IMPACT STUDIES ON FIXED END RODS

by

Richard J. Charles

B.A.Sc., University of British Columbia

1948

M.A.Sc., University of British Columbia

1949

Submitted in Partial Fulfillment of the

Requirements for the Degree of

DOCTOR OF SCIENCE

from the

Massachusetts Institute of Technology

1954

Signature of the Author
Department of Metallurgy
April 30, 1954

Signature of Professor
In Charge of Research

Signature of Chairman
of Department Committee
on Graduate Students

IMPACT STUDIES ON FIXED END RODS

by

Richard J. Charles

Submitted to the Department of Metallurgy

on April 30, 1954

In Partial Fulfillment of the Requirements for the Degree of

DOCTOR OF SCIENCE

ABSTRACT

This thesis is concerned with the study of longitudinal impact of fixed end rods as it affects the transfer of impact kinetic energy to strain energy within the rods. From theoretical considerations the amount of fractured material produced during structural failure of a brittle solid should be related to the amount of strain energy in the solid prior to fracture. The transfer of kinetic energy to strain energy by impact, therefore, is an important step in comminution processes.

Estimations of the amount of strain energy absorbed in pyrex glass and mild steel rods were made from an analysis of the strains produced at various sections of the rods during impact. Experiments were made under varied conditions of impact and a correlation made between these conditions and the maximum amounts of strain energy absorbed during the impacts.

The experiments showed that a maximum transfer of kinetic energy to strain energy could be obtained if the time of contact of the impacting hammer and the rod was a fractional part of the period of vibration of the rod and if the impacting blow consisted of a single pulse. Under the most favorable impact conditions for the rod systems investigated the maximum amount of strain energy observed in the rods never exceeded one-half of the kinetic energy of impact. The experiments also showed that the time of contact and the shape of the impact pulse were mainly determined by the mass of the impacting object.

A theoretical analysis of longitudinal impact of rods, along the lines proposed by Timoshenko and Frankland, illustrated that the transfer of impact energy to strain energy could be profoundly affected by the conditions of impact and that for any simple structure one of these conditions results in a maximum energy transfer.

Thesis Supervisor: P.L. deBruyn
Title: Assistant Professor of Metallurgy

TABLE OF CONTENTS

LIST OF TABLES

APPENDIX I

EXPERIMENTAL EQUIPMENT

APPENDIX II

EXPERIMENTAL DATA

LIST OF FIGURES

APPENDIX I - EXPERIMENTAL EQUIPMENT

APPENDIX II - EXPERIMENTAL DATA

APPENDIX III - THEORETICAL CALCULATIONS

ACKNOWLEDGMENTS

The author wishes to thank Professor P. L. de Bruyn for his guidance, constructive criticism, and invaluable assistance which made completion of this work possible.

The research presented in this thesis was done in the Richards Mineral Engineering Laboratory of the Massachusetts Institute of Technology and was jointly sponsored by the United States Atomic Energy Commission, The Engineering Foundation, and the private industrial concerns who support the Comminution Research Program at M.I.T. The author is grateful for the financial assistance which gave him the opportunity of conducting this research program and continuing his studies in Mineral Engineering.

The author is greatly indebted to Professor A. M. Gaudin, Richards Professor of Mineral Engineering, M.I.T., and Mr. H. R. Spedden, presently with the Metals Research Laboratories of the Union Carbide and Carbon Corporation, for their valuable assistance in initiating the research problem and their continued guidance and interest throughout the investigation.

For the many favors and friendly associations afforded him, the author wishes to thank the entire mineral engineering staff.

I. INTRODUCTION

The main object in comminution of brittle materials is to bring about size reduction by causing fractures to originate and propagate. Although many of the properties of fracture are in debate it is well established that the initiation and propagation of fractures are brought about by changing stress conditions within the material. The changing stress conditions may be the result of external loading, thermal effects or changes in the physico-chemical nature of the material. In order that fractures may propagate it is logical to assume that the stress conditions must exceed some critical value that would be determined by the binding forces between atoms or molecules of the material. On this basis theoretical "strengths" of certain materials have been calculated[1,2] and these calculated values are always much higher than the strengths actually exhibited by the materials.

The difficulty in determining strengths of brittle materials and the correlation of these strengths to theoretical values led Griffith[1] to postulate a theory of brittle rupture which, from the comminution standpoint, offers two important ideas. These are as follows:

1) Comminuting practises are mainly dependent on the existence of flaws, weaknesses and micro-cracks within the material being broken. If this were not the case and brittle materials exhibited their theoretical strengths then much greater difficulty would be encountered in the size reduction of these materials than is generally experienced.

2) A simple comminuting system can be outlined in which the amount of new surface produced is shown to be dependent on the reduction of strain energy of the system. The above statement is, in actuality, a corollary of the well

known Rittinger's hypothesis for crushing and grinding, which has never had a sound fundamental basis.

For a certain glass Griffith calculated a theoretical strength in tension of 1.6×10^6 pounds per square inch while specimens of the glass failed in tensile tests at values around 26,000 pounds per square inch. He showed that this discrepancy could be accounted for if flaws or micro-cracks were assumed to exist in the material. The flaws would act as centers of stress concentration and permit spreading of the cracks. For purposes of calculation Griffith considers a rigidly constrained specimen in which a crack is allowed to extend. Since the specimen is rigidly constrained the increase in surface free energy due to a spontaneous increase in crack length must equal the decrease in potential (strain) energy of the specimen. By equating these two energy changes Griffith was able to show, with the aid of elastic theory, that the overall tensile strength of the specimen is related to the surface free energy of the material and the crack length in the following manner.

$$S_{cr} = \sqrt{\frac{4E\gamma}{\pi l}} \qquad (1)$$

S_{cr} = tensile strength of the specimen

γ = surface free energy of the material

E = Young's Modulus

l = crack length

Griffith carried out experiments with glasses in which cracks of known lengths were formed and obtained satisfactory agreement with Equation 1. Thus the strength of a brittle material was shown to be mainly dependent on the flaws and cracks in the material.

Piret[2] has conducted experiments on the crushing of quartz particles in which he showed that the amount of new surface produced was proportional to the strain energy absorbed by the particles and thus the results were in qualitative agreement with the fundamental basis of Griffith's theory.

The problem of fracture may be further complicated in that gases and liquids may enter the cracks and radically change the nature of the surfaces and alter the physical and chemical conditions at the tip of the cracks. If the material around the flaw is under tension it may be greatly weakened and the crack will progress. If the flaw does not extend the chemicals may alter the surfaces and round out the crack tips so that the material is actually strengthened. Theory and experiment have shown that to speak of strength as a physical property of most brittle materials has little meaning and that rupture is a result of many causes including the stress conditions, the characteristics of the flaws and the penetration of weakening or strengthening reagents.

In many crushing and grinding operations, as well as in many testing methods used for determining grinding efficiencies, impact processes are used to bring about fracture. The analysis of these comminuting procedures must include an examination of the energy changes that occur. Kinetic energy of impact is changed into a number of forms including strain energy of the masses, kinetic energy of translation, kinetic energy of vibration and energy dissipated in plastic deformation. In explaining the fracture process the strain energy absorbed is the important quantity to be considered since it is from this source, and this source only, that the energy to produce fracture will be drawn.

From this brief review it is apparent that any increase in the efficiency

of transfer of the source energy of comminution to strain energy of the material must result in an increase in the overall efficiency of the comminution process. Thus a study of impact and energy transfer by impact may greatly contribute to the general theory of comminution.

This thesis presents a study of the transfer of kinetic energy of impact to strain energy of an impacted body and illustrates some of the conditions of impact that affect this transfer.

II. THEORETICAL CONSIDERATIONS OF IMPACT

Application of the Law of Conservation of Momentum to Impact

The application of the Law of Conservation of Momentum is helpful in studying impact since it can generalize some of the overall effects of the process. Consider a stationary object of mass m_1, which is struck by another object of mass m_2 initially moving at a velocity of v_2, and consider that the two masses remain together after impact and move at a velocity of $v_{1,2}$. Then, from conservation of momentum,

$$m_2 v_2 = (m_1 + m_2)\, v_{1,2} \tag{2}$$

Let E_2 equal the initial kinetic energy of m_2 and $E_{1,2}$ equal the kinetic energy of the combined mass after impact, then

$$\frac{E_{1,2}}{E_2} = \frac{1/2(m_1 + m_2)(v_{1,2})^2}{1/2(m_2)\, v_2^2} = \frac{m_2}{m_1 + m_2} \tag{3}$$

Thus Equation 3 shows that the smaller the ratio m_2/m_1 the larger the amount of kinetic energy that is lost in the impact process. The loss of kinetic energy is taken up as strain energy of the masses, heat and perhaps by permanent deformation of the colliding objects. The above equation shows why small hammers at high velocities are used in forging processes where a maximum amount of deformation is required and why large hammers at relatively slow velocities are used in pile driving where the object is to give the pile as much kinetic energy as possible.

The application of the law of conservation of momentum to two objects colliding is quite straightforward since the problem is concerned with the

the effects after impact; however, in comminuting processes the system may change drastically if fracture takes place during impact. The impact process is not instantaneous and during the process translatory kinetic energy of the impacting mass changes to strain energy and kinetic energy of vibration of the masses as well as to other forms of energy. In this case it is difficult to determine the distribution of kinetic energy to the elemental parts of the system and consequently difficult to determine the loss of initial kinetic energy to other forms of energy. As a general rule, however, the case of comminution may be considered analagous to the case of forging in that light hammers at high velocities would be advantageous. An objection may be raised to the above rule in that, in comminuting devices where impact is employed, the impacting medium will lose all its kinetic energy either by a single impact or a number of further impacts and so nothing would be gained by adjustment of the weights of the impacting masses. The main object however, is to cause fracture and unless the impacts raise the strain energy of the impacted material above a certain level, the energy input is lost in the form of heat and does not contribute to the comminuting process. If fracture is to be obtained by impact it is desirable for the impacting masses to lose as much kinetic energy as possible during a single impact so that a maximum amount of energy would be available for fracture.

Displacements and Stresses Arising from Forced Loading

In the foregoing no attention was given to the stress values arising from impact and since the strain energy density in the impacted object would, in general, not be constant throughout, the stress conditions would be a better criterion for predicting fracture than the total strain energy of the masses.

The stress conditions set up in bodies undergoing impact are usually

very complicated since propagation of stresses as travelling pressure waves must usually be taken into account. In static loading any change in applied force is so slow compared to the velocity of stress propagation that the specimen may be considered to readjust instantaneously at all points under the change in loading. In the case of impact the changes in the applied force are usually so rapid that the time necessary to transmit the changes in stress to all parts of the specimen must be considered. An analysis of the wave equation illustrates the effect of travelling waves and shows how the wave velocities are dependent on the physical characteristics of the material through which the waves are transmitted.

Consider Figure 1 in which a uniform stress, σ, is suddenly applied to the end of a bar.

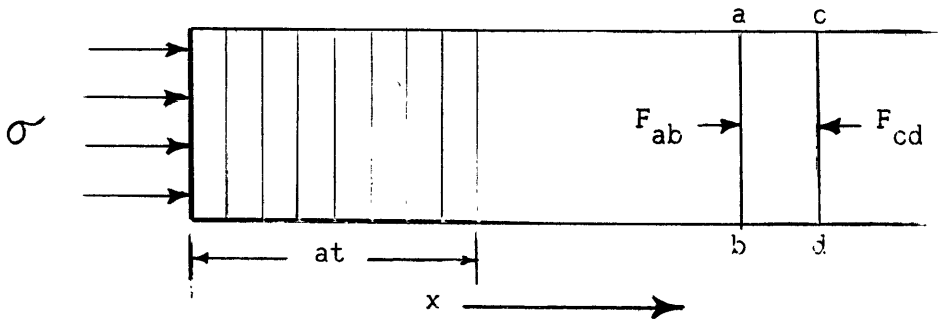

Figure 1. Schematic Illustration of End Loaded Bar

The stress is transmitted along the bar at some velocity, a, which is the velocity of wave propagation in the material. The velocity, v, of the particles in the stressed zone would not be equal to the wave velocity since the compressed zone is shortened by the amount $(\sigma/E)at$, where σ is the stress, E is the Young's Modulus of the material, and t is the time during which the stress is applied. The velocity of the particles at the end of the

bar where the stress is applied would be

$$v = \frac{a\sigma}{E} \tag{4}$$

The velocity of wave propagation can be found by applying the equation of momentum. The compressed zone, initially at rest, has a velocity v and a momentum of $Aav\rho t/g$ at the time t, where A is the area of the rod and ρ is the density of the material and g is the acceleration of gravity. The momentum of the compressed zone must equal the impulse of the applied force and thus

$$A\sigma t = Aa\rho v/g \tag{5}$$

and therefore $$a = g\sigma/\rho v \tag{6}$$

and since $$v = a\sigma/E$$

then $$a = \sqrt{Eg/\rho} \tag{7}$$

Thus the velocity of wave propagation is dependent only on the characteristics of the material and is independent of the applied force.

Again, referring to Figure 1, if the displacement of any element from its rest position is 'u' then the strain at that element, equal to the unit elongation or contraction at that section, is equal to $\partial u/\partial x$. The corresponding force on the bar would be $AE\,\partial u/\partial x$. The force would be positive or negative depending on whether the force was tensile or compressive. An element of the bar, bounded by the sections ab, cd, if in motion would have forces of different values acting on the sides ab and cd. The resultant of these forces causes an acceleration of the element according to Newton's Third Law. Thus

$$\text{Force}_{(ab)} - \text{Force}_{(cd)} = \text{Force}_{(\text{resultant})}$$

$$AE\left(\frac{\partial u}{\partial x} + \frac{\partial^2 u}{\partial x^2}dx\right) - AE\frac{\partial u}{\partial x} = AE\frac{\partial^2 u}{\partial x^2}dx \tag{8}$$

$$\text{Force}_{(\text{resultant})} = \text{mass} \times \text{acceleration}$$

$$AE \frac{\partial^2 u}{\partial x^2} dx = (A\rho/g) \frac{\partial^2 u}{\partial t^2} dx \tag{9}$$

Rearranging terms the following equation of motion, which is generally known as the wave equation, results

$$\frac{\partial^2 u}{\partial t^2} = a^2 \frac{\partial^2 u}{\partial x^2} \tag{10}$$

where $a = \sqrt{Eg/\rho}$ as found for the velocity of wave propagation in Equation 7.

As a solution to the wave equation Timoshenko[4] shows that any longitudinal vibration of a prismatic bar, fixed at one end and under no external forces, can be represented in the following form

$$u = \sum_{i=1,3,5\ldots}^{i=\infty} \sin \frac{i\pi x}{2\,l} \left(A_i \cos \frac{i\pi at}{2\,l} + B_i \sin \frac{i\pi at}{2\,l} \right) \tag{11}$$

where u = displacement of an element from its rest position

x = coordinate value of an element

a = wave velocity

l = bar length

t = specific value of time

A_i, B_i = constants

If at the initial moment the displacement may be given as

$$(u)_{t=0} = f(x) \tag{12}$$

and the initial velocities of the elements being displaced are given as

$$(du/dt)_{t=0} = f_1(x) \tag{13}$$

then the coefficients, A_i and B_i, may be determined from the known functions f and f_1 in a manner similar to the determination of coefficients in Fourier

Series analysis.

If an external force acts on the free end of the bar an expression must be added to Equation 11 to take into account the vibrations produced by the external force, thus

$$u = \sum_{i=1,3,5\ldots}^{i=\infty} \sin\frac{i\pi x}{2l}\left[A_i\cos\frac{i\pi at}{2l} + B_i\sin\frac{i\pi at}{2l} + K/i\int_o^t P\sin\frac{i\pi at}{2l}(t-t_1)dt_1\right] \quad (14)$$

where t_1 = time

P = external force

$K = 4g/A\rho a\pi$

For the case of impact wherein the disturbing force produces the vibration and the bar was at rest prior to the blow then

$$A_i = B_i = 0$$

and

$$u = \sum_{i=1,3,5\ldots}^{i=\infty} \sin\frac{i\pi x}{2l}\left[\frac{K}{i}\int_o^t P\sin\frac{i\pi a}{2l}(t-t_1)dt_1\right] \quad (15)$$

For the particular case of the deflection at the struck end of the bar, i.e., $x = l$

$$u_{(x=l)} = K\sum_{i=1,3,5}^{i=\infty}\frac{1}{i}\int_o^t P\sin\frac{i\pi a}{2l}(t-t_1)dt_1 \quad (16)$$

Equation 15 thus gives the position of any section of a prismatic bar as a function of time when a force, P, is applied to the originally free end of the bar. If the positions of the elements of the bar are known then the stress distribution throughout the bar may also be calculated. The application of this equation to impact problems would therefore be possible if the applied

force, P, which is derived from the impact and is a function of time, were known.

Summation terms in Equations 15 and 16 indicate that in the end-loading of a prismatic bar an infinite number of modes of vibration of the bar contribute to the complete displacement of any single element of the bar during vibration. Equations 15 and 16 also show that the higher the mode of vibration the less is the amount of displacement attributable to this mode. Each mode of vibration may be considered as defining a single coordinate system for locating any element of the bar and since an infinite number of modes of vibration are present in the above solution the problem is considered as one involving an infinite number of degrees of freedom*. It often occurs in impact systems that one of the degrees of freedom (or one of the modes of vibration) is so important that it determines the behavior of the system for all practical purposes; the problem can then be greatly simplified by analysis on the basis of a single degree of freedom.

Frankland[5] has dealt with the problem of impact by focusing attention on simple systems of one degree of freedom. Figure 2 illustrates such a system in which a force acts upon a rigid mass which is separated from a reference plane by a weightless spring. The system illustrated is analogous to the case of a rod with a fixed end which undergoes impact on the free end if the rigid mass is considered to be represented by the rod mass and the spring to be represented by an imaginary spring whose properties are determined by the elastic and dimensional characteristics of the rod.

---

*A mechanical system is said to have n degrees of freedom if it requires n independent coordinates to completely specify the configuration of the system.

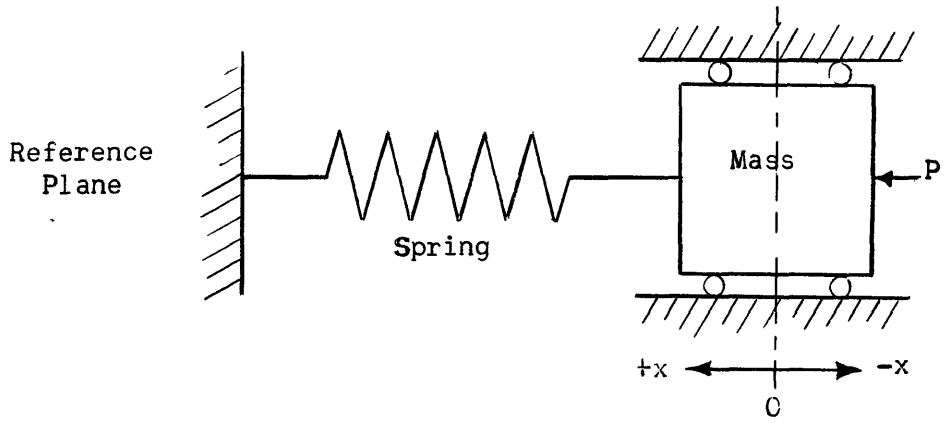

Figure 2. Mechanical System of One Degree of Freedom

In this case the differential equation of motion of the mass is

acceleration force + spring force = applied force

$$md^2x/dt^2(t) + kx(t) = P(t) \qquad (17)$$

where m = mass of the rigid body

x = coordinate position of body from equilibrium

t = time

k = spring constant

P = applied force

A general solution of the above equation is,

$$u(t) = K' \int_o^t P(t_1)\sin \beta(t-t_1)dt_1 \qquad (18)$$

where $\beta^2 = k/m$

u(t) = displacement as a function of time

K' = a constant

t_1 = time

t = a specific value of time

This equation is very similar to Equation 16 with the exception that no summation term,which indicates the higher modes of vibration of the system, occurs. In this case, where only the fundamental mode of vibration of the system

is considered to be excited, the positions of the mass and the elemental positions of the spring may be described by a single coordinate value at any time and consequently the system has only one degree of freedom.

In order to generalize the results of his investigations Frankland introduces two non-dimensional terms as follows;

disturbance p -- ratio between the applied force, P, at any time and the maximum value of the applied force, P_o. (i.e. $p = P/P_o$)

response u_x -- ratio of the dynamic displacement, x, of the mass under sudden application of a load and the static displacement, x_o, of the mass under a static load equal to P_o. (i.e. $u_x = x/x_o$)

In the experimental work of this thesis a loading pulse approximating the shape of the first half cycle of a sine wave assumes importance. The effect of such a pulse on the simple system described above has been determined by Frankland in the following manner.

The boundary conditions for solving Equation 18 when a single sinusoidal load pulse acts on the system in Figure 2 are as follows,

$$\begin{aligned} p &= 0 && t_1 < 0 \\ p &= \sin \pi t_1/t && 0 \leqq t_1 \leqq t \\ p &= 0 && t_1 > t \end{aligned} \qquad (19)$$

where t_1 = time

t = impulse time

For these boundary conditions the solutions for the responses are,

$$u_x = \frac{2}{\frac{T}{t} - \frac{4t}{T}} \left(\sin \beta t_1 - 2\frac{t}{T} \sin \pi \frac{t_1}{t}\right) \quad 0 \leqq t_1 \leqq t \tag{20}$$

$$u_x = \frac{2}{\frac{T}{t} - \frac{4t}{T}} \left[(1 + \cos \beta t) \sin \beta t_1 - \sin \beta t \cos \beta t_1\right] \quad t_1 \geqq t \tag{21}$$

where T = period of oscillation of system

Equations 20 and 21 are indeterminate for t = 0.5T. For this particular case the response is,

$$u_x = 1/2 \left(\sin \beta t_1 - K\, t_1 \cos \beta t_1\right) \quad 0 \leqq t_1 \leqq 0.5T \tag{22}$$

$$u_x = \frac{-\pi}{2} \cos \beta t_1 \qquad t_1 \geqq 0.5T \tag{23}$$

A plot of response versus time utilizing Equations 20 and 21, as given by Frankland, is reproduced in Figure 3. The pulse time of the disturbance, t, is expressed in terms of the period of fundamental vibration, T, of the system. The dotted curve in Figure 3 is included to show the shape of the sinusoidal pulse.

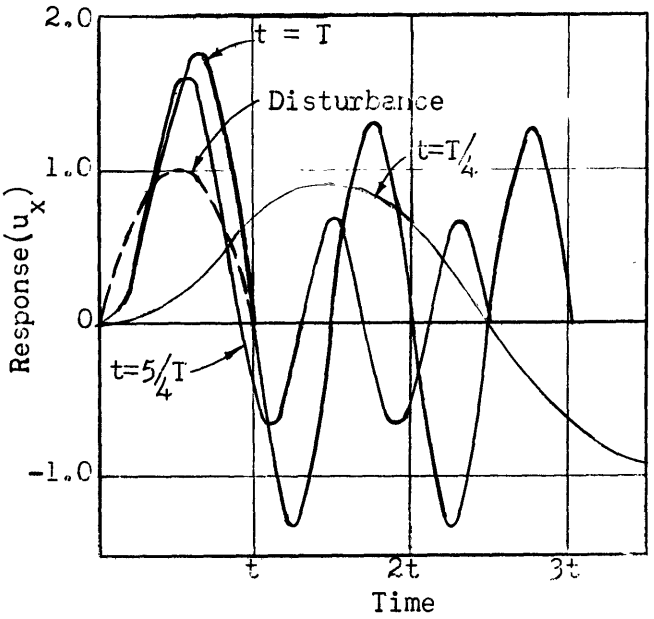

Figure 3. Response of System of One Degree of Freedom Under Sinusoidal Pulse Loading

Since the spring is assumed to follow Hooke's Law the response of the system may be used to represent ratios of spring force as well as displacements. Since a displacement of x_o is obtained under a load of P_o the spring reaction, S, would be equal to $P_o(x/x_o)$ at any time under dynamic loading. It is convenient to denote the numerical maximum of the response factor, x/x_o, as the dynamic load factor, n, which is the maximum ordinate in Figure 3 for any specific impact. This factor when multiplied by the peak value of the load, P_o, gives the maximum spring reactive force during the impact. Figure 4 is a plot from Frankland's work showing the dynamic load factor for sinusoidal pulse loading as a function of the time ratio t/T, where t is the pulse time and T is the period of the fundamental oscillation of the system.

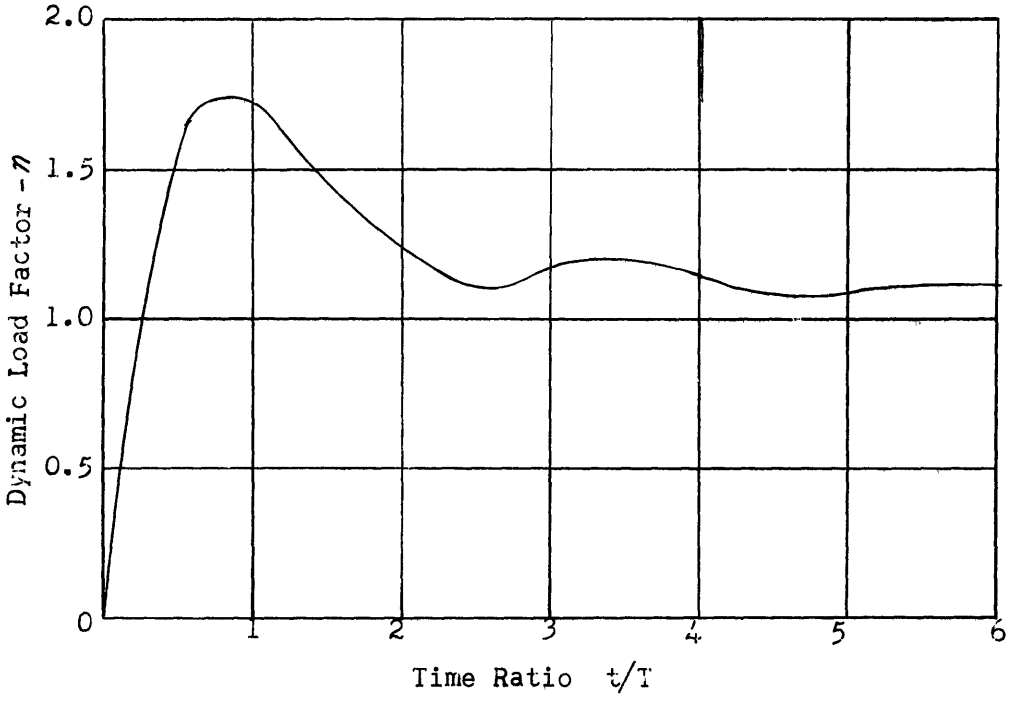

Figure 4. Dynamic Load Factor for Sinusoidal Pulse

Figure 4 shows that the dynamic load factor reaches a maximum when the time of loading is between 0.5T and T.

Determination of Pulse Loading for Lateral Impact on Bars

As shown in the previous section the deflection of an end-loaded rod can be calculated if the force producing the deflection is known. In the discussion of Timoshenko's method the loading force is considered as any arbitrary force which varies with time and this force-time relationship must be known to solve the deflection equation. In the cases given by Frankland specific force-time relationships are assumed in the calculation of responses and displacements.

For the solution of the impact problem the value of the contact force between the impacting objects and the manner in which it varies with time may be obtained from the conditions of impact, as shown in the following treatment.

Consider a rigid object striking the end of a bar and being decelerated; the velocity of the object at any moment, t_1, would then be,

$$v = v_o - 1/m \int_o^{t_1} P dt_1 \qquad (24)$$

where v = velocity

v_o = initial velocity

P = force of contact

m = mass of the object

t_1 = elapsed time

The distance, d, the object moves up to a specific time, t, is

$$d = v_o t - \left(\int_o^t dt_1/m\right) \int_o^{t_1} P dt_1 \qquad (25)$$

This distance, d, must also be the distance the end of the bar moves during time t, therefore,

$$v_o t - \left(\int_o^t dt_1/m\right) \int_o^{t_1} P dt_1 = \sum_{i=1,3,5\ldots}^{i=\infty} (K/i) \int_o^t P \sin(i\pi a/2\ l)(t-t_1)dt_1 \qquad (26)$$

where the right hand side of the above equation is the deflection equation as given by Equation 16.

Equation 26 may be integrated numerically and the relation $P = f_1(t)$ obtained, where f_1 is the function to be determined.

In experimental work it is difficult to obtain a uniform impact force on a flat ended bar and if the bar end is rounded to assure symmetrical and reproducible impacts, the above equation is not valid because of the local deformation produced at the point of contact. The local deformation may be accounted for by using the known solution of Herz[6] for impact of spheres.

The total distance the striking object moves during impact equals the deflection of the end of the bar plus the local flattening of the bar, i.e.,

$$d = \alpha + y \qquad \begin{array}{l} d = \text{total bar deflection} \\ \alpha = \text{local flattening} \\ y = \text{bar deflection} \end{array} \qquad (27)$$

According to Herz,

$$\alpha = k_1 P^{2/3} \qquad \begin{array}{l} P = \text{force of contact} \\ k_1 = \text{proportionality constant} \end{array} \qquad (28)$$

Thus, by combining the Herzian equation and Equation 26 the final impact equation would be,

$$v_o t - \left(\int_o^t dt_1/m\right) \int_o^{t_1} P dt_1 = k_1 P^{2/3} + \sum_{i=1,3,5\ldots}^{i=\infty} (K/i) \int_o^t P \sin(i\pi a/2\ l)(t-t_1)dt_1 \qquad (29)$$

Again this equation may be integrated numerically and once the function $P = f_1(t)$ is determined the conditions of stress at any point in the bar may also be determined by integrating Equation 15.

The general impact equation as given above will be used in a further chapter to theoretically derive impulse force-time relationships for comparison with force-time loading pulses obtained by experiment.

III. OUTLINE AND PLAN OF WORK

The primary object of this research is to determine the effects of impact on simple geometric bodies, to measure the magnitude of the variables which permit an estimation of the transfer of kinetic energy of impact to strain energy of the impacted masses and to determine the conditions of impact that control the energy transfer.

The principle steps of the experimental work are as follows:

(1) The design and construction of an apparatus by which reproducible impacts can be made on rods with fixed ends.

(2) The design and construction of suitable instruments for the measurement of quickly varying strains and for the measurement of impact times.

(3) The observation of time-strain relationships for glass and mild steel rods.

(4) The calculation of strain energy values brought about by impact.

(5) The measurement of impact times as a function of the conditions of impact.

IV. EXPERIMENTAL METHOD

Experimental Materials

The impact tests were made on bars of pyrex glass and mild steel. The specimens were 10 inches long and 1 inch in diameter with the ends rounded to a radius of 6 inches. The ends were rounded to facilitate reproducible impacts. The specimens were made of the above materials and were made 10 inches long so that their natural frequencies of longitudinal vibration would be approximately 10 kilocycles. The Young's Modulus-density ratios of the above materials are such that the velocity of sound is nearly the same in both of them and thus objects of similar dimensions would have similar vibrational characteristics. The main portion of the experimental work was done on pyrex rods for the following reasons.

(a) Pyrex glass is almost perfectly elastic and will not permit measurable plastic deformation[7].

(b) The Young's Modulus of pyrex has been shown to be constant up to the fracture point[1,8].

(c) Pyrex glass has many characteristics that are similar to those of the materials encountered in crushing and grinding operations.

The hammers which were used to impact the rods were made of mild steel. Six hammers, which were swung as pendulums, were constructed from one inch mild steel rod. These hammers varied in weight from 100 to 600 grams at almost equal increments of 100 grams. Four hammers, which were individually shot from a spring loaded gun as projectiles, were constructed from one-half inch mild steel rod. These hammers weighed, respectively, 19.7, 39.5, 59.3 and 78.1 grams. The impacting ends of all the hammers were rounded to a

six inch radius.

Experimental Apparatus

(a) Impact equipment

Figures 5 and 6 illustrate the impact equipment. As shown in Figure 5 the rods were mounted horizontally in v-notches on a rest with a heavy steel anvil at one end. The anvil and rests were securely bolted to a 300 pound block of concrete in order to obtain as rigid end conditions as possible for the impacted bars. Figure 5 also shows the manner in which the pendulum impacts were accomplished. Figure 6 is a photograph of the rod (a), the anvil (b), the concrete block (c) and the spring loaded gun (d).

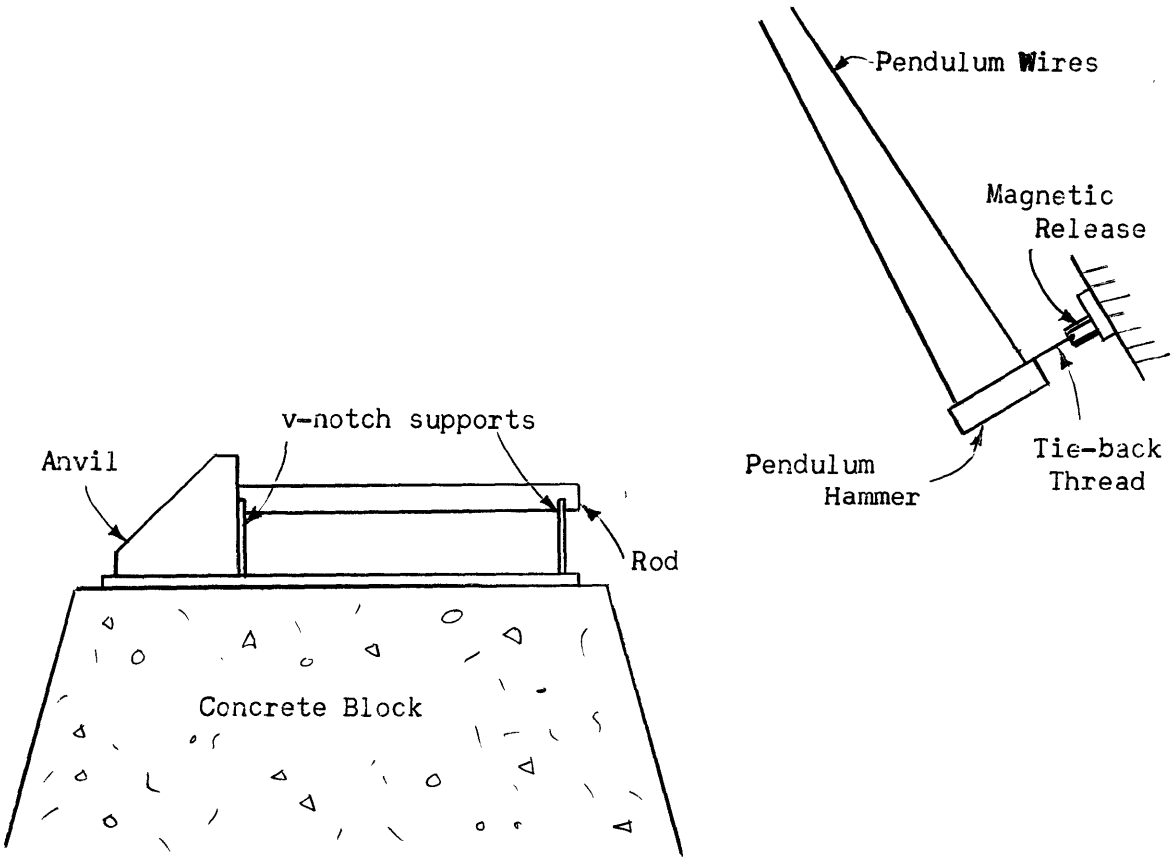

Figure 5. Arrangement for Pendulum Impacts of Rods

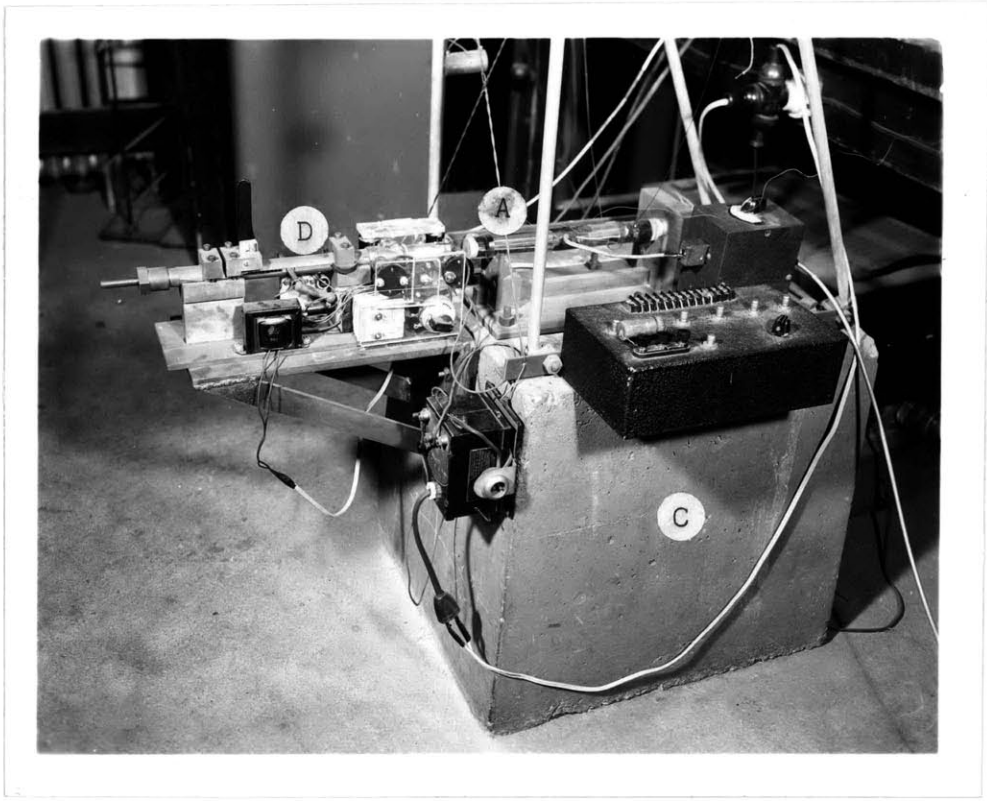

Figure 6. Photograph of Impacting Arrangement with Spring Loaded Gun

Measurements of the kinetic energies of the impacting hammers just prior to impact were required in the experimental work. In the case of the pendulum hammers the kinetic energies of impact were obtained by measuring the heights of fall of the centers of gravity of the hammers before and after impact and multiplying these values by the weights of the hammers. The heights of fall were measured by means of a levelling telescope which could be moved up and down a graduated post. By means of a vernier scale on the graduated post measurements could be made to within 0.2 mm. On this basis the accuracy of measurement of a 20 cm fall would be 0.1 percent and for a small drop, such as 2 cms the accuracy of measurement

would be about 1 percent.

The kinetic energies of the projectile hammers were determined by measuring the velocities of the projectiles prior to impact and calculating the kinetic energy values. The velocities of the projectile hammers were measured by means of an electronic device employing light sources and slits, phototubes and a constant frequency source. The mounting arrangement for the slits, lights and phototubes is shown in Figure 7 and the circuit arrangement for the velocity measurement device is given in Appendix I. Velocity measurements were made by timing the path of flight of the projectiles as they passed between two 0.5 mm slits of light set 8 cm apart. The optical arrangement could therefore permit a maximum error of 1 mm in 80 mm or 1.25 percent. Since the velocity measured is the average of the projectile velocity as it passes between the beams of light, the value arrived at may be greater than the actual velocity at impact due to frictional deceleration of the projectile in the gun barrel. Measurements were made of the coefficient of friction between the projectiles and the gun barrel so that the magnitude of the change in velocity due to frictional effects could be calculated. These calculations, which are given in Appendix I, show that no serious error of velocity measurement due to frictional forces should be encountered for velocity measurements above 200 cm per second. At 100 cm per second the error would be about 10 percent while at 200 cm per second it would be 2.5 percent.

(b) Strain measurement equipment

In order to measure the quickly varying strains set up in the rods by impact a technique involving wire resistance strain gages was used. Wire resistance strain gages are particularly suitable for strain measurements

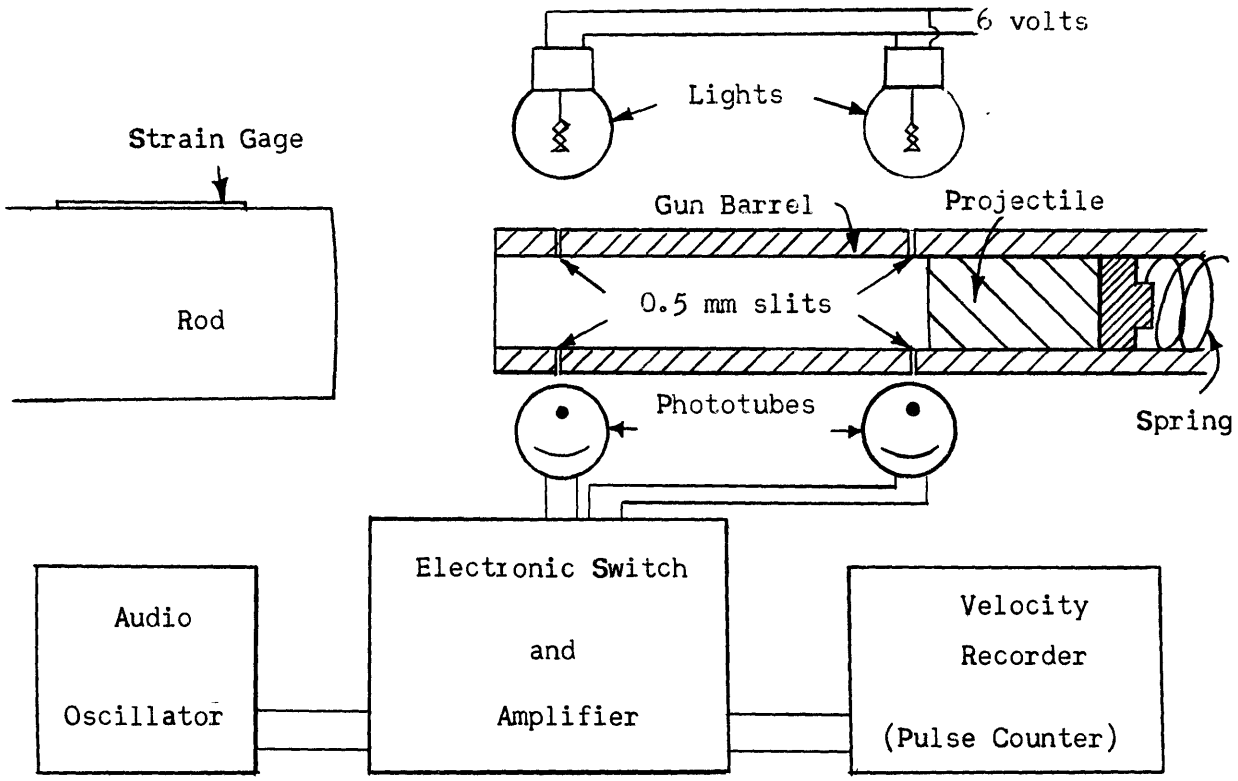

Figure 7. Mounting Arrangement for Velocity Measuring Device

since they have negligible inertia effect on the system, have good sensitivity and have a large range of frequency response (0-50 kc)[9].

The measurement of strain with wire resistance strain gages depends on a change in resistance of the gages as they are extended or compressed under the changes of strain of the object to which they are attached. If a constant current flows through the gage then a change in voltage occurs when the overall resistance is changed. The change in voltage may be applied to an amplifier by means of a blocking capacitor and the signal amplified to some value suitable for measuring or observing on an oscilloscope. The strain gage circuit used in the investigation is shown in Figure 8. The strain gage

equation is as follows,

$$\frac{\Delta l}{l} \Big/ \frac{\Delta R}{R} = F \qquad (30)$$

ΔR = resistance change

Δl = change in length

R = gage resistance

l = gage length

F = gage factor

since $\Delta v = i \Delta R$, and 'i' is constant then,

$$\mathcal{E} = \frac{\Delta l}{l} = \frac{\Delta v}{iRF} \qquad (31)$$

Δv = voltage change when resistance change is ΔR

i = current

$\mathcal{E}$ = strain

The above equation shows that the change in voltage is proportional to the strain. Since the voltage changes given by strain gages under normal strain applications are of the order of 1 millivolt the amplification of the signals sometimes presents difficulties because stray signals of the same order of magnitude as the strain signals may be picked up in the electrical system. For this reason a well shielded,battery operated amplifier was constructed so that 60 cycle signals from transformers, chokes and heater filaments could be eliminated. Figure 2, in Appendix I, gives the circuit of the amplifier along with its amplification and frequency response characteristics. Table 1, Appendix I, lists the manufacturers data on the strain gages used in the investigation. Both the resistance and gage factors of the strain gages were listed with tolerances of 1 percent.

Figure 9 is an illustration showing the positions where the strain gages were attached to the pyrex and mild steel rods.

(c) Recording and calibrating equipment

The experimental data throughout the investigation was obtained in the

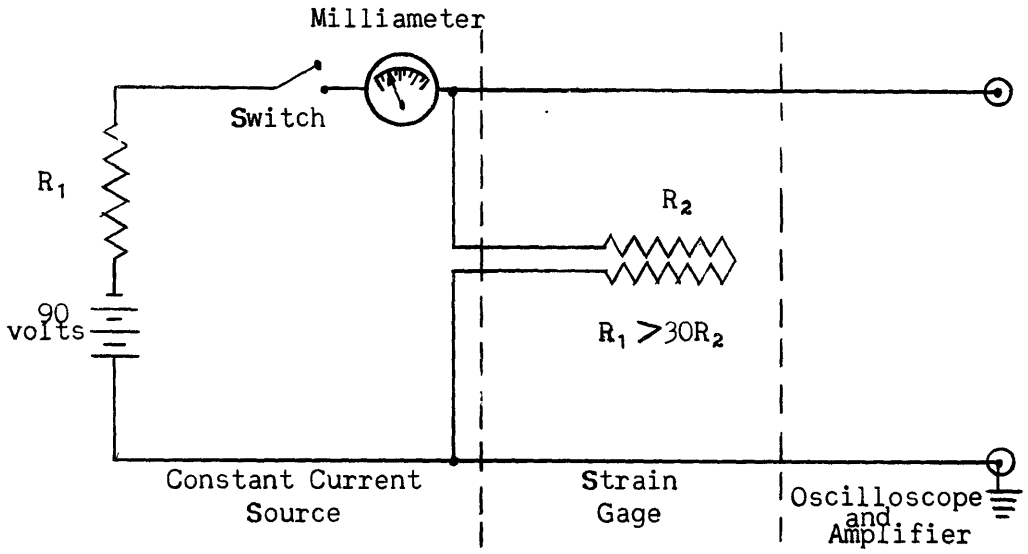

Figure 8. Strain Gage Circuit

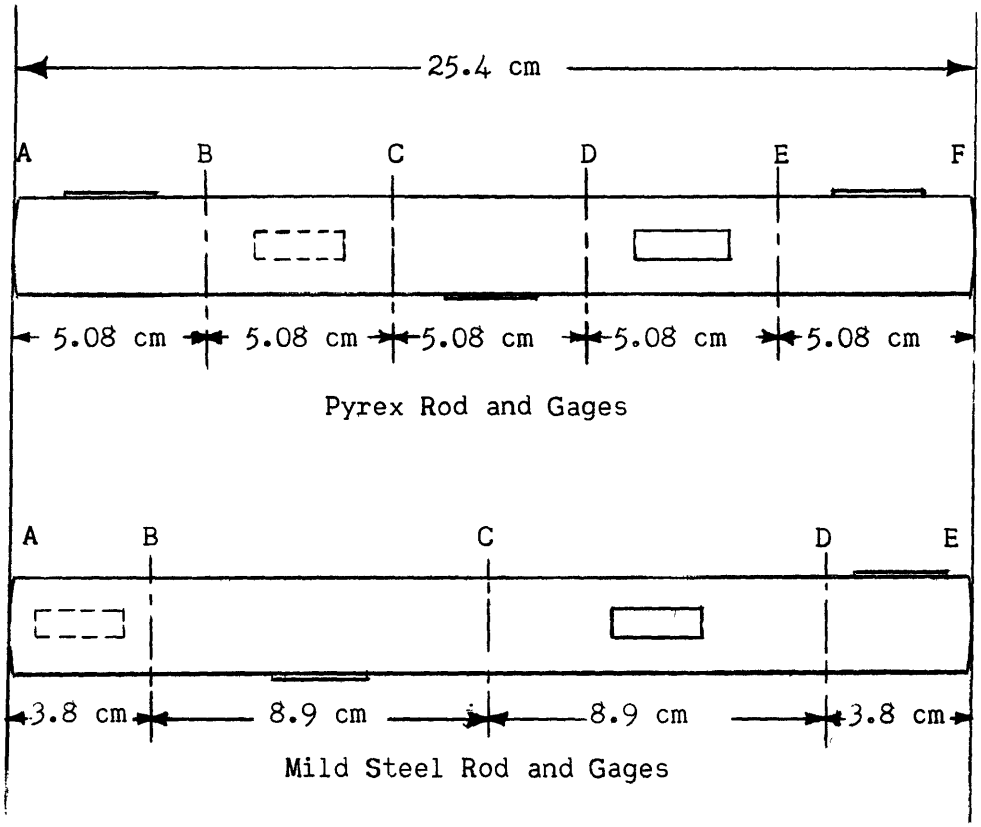

Figure 9. Positions of Strain Gages on Rods

form of oscillographs from a Dumont Type 248 oscilloscope. A camera, which held either 2 1/2 inch by 3 1/2 inch cut film or 35 mm roll film, was used to photograph the oscilloscope patterns. The oscilloscope was arranged so that a single sweep could be driven across the oscilloscope screen by an external circuit that was tripped when the hammer and rod made contact. After the sweep was started the amplified signals from the strain gages deflected the trace vertically. The duration of sweep selected for the strain measurements was 1,000 microseconds and the trace, due to the single sweep, was interrupted by markers every 100 microseconds from the beginning of the sweep. A General Radio Microvolter and a Hewlett Packard Oscillator were used to calibrate the oscilloscope and amplifier so that the value of a signal producing a specific vertical response on the screen could be determined. Calibration signals were photographed with all voltage-time records since the screen of the oscilloscope did not give a linear response to the input voltage. Figure 10 is a photograph illustrating the complete experimental apparatus.

Experimental Procedure

The procedure for obtaining voltage-time records of the impacts on the bars, once standardized, was repeated without change for the various impact conditions that were studied. The procedure was as follows.

The pendulum apparatus or the spring loaded gun, whichever was being used, was adjusted so that the kinetic energy of impact, when measured, would have a value near that desired for the particular impact test that was being made. The impacting hammer was released and at the same time the shutter of the oscilloscope camera opened. Contact of the impacting hammer and the rod discharged a condenser such that the voltage change on the discharging

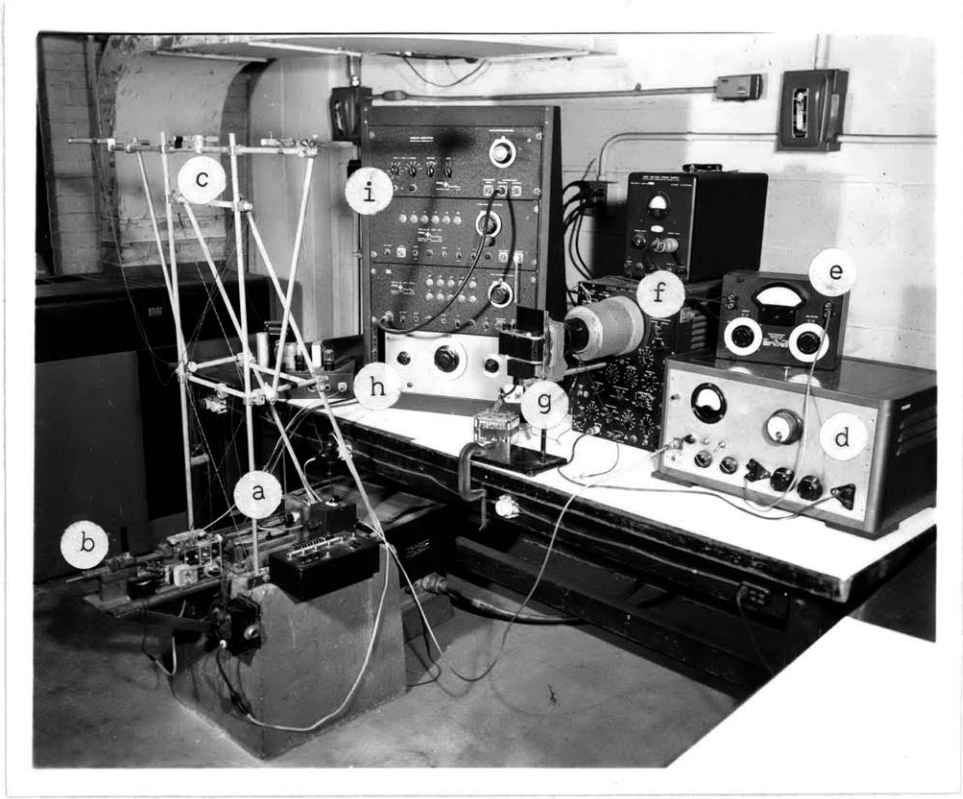

(a) Specimen rod, rests and anvil

(b) Spring loaded gun

(c) Support for pendulum hammers

(d) Amplifier for amplifying the strain gage signals

(e) Microvolter for calibrating the amplifying system

(f) Oscilloscope and high voltage supply

(g) Oscilloscope camera

(h) Audio oscillator used as a signal source for the microvolter and the velocity measuring device on the spring loaded gun

(i) Amplifier and scaler used as a recorder for the velocity measuring device

Figure 10. Experimental Equipment Used in the Investigation

condenser caused the oscilloscope tripping circuit to start a single trace to travel across the screen. The amplified signal from the strain gage deflected the trace vertically as it moved across the screen and thus a time-voltage record was obtained. A constant frequency signal source (10 kc) was then substituted for the strain gage by means of a switching arrangement and a companion photograph taken of several precisely known voltages. The voltage levels were selected so that they would bracket any expected signal voltage on the voltage-time trace. From these calibration voltages it was possible to convert the voltage-time traces into a strain-time relationship.

After the voltage-time and calibration records were made, an oscillograph was made of the contact time of the hammer and rod. Figure 11 illustrates the circuit used in determining the times of contact and with reference to this figure the procedure was as follows.

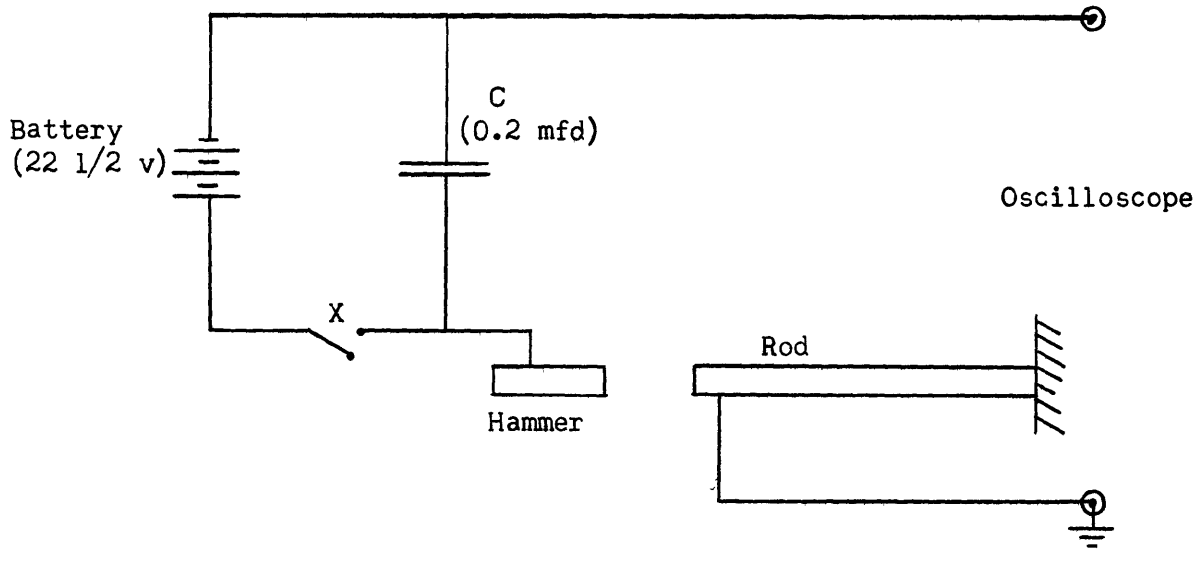

Figure 11. Circuit for Measuring Time of Contact

Condenser C was charged up by closing switch X. The shutter of the oscilloscope camera was opened and the hammer released. When the hammer and rod made contact a direct current signal equal to the charging voltage on the condenser tripped the oscilloscope and a single horizontal trace travelled across the screen until the hammer and rod separated. The trace then dropped to the zero base line and continued for the remainder of the single sweep. The capacity of the condenser was large enough to maintain discharge at nearly constant voltage during the time of impact. The trace was interrupted every 100 microseconds to provide a time scale so that the impact times could be determined. Contact traces are included in the oscillographs given in the following chapter.

Errors up to 10 percent in the measurement of strains and impact times were estimated as being possible because of the breadth of the oscilloscope traces and because the oscilloscope marking scale was not completely linear.

V. EXPERIMENTAL RESULTS

The experiments in the investigation of the effects of impact on rods of various materials were made to determine the strain at various sections of the rods as a function of the impacting kinetic energies of the hammers, the durations of impact and the Young's Moduli of the materials.

Interpretation of Oscillographs

The oscillographs obtained from the impact tests showed a voltage-time relationship which was obtained from the amplified signals of the strain gages. With the aid of the calibration signals included with each oscillograph and the strain gage equation as given in Chapter III any signal height on the traces could be converted to a strain value. The oscillographs were examined with an enlarger and a calibration graph of signal height in centimeters versus signal voltage in millivolts prepared. The voltage-time traces were then analyzed.

The most important measurement taken from each voltage-time oscillograph was the voltage value at the instant when the bar was considered to have absorbed the greatest amount of strain energy during its particular impact. The time of contact trace helped to determine the position on the oscillographs of this instant. The point of maximum strain energy absorption would be at, or very near, the instant when the impacting hammer had lost all its kinetic energy of translation. If the impact is assumed symmetrical then the point in time when the hammer was at a standstill would be one-half the time of impact. Examination of the oscillographs showed that strain peaks occurred either at the struck end or the fixed end of the bar at approximately half the contact times and so these peaks were used as time references for

measuring the impact strains at all the strain gage sections.

Measurements of the contact times were made by comparing the point of the trace where the initially elevated voltage trace dropped to the zero base line with the time markers which interrupted the trace.

From the large number of impacts on pyrex and steel rods the oscillographs shown in Figures 12, 13, 14, 15, 16 and 17 have been selected as typical examples of the voltage-time traces obtained. Since, as has been shown previously, the voltages produced by the strain gages are proportional to the strain and since no ordinate values are given on the above figures the voltage-time traces may be referred to as strain-time traces. The vertical dashed line in each of the figures indicates the time after the beginning of impact at which the strain values were measured. Traces marked 'X' show the time of contact of the hammers and rods and the traces marked 'Y' are portions of the calibration signals. The solid vertical line near the center of the traces indicates the end of impact. The gage sections on the specimens, from which the signals have been obtained, have been designated by two letters at the left of the figures which correspond to the gage positions as given in Figure 9.

All the traces show an initial period of loading of the rods during the impact and then a period after impact in which the rod is left in a state of vibration.

Determination of the Young's Moduli of the Materials

In order to calculate stress and strain energy values of the impact loaded rods several measurements were made of the Young's Moduli of the materials of which the rods were constructed. It has previously been shown (Equation 7) that the pressure wave velocity in solids is dependent only

on the Young's Modulus and the density of the solids. The fundamental period of oscillation of the rods would therefore be dependent only on these two characteristics and the dimensions of the rods. The Young's Modulus of the material composing a specific rod can be determined from the following equation.

$$E = \frac{4 l^2 \rho}{T^2 g} \qquad (32)$$

E = Young's Modulus

l = rod length

ρ = density

T = period of fundamental oscillation

g = acceleration of gravity

The period of oscillation, T, was determined by examining the free vibration portion of the strain-time traces obtained by impacting the rods. The time taken for eight complete oscillations of a rod was measured and an average period of fundamental oscillation calculated. Table 1 shows the results obtained and comparisons are given for generally accepted values listed in handbooks[10].

TABLE 1

Young's Moduli of the Materials Used in the Investigation

Material	Period of Oscillation T microseconds	Density ρ gms/cm^3	Rod Length l cm	Young's Moduli E gm/cm^2	
				Measured	Listed
Mild Steel	98.0	7.79	25.4	21.3×10^8	21.1×10^8
Pyrex Glass	93.7	2.31	25.4	6.93×10^8	6.5×10^8 to 7.75×10^8

Effect of Hammer Weight on Strain

(a) Pyrex rods

Strain versus time during impact: In Figures 12 and 13 the trace for Gage Section EF for the struck end of the rod shows two peaks during the time of impact. The occurrence of two peaks indicates that during the overall time of impact the rod received two separate blows, one following the other so rapidly that without sensitive methods of detection the impact would appear as one blow. The multiple blow effects were obtained when hammers weighing greater than 200 grams were used for the impacts on the pyrex rods. The corresponding trace for Gage Section EF in Figure 14, which was obtained from an impact with a hammer weighing about 200 grams, also shows the double blow effect. The second blow, however, is much less prominent than the initial blow. Figure 15 shows the corresponding trace obtained when the pyrex rods were impacted with a hammer weighing about 60 grams. In this case the impact consists of a single blow of short duration.

In Figure 12 the trace for Gage Section AB indicates the strain conditions near the fixed end of the bar. In this trace a single strain peak occurs considerably after the beginning of impact. The peak height shows that the strain (or stress) at the fixed end of the rod is much larger than in any other section of the rod during the impact. At the same instant when the strain reaches a maximum at the fixed end the strains at successive Gage Sections in the direction of the struck end become progressively smaller until at the struck end the strain is very nearly zero. In Figures 13 and 14 the same effect of a strain peak at the fixed end is evident. However, in Figure 15 the maximum strain occurs at the struck end of the bar.

Reference to the strain-time figures show that when two strain peaks

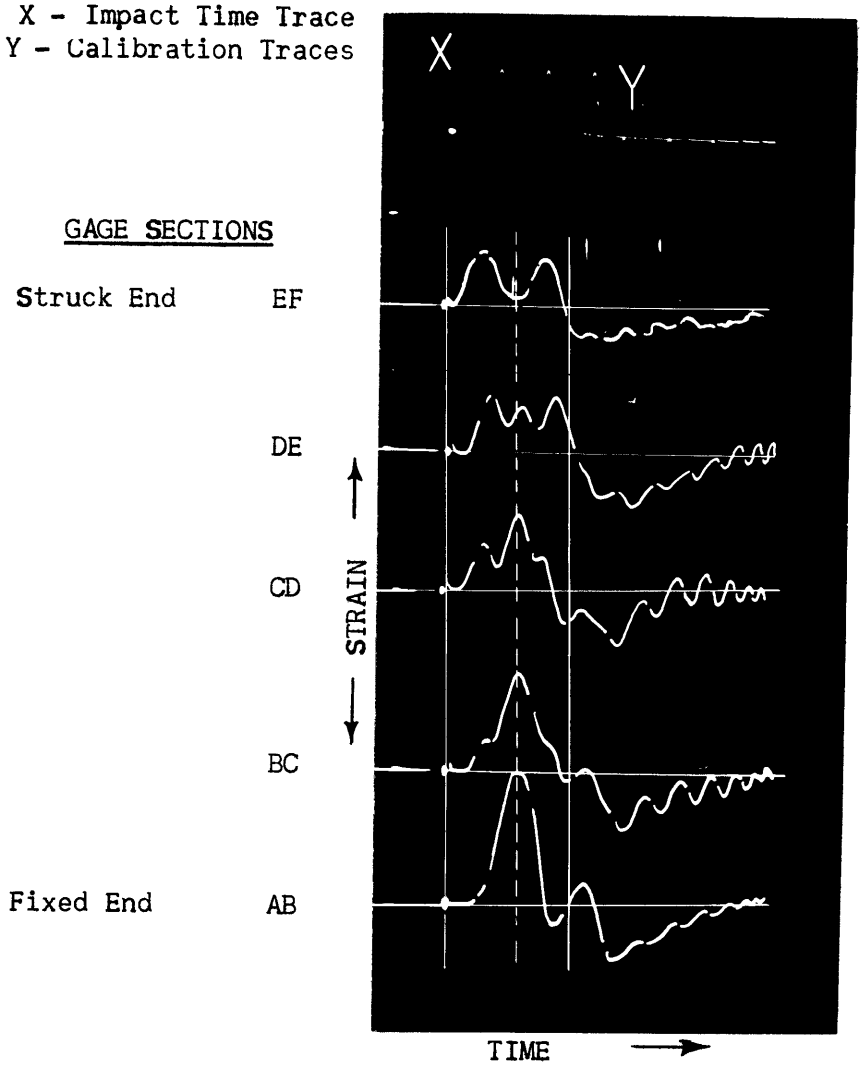

Figure 12. Strain-Time Traces For Impacts on a Pyrex Rod with a 593 gram Hammer

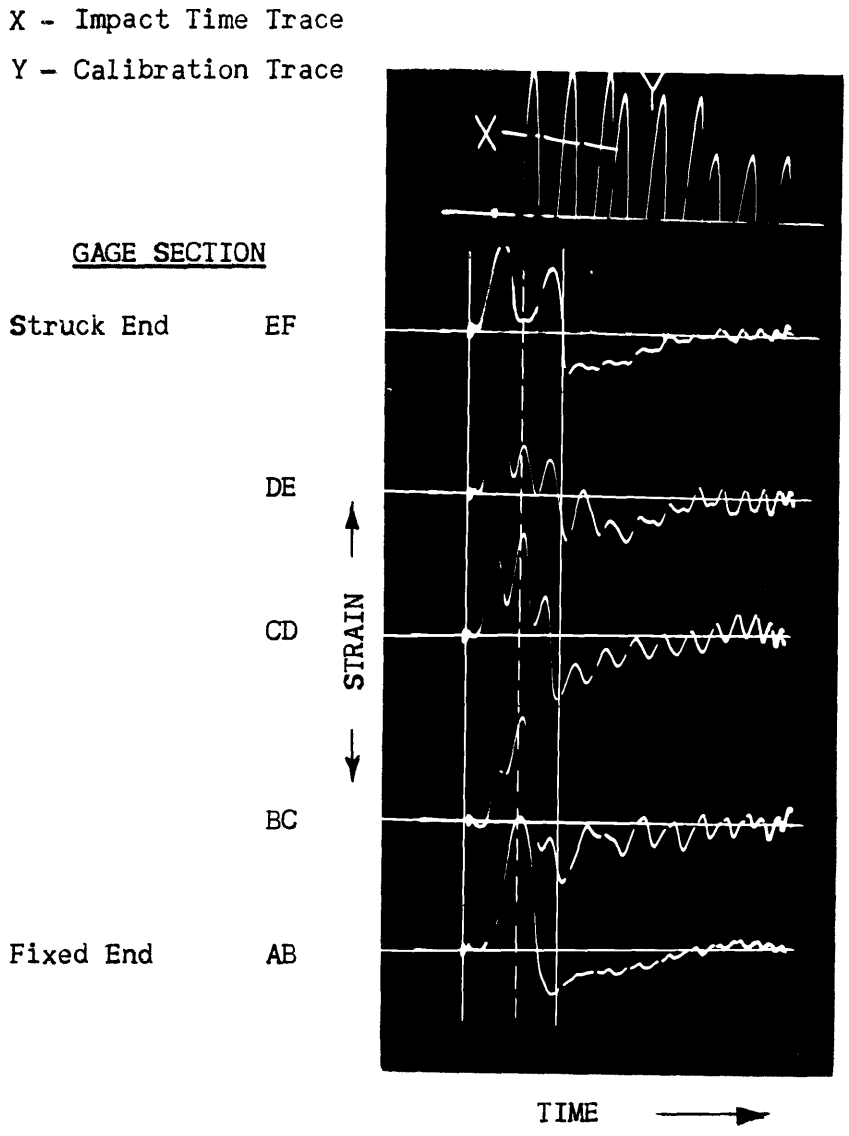

Figure 13. Strain-Time Traces for Impacts on a Pyrex Rod with a 393 gram Hammer

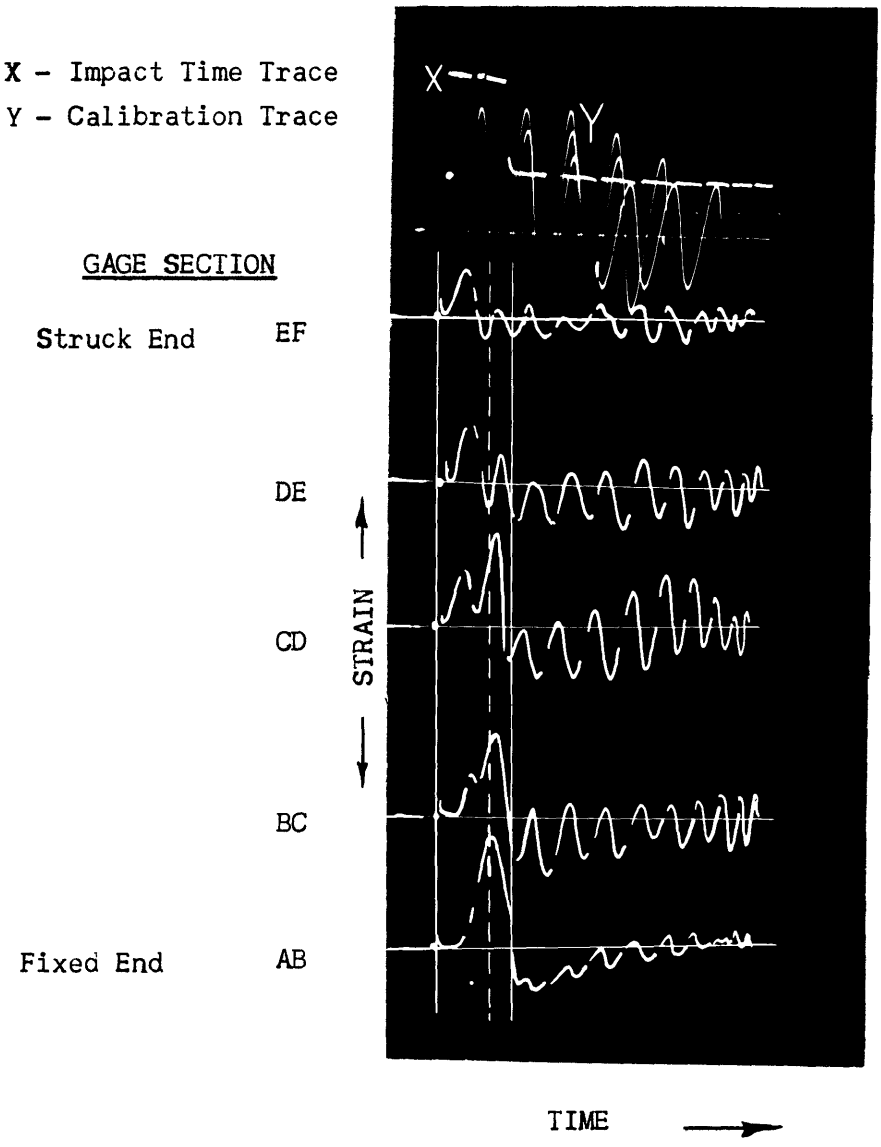

Figure 14. Strain-Time Traces for Impacts on a Pyrex Rod with a 199 gram Hammer

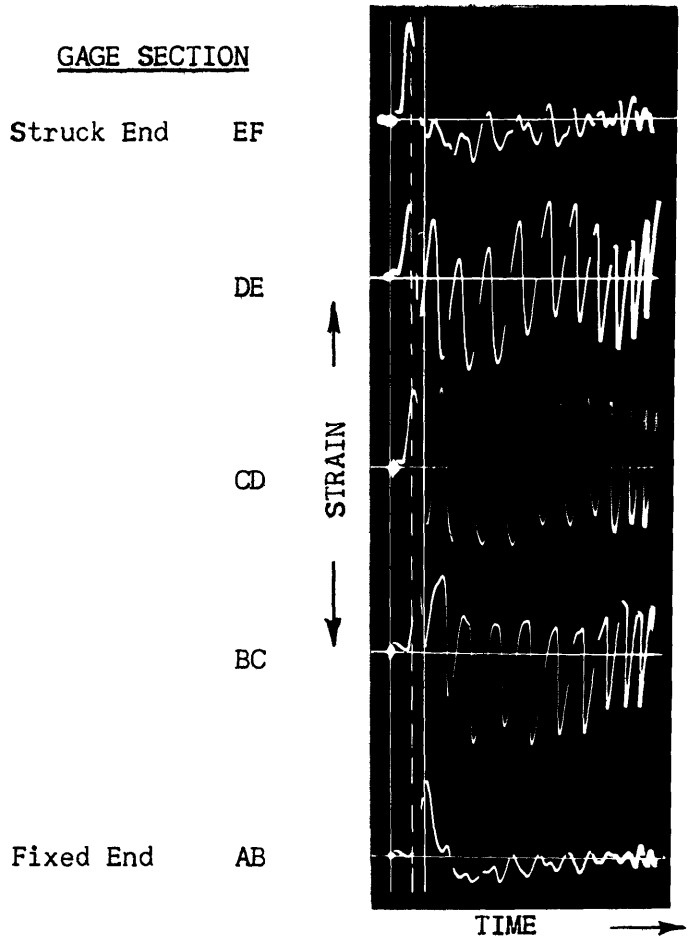

Figure 15. Strain-Time Traces for Impacts on a Pyrex Rod with a 59.3 gram Hammer

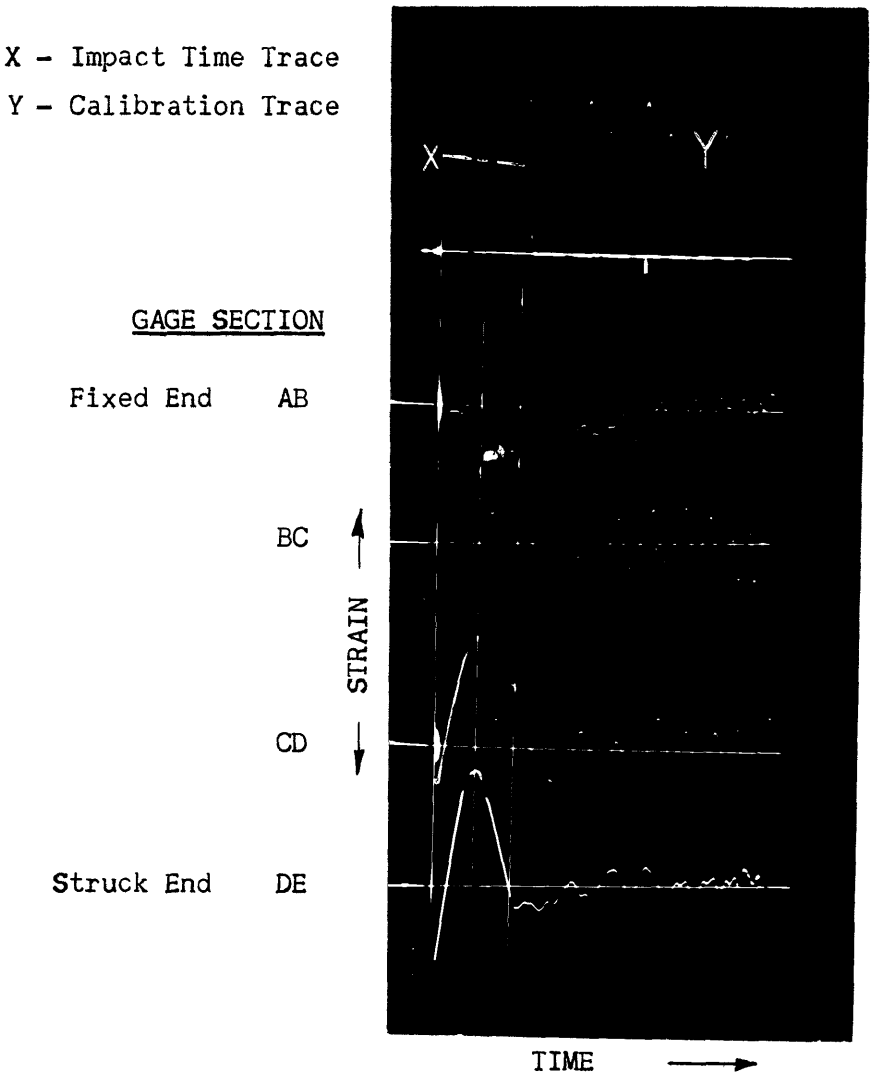

Figure 16. Strain-Time for Impacts on a Mild Steel Rod with a 593 gram Hammer

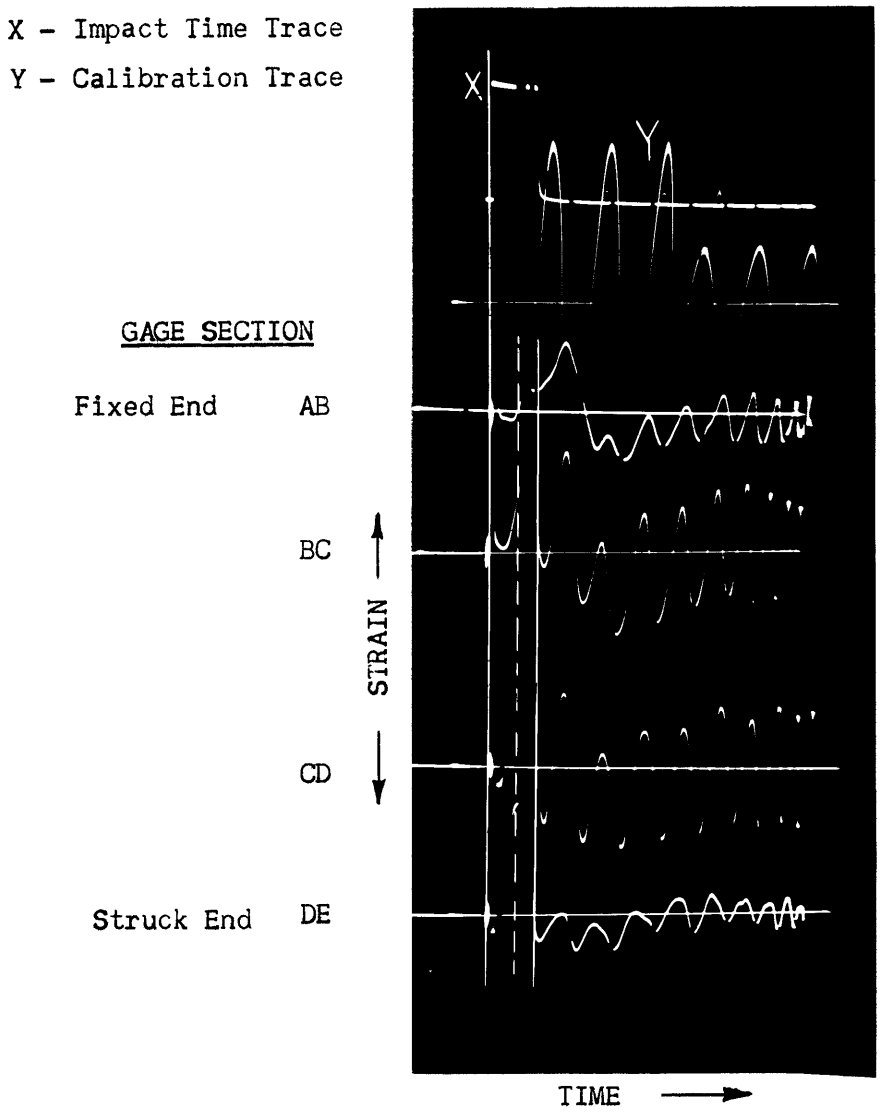

Figure 17. Strain-Time for Impacts on a Mild Steel Rod with a 199 gram Hammer

are present in the loading pulse the maximum strain is developed at the fixed end of the rod. The maximum strain at this point occurs at approximately half the time of impact as can be seen by comparing the time of contact trace with the trace from Gage Section AB. The point of minimum strain, at this time, occurs at the struck end of the rod and falls between the two peaks of the loading pulse. The minimum strain at the struck end during contact was usually only slightly greater than zero and thus it was concluded that the impacting hammer was at rest and exerted only a small force on the rod at this time. The impacting hammer, being at rest, would have lost all its kinetic energy and therefore the strain measurements for determining strain energy absorption in the rod were made at this time. When the trace for the struck end falls to zero after the second peak the impact ends since the hammer rebounds and the struck end of the rod becomes a free end on which no stress is possible. Thus by examination of the trace from the struck end an indirect measurement of the time of contact can be made and this time can be compared to that arrived at by direct measurement.

When a single strain peak is present in the loading pulse the maximum strain is developed at the struck end (Figure 15). Again, when the trace for the struck end returns to zero the impact ends. At approximately one-half the time of impact the force on the struck end of the rod reaches a maximum and thus it was concluded that the hammer had come to rest at this point. The strain measurements for the calculation of absorbed strain energy during single pulse impacts were therefore made at this time.

Strain versus time after impact: An interesting effect can be observed in the strain-time records in regard to the amplitude of vibration of the rods after the impact has been completed. When the hammer rebounds after impact, the rod continues to oscillate and, since both ends of the

rod are now free, the oscillation is essentially a harmonic vibration at the fundamental frequency of the rod. Under longitudinal harmonic oscillation all points of the rod pass through their equilibrium positions at the same instant and thus the signals from the various strain gages are in phase. The greatest strain is developed at the center of the rod and if the amplitudes of these strain signals (Gages CD) are compared, it is noted that in the case of short impact times, the maximum amplitudes during free vibration are almost equal to the maximum peak amplitude during impact; whereas, in the case of long impact times with heavy hammers the maximum amplitude during free vibration is much less than that during the impact. It appears that the heavy hammers, in rebounding, extract a much greater proportion of the strain energy and kinetic energy of vibration from the rods than do the light hammers where the impact times are relatively short. No experimental measurements were made of rebound velocities in this investigation since the conditions of the impact system after the completion of impact are only of passing interest and lend no information as to the conditions of impact during the impact time.

(b) Mild Steel Rods

Figures 16 and 17 are oscillographs showing the strain-time relationships observed for impacts on the ten inch mild steel bar. As in the previous oscillographs the traces marked X are time of contact traces and the traces marked Y are calibration signals.

Strain versus time during impact: In contrast to the strain-time oscillographs obtained from impacting the pyrex rods, the strain-time traces for the struck end of the steel bar showed only a single blow even with the heaviest impacting hammer (600 grams). The point in time

for the measurement of the maximum strain energy absorbed was therefore the time when the impact loading pulse, as shown by Gage Section DE, reached a maximum. The strain, at this time, was a maximum at the struck end and decreased in intensity at successive gage positions towards the fixed end of the rod until at the fixed end the strain was nearly zero. Shortly after the impact was completed the state of strain of the rod reversed, the fixed end reached a maximum strain and at this time the strain at successive gage sections towards the struck end decreased in intensity.

Strain versus time after impact: As in the case of impacts on the pyrex glass rods the impacts on the steel rod show that the maximum peak amplitude during free vibration is almost equal to the maximum peak amplitude during impact for short impact times. For relatively long impact times with heavy hammers the maximum amplitude during free vibration is much less than that during the impact.

Effect of Hammer Weight on Time of Impact

Figures 18 and 19 show the experimental relationship obtained between the measured contact times of the hammers and rods and the weight of the hammers used in the impacts. Each of the solid vertical lines in these figures indicates the variation of the measured values for the impact times of any single hammer weight. Since the relative variation of the measured values of impact times increased with hammer weight the data is presented as varying over ranges rather than as single points representing averages of the experimental measurements.

Some of the experimental data from which the above figures were prepared (Table 1, Appendix II) indicates that the kinetic energy of impact may be a factor in determining the impact time for any single impact. The

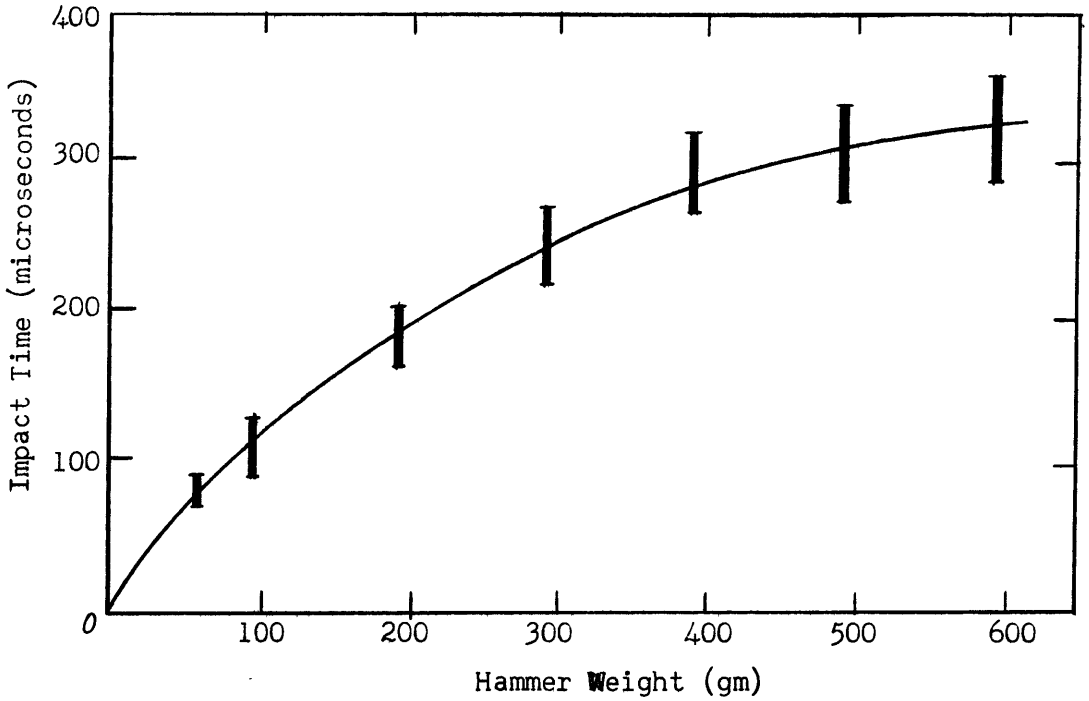

Figure 18. Impact Time Versus Hammer Weight for Impacts on a 10 inch by 1 inch Pyrex Glass Rod

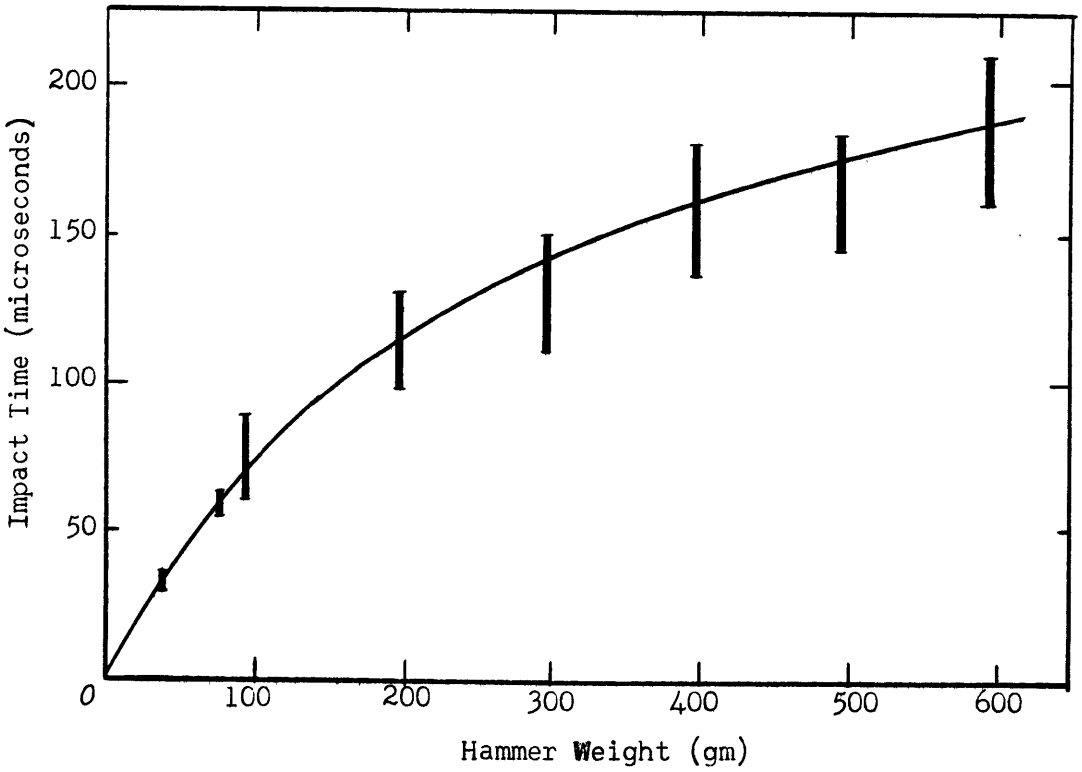

Figure 19. Impact Time Versus Hammer Weight for Impacts on a 10 inch by 1 inch Mild Steel Rod

relatively large errors inherent in the method of measuring impact times, however, prevented a quantitative determination of this effect. Continuous curves, therefore, have been drawn through the vertical lines in the above figures to represent average impact time versus hammer weight.

Strain as a Function of Kinetic Energy of Impact at Constant Hammer Weight

The main object of this investigation was to obtain experimental data which would provide a means of calculating the maximum amount of strain energy absorbed by the rods during impact for any specific impact. In order to calculate strain energy values the variation of strain with position along the rods must be determined as a function of the kinetic energy of impact. The impact tests with any specific hammer weight showed that at the instant when the rod had absorbed a maximum amount of strain energy the strains at any of the bar sections were proportional to the square root of the impacting energy.

Figures 20 and 21, in which strains at various rod sections are plotted against the square roots of the kinetic energies of impact, show the above linear relationship for impacts of hammers weighing 593 and 59.3 grams on the pyrex rods. The above graphs have been selected as representative of the results with two of the hammers used in the investigation on pyrex rods and the remainder of the graphs for the other hammer weights are given as Figures 1 to 8 in Appendix II. In all the above figures a linear relationship between strain at any gage section of the rod and the square root of the impacting energy is shown.

Figures 22 and 23 are representative graphs showing strain as a function of kinetic energy of impact for the case of the steel rods. The hammers used in the impacts from which the above figures were derived were again those weighing 593 and 59.3 grams. The remainder of the graphs for other hammer weights impacting steel rods are given in Appendix II as Figures 9 to 16 inclusive.

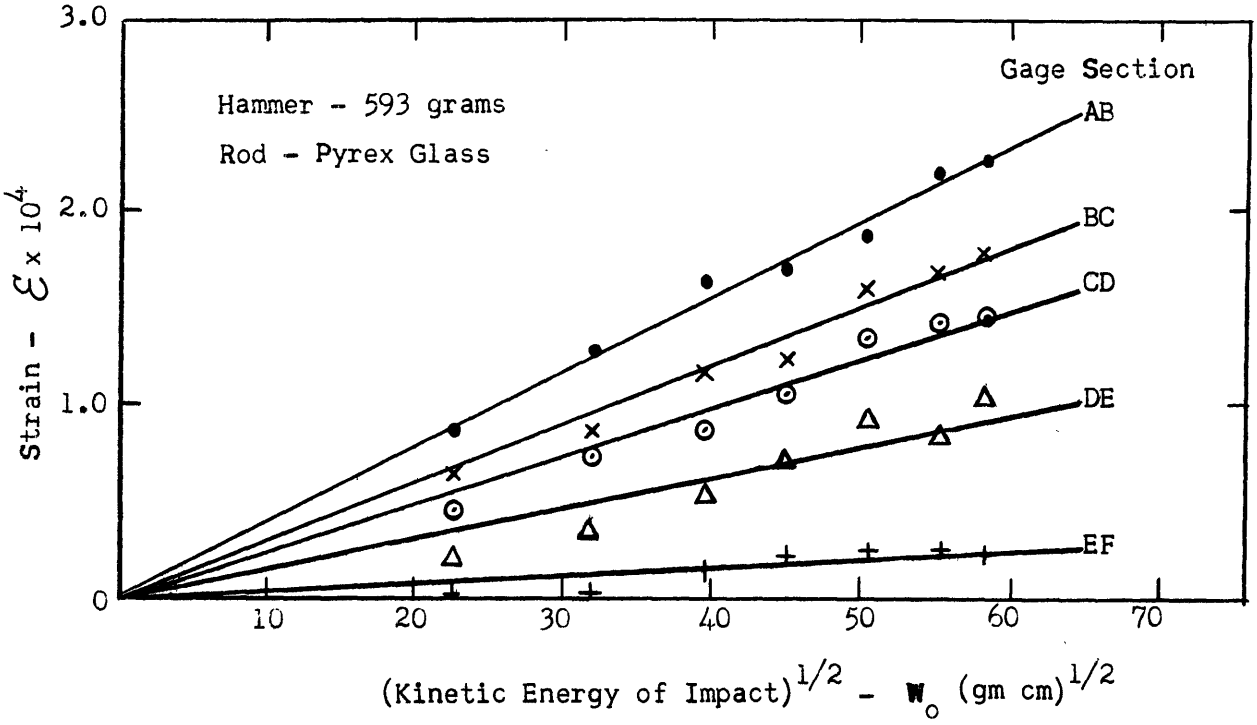

Figure 20. Strain Versus Square Root of the Kinetic Energy of Impact

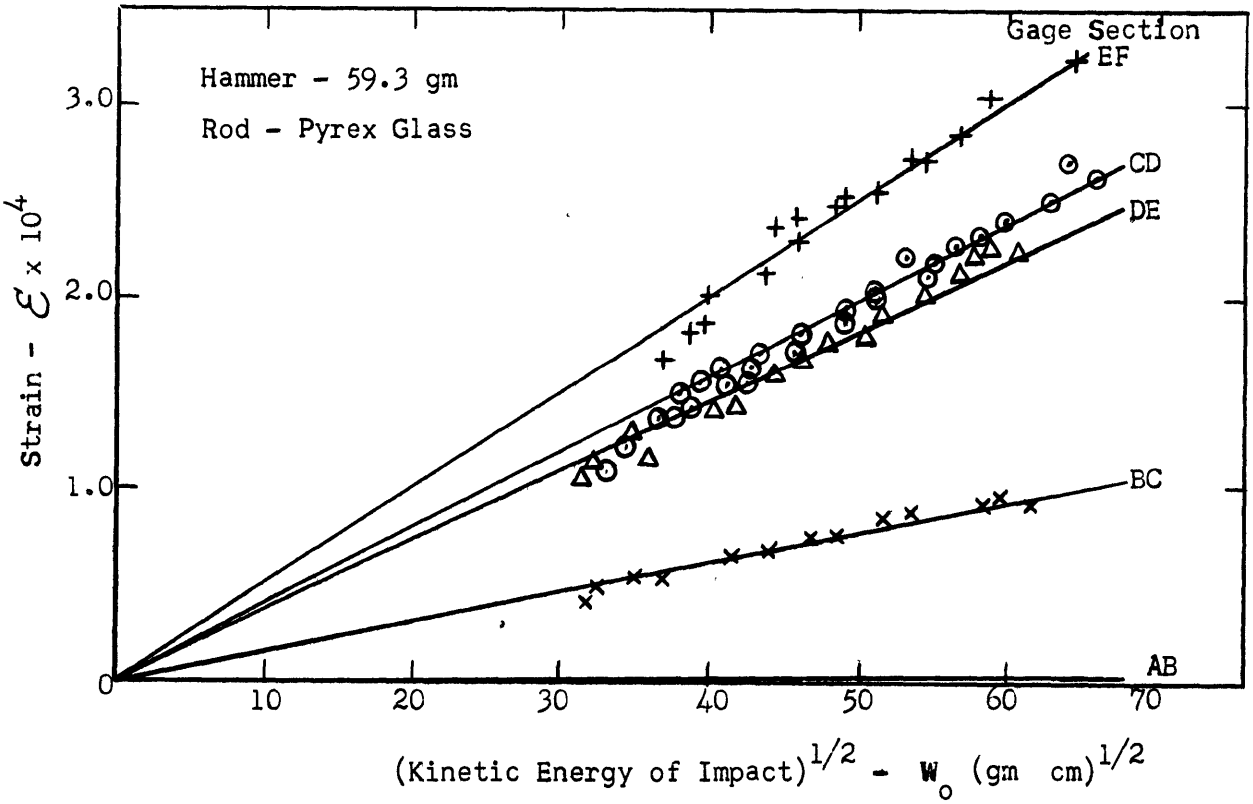

Figure 21. Strain Versus Square Root of the Kinetic Energy of Impact

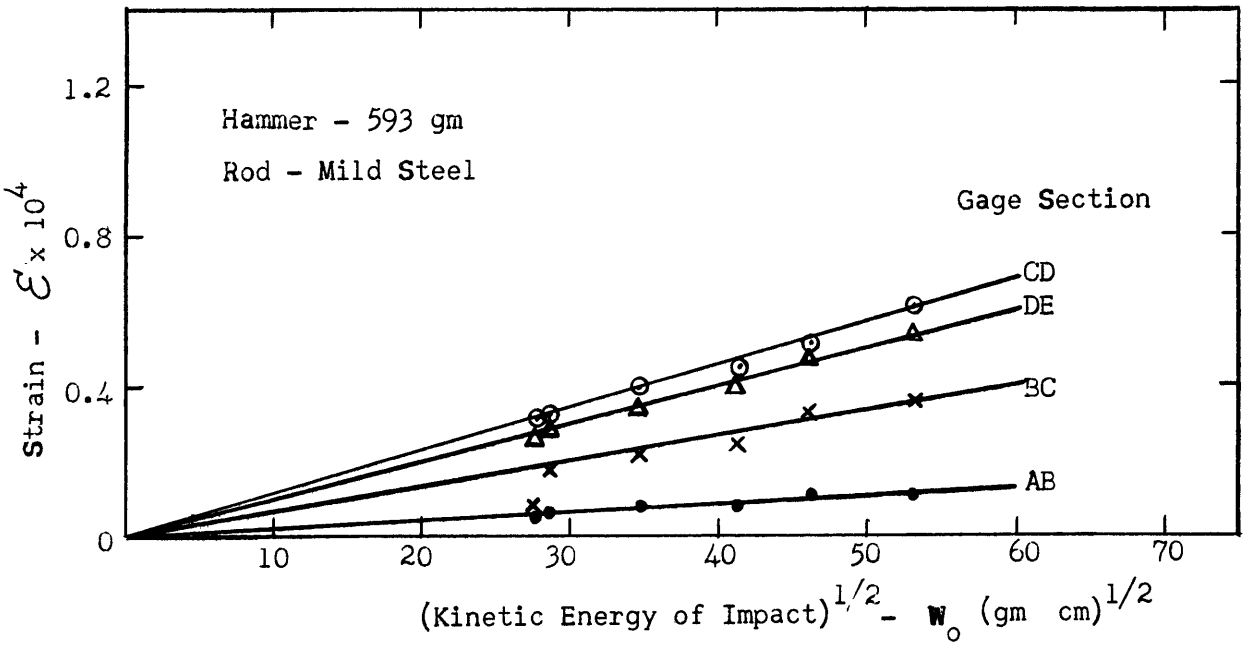

Figure 22. Strain Versus Square Root of the Kinetic Energy of Impact

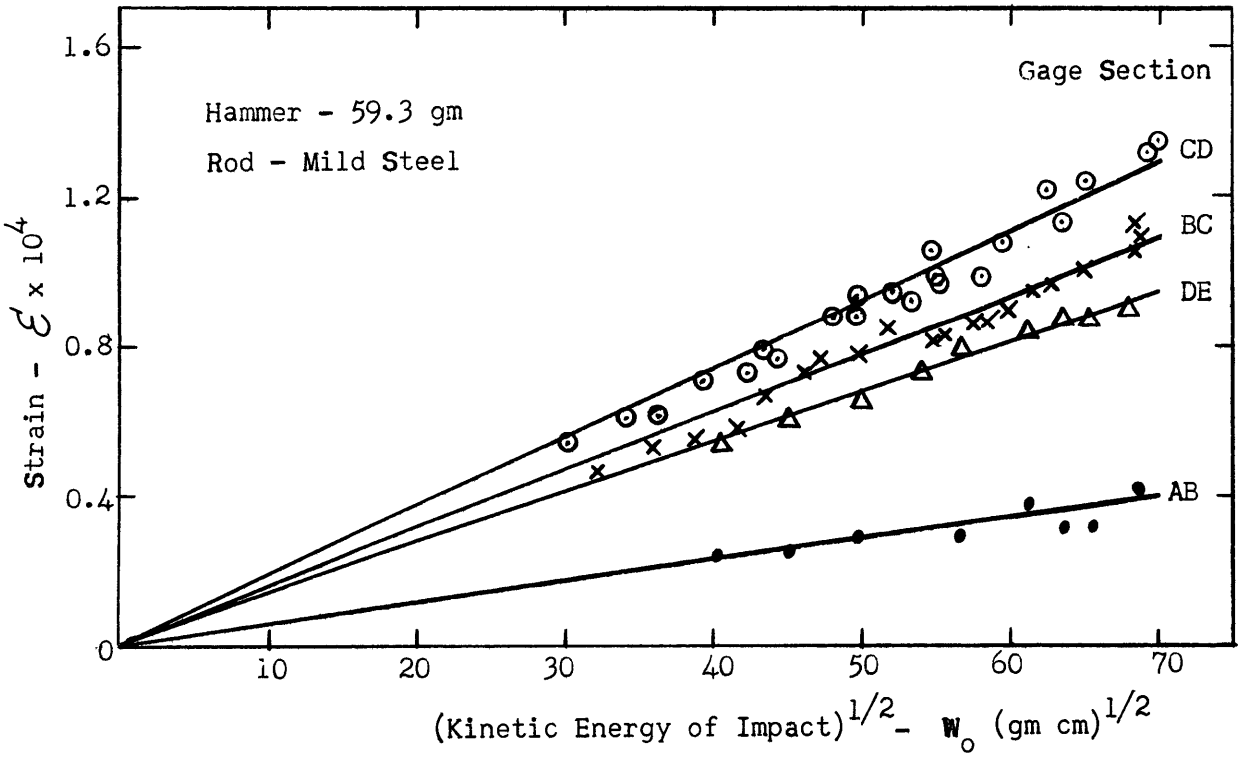

Figure 23. Strain Versus Square Root of the Kinetic Energy of Impact

VI. DISCUSSION OF EXPERIMENTAL RESULTS

The experimental results from this investigation provide data for the analysis of the loading forces which are derived from impact on the glass and steel rods and for the calculation of the maximum amounts of energy which are transformed from kinetic energy of impact to strain energy of the rods during impact. The data are also used to illustrate the effect of the mass of the impacting weight and the time of impact on the energy transfer process during impact.

A. The Analysis of the Impact Loading Forces

The stress and energy conditions arising from longitudinal impact of a solid rod have been shown, in Chapter II, to be greatly dependent on the character of the force that is built up at the point of contact of the colliding objects. This force will be referred to as the contact force. The experimental results from these investigations show that for the impacts considered two main types of contact force-time relationships occur. The simplest of these relationships consists of a single pulse of variable duration (Gage Section EF, Figure 15, Chapter V). The other force-time relationship is more complex and consists of two separate and symmetrical pulses which are separated by a short interval of time during which the contact force is almost zero (Gage Section EF, Figure 12, Chapter V).

Solutions of the general impact equation (Equation 29) for specific cases of impact show that single and multiple loading pulses should be expected as a result of the forced vibration of the rod during the time of contact of the impacting object and the rod.

By a process of stepwise numerical integration the general impact

equation has been solved to obtain the contact force as a function of time for two cases of impact. The method of solution is given in Appendix III. The results of these calculations are compared with experimental contact force-time curves as shown in Figures 24 and 25.

Curves A and B, Figure 24, illustrate the experimental and calculated contact force as a function of time for the impact of a 393 gram hammer on the steel rod at a velocity of 127 centimeters per second. In this case, a loading pulse with a single peak results. Curves A and B, Figure 25, illustrate the experimental and calculated contact force as a function of time for the impact of a 593 gram hammer on the glass rod at a velocity of 120 centimeters per second. In this case the loading pulse consists of two well defined peaks.

In both of the above figures the theoretical values of contact force are higher than those observed experimentally. This discrepancy is probably due to the fact that the impact equation is based on the assumption that the contacting surfaces are perfectly smooth and spherical. Such conditions are difficult to obtain experimentally and consequently some impacting energy may be absorbed in flattening local irregularities. Therefore the actual forces built up would be less than those expected from theory.

In the following section of this chapter it is shown that when double peaks are observed in the contact force-time relation the amount of impact energy transferred to strain energy is less than when the loading pulse consists of a single peak. Multiplicity of peaks in the loading pulses may have a direct influence on the energy transfer. However, it is impossible to analyze the experimental data for the effect of pulse shape alone since the pulse shape is determined from the conditions of impact and cannot be considered as an independent variable in experimentation.

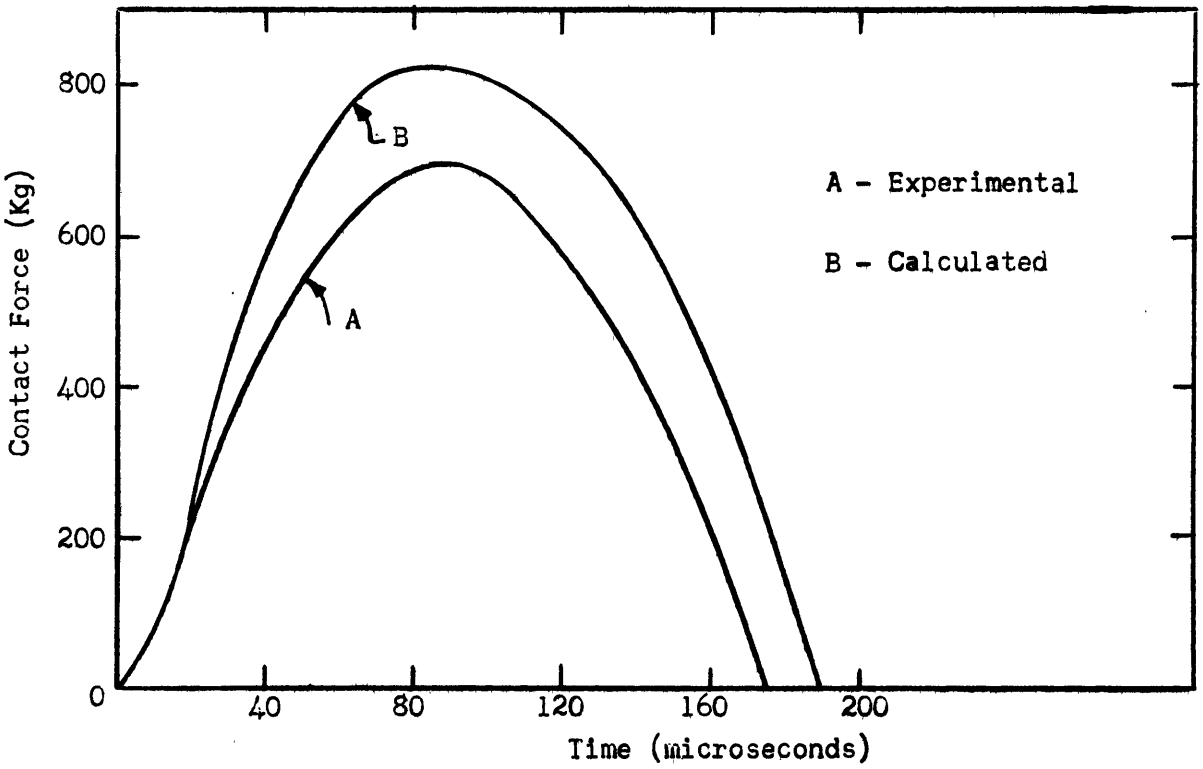

Figure 24. Contact Force Versus Time for Impacts on 10 inch Steel Rod With 493 gram Hammer

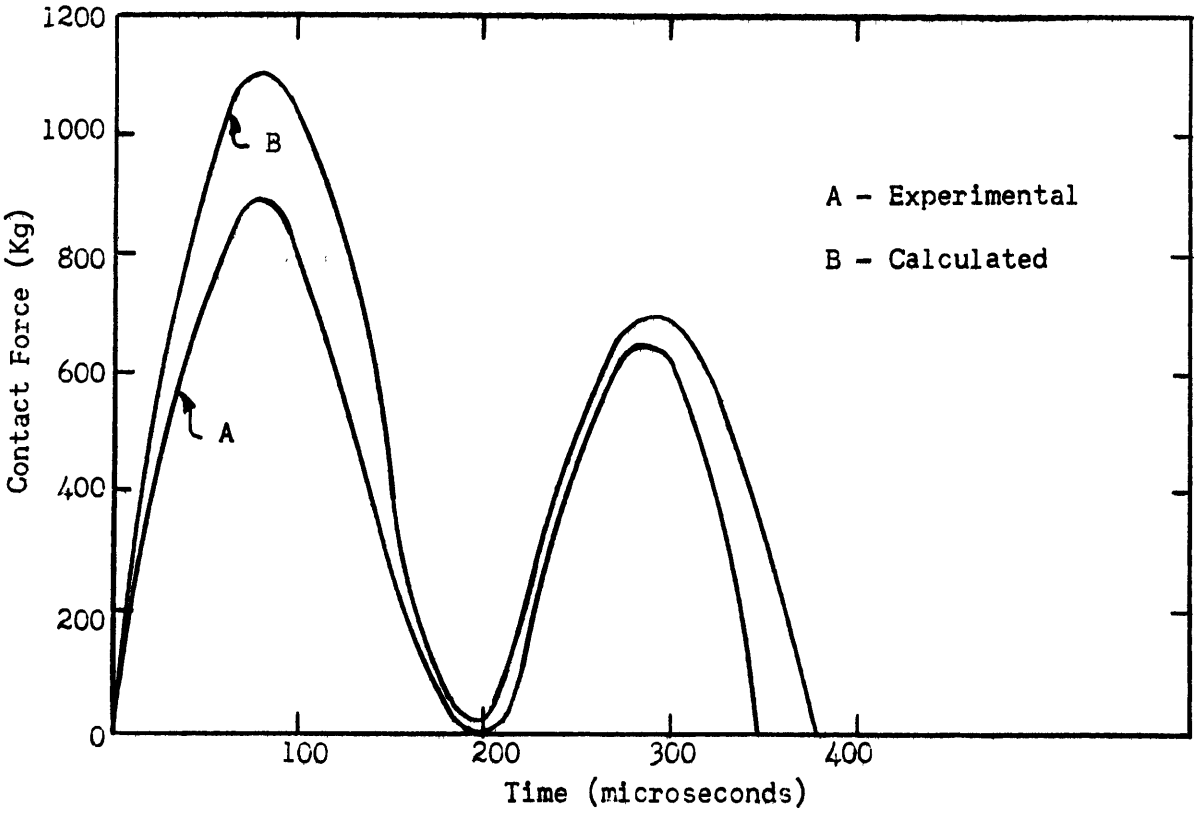

Figure 25. Contact Force Versus Time for Impacts on 10 inch Pyrex Glass Rod With 593 gram Hammer

B. Determination of Transfer of Kinetic Energy of Impact to Strain Energy

When rods of various materials are supported with a fixed end and subjected to longitudinal impact the distribution of energy during the impact is generally very complex; but the forms into which the original kinetic energy of impact changes are relatively simple and provide a means of understanding how the energy transfer process takes place. At a moment just prior to impact all the energy of the system is composed of kinetic energy of translation of the hammer. During impact part of this energy changes into strain energy of the rod and the hammer and another portion changes to kinetic energy of vibration in the rod and hammer. If the fixed end of the rod is perfectly rigid no vibrational or strain energy will be imparted to the rod support. In practice no support can be made perfectly rigid and energy leaves the rod and hammer system as vibrational, strain,or kinetic energy of translation of the support. While the impact is in progress another portion of energy is being lost in the form of heat that is generated due to the damping action of the materials through which the stress waves are travelling. This loss is generally small and is usually neglected in analyzing impact effects.

If the rod support is considered rigid, then when the hammer is decelerated to zero velocity all its original energy of translation has been changed to other forms and the strain or potential energy of the hammer and rod system is a maximum. As the impact continues the strain and vibrational energy of the system is partially reconverted to kinetic energy of translation of the hammer and rebound occurs.

The only form of energy which is directly usable in a comminuting or fracturing process is the strain energy that has been momentarily stored

in the rod and the hammer. The experimental data of this investigation permit the calculation of the maximum amount of strain energy absorbed by the rod expressed as a fraction of the total kinetic energy of impact. The calculations are carried out as follows.

If a prismatic bar is under a state of strain such that the strain at any cross-section is uniform but the strains at various cross-sections along the length of the bar are variable then the total strain energy of the bar may be calculated as follows,

Let w_s = strain energy density (strain energy per unit length of rod)

l = length of rod

W_s = total strain energy of the rod

then

$$W_s = \int_o^l w_s dl \tag{33}$$

The strain energy density at any section is related to the strain at that section by the following equation,

$$w_s = AE\mathcal{E}^2/2 \tag{34}$$

where A = cross-sectional area of the rod

E = Young's Modulus of the rod material

$\mathcal{E}$ = strain

therefore

$$W_s = (AE/2)\int_o^l \mathcal{E}^2 dl \tag{35}$$

In the case where the strain conditions in the rod are brought about by longitudinal impact the amount of strain energy in the rod at any time may be expressed as a fraction of the kinetic energy of impact. Thus, if the kinetic energy of impact is W_o then,

$$W_s/W_o = (AE/2)\int_o^1 (\mathcal{E}^2/W_o)dl \qquad (36)$$

Figures 20 to 23 in the preceding chapter and Figures 1 to 16 in Appendix II show a linear relationship between the square root of the kinetic energy of impact and the strain produced at any gage section if the impacts on the steel and glass rods are made with a specific hammer weight and if the strains are measured when the amount of strain energy absorbed is a maximum. Therefore, the ratio $(\mathcal{E}\ \text{max})/\sqrt{W_o}$ is constant for impacts with any single hammer. The ratio $W_s\text{max}/W_o$, which represents a linear function of the summation of all the values of the term $(\mathcal{E}\ \text{max})^2/W_o$ along the length of the rod must also be a constant for impacts with any single hammer. The quantity, $(\mathcal{E}\ \text{max})^2/W_o$, is a measure of the fraction of kinetic energy of impact which is transformed to strain energy in the gage section considered when the amount of strain energy absorbed by the complete bar is a maximum; it may be evaluated by squaring the value for the slope of any of the straight lines in the above mentioned figures.

If the values of $(\mathcal{E}\ \text{max})^2/W_o$, for impacts with any single hammer, are plotted versus gage position on the impacted rods a smooth curve may be drawn through the points and the graph thus obtained shows the distribution of strain energy in the rod as a function of impact energy for the instant when the strain energy is a maximum.

A value for $W_s\text{max}/W_o$ can now be calculated by graphically integrating the area under the strain distribution curve and multiplying the result by the factor AE/2 as indicated by Equation 36. The ratio $W_s\text{max}/W_o$ will be referred to as a Strain Energy Absorption Coefficient. Such a coefficient

expresses the maximum fraction of kinetic energy of impact transferred to strain energy for impacts with any single hammer.

Figures 26 to 29 show the strain energy distributions in pyrex and mild steel rods for impacts with the 593 and 59.3 gram hammers. The strain energy distributions obtained with other hammers used in the investigation are given as Figures 1 to 16 in Appendix III. Table 2 lists the calculated values of the Strain Energy Absorption Coefficients as determined from the strain energy distribution graphs. Examination of these coefficients shows that a maximum value is reached for both the mild steel and pyrex rods and that no value of these coefficients exceeds 0.502.

TABLE 2

Strain Energy Absorption Coefficients

Hammer Weight Grams	Strain Energy Absorption Coefficients $W_s(max)/W_o$	
	Pyrex Rod	Mild Steel Rod
593	0.299	0.105
493	0.282	0.115
393	0.238	0.139
296	0.266	0.162
199	0.328	0.180
93.0	0.376	0.235
78.1	0.462	0.258
59.3	0.502	0.310
39.5	0.449	0.263
19.7	0.425	0.216

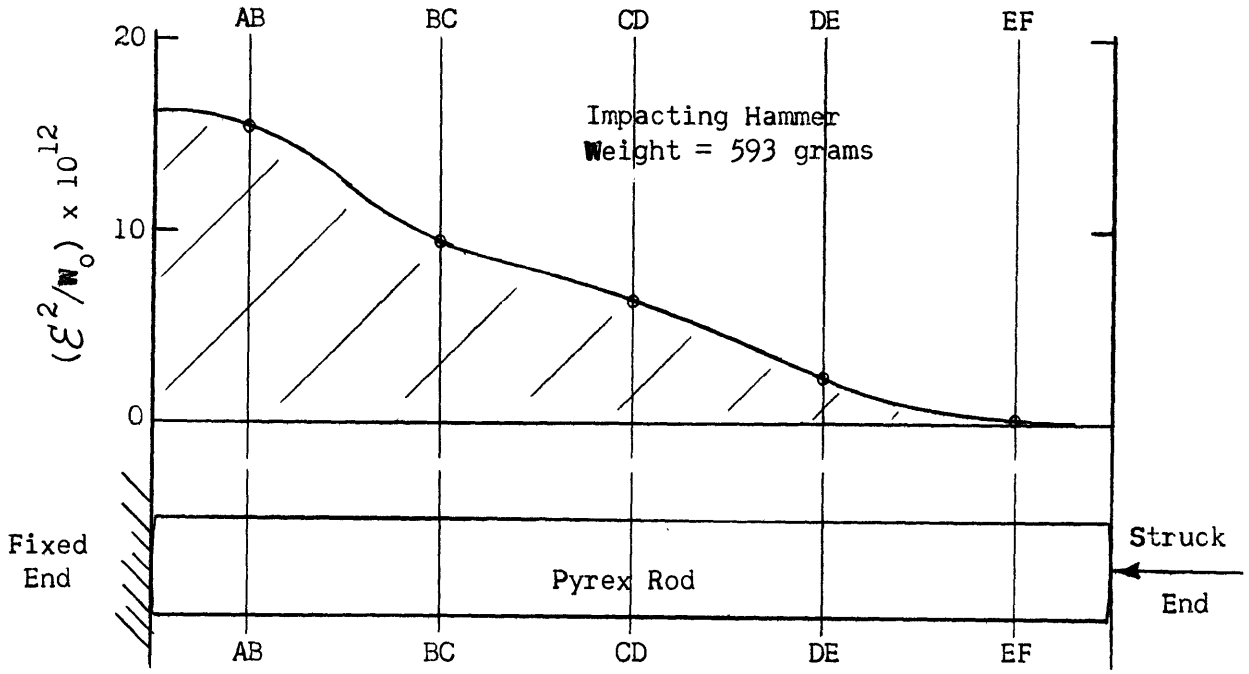

Figure 26. Distribution of Strain Energy in Impacted Pyrex Rod as a Function of Kinetic Energy of Impact

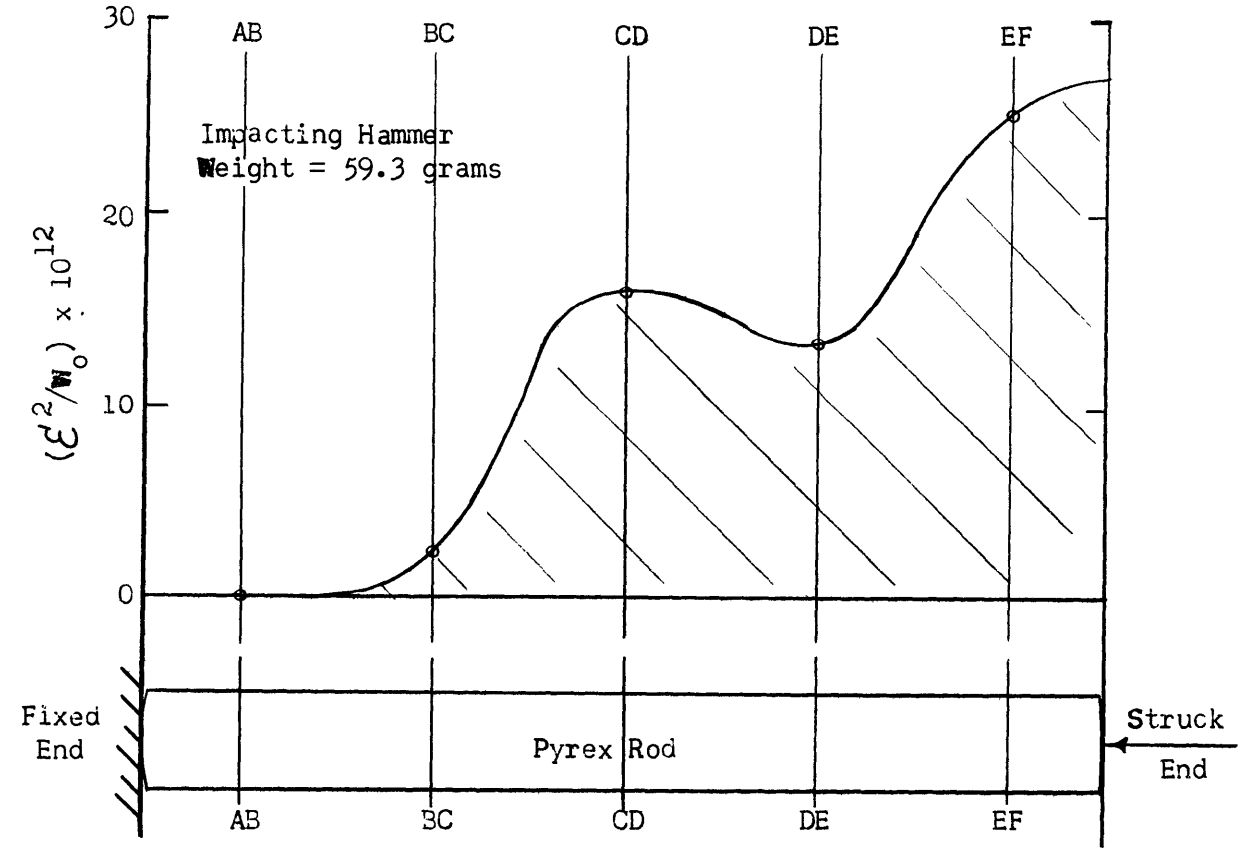

Figure 27. Distribution of Strain Energy in Impacted Pyrex Rod as a Function of Kinetic Energy of Impact

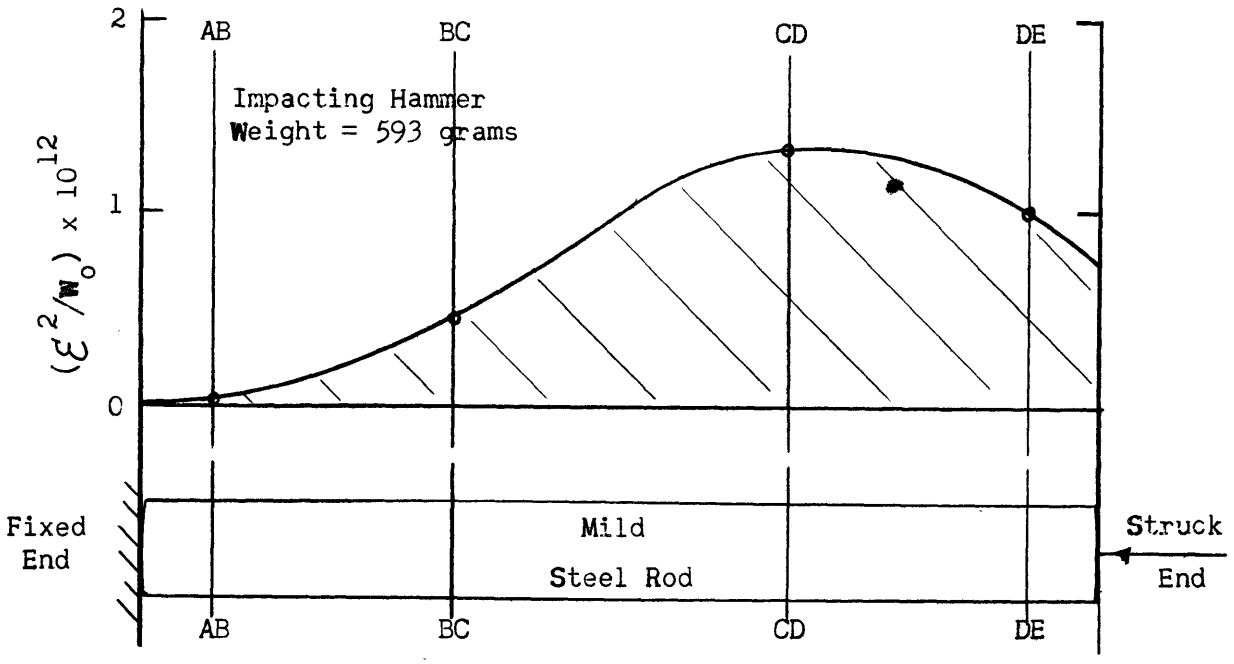

Figure 28. Distribution of Strain Energy in Impacted Mild Steel Rod as a Function of Kinetic Energy of Impact

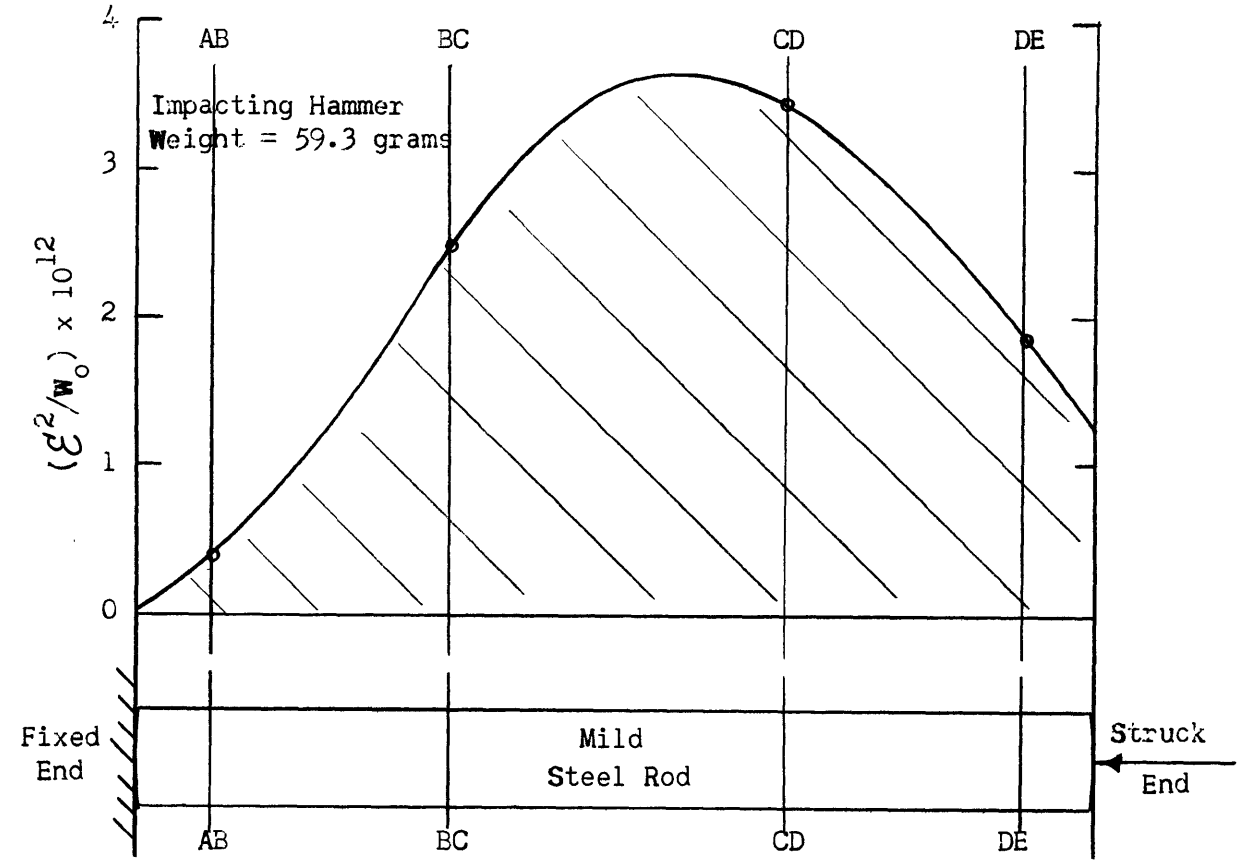

Figure 29. Distribution of Strain Energy in Impacted Mild Steel Rod as a Function of Kinetic Energy of Impact

C. Conditions That Influence Impact Times

The experimental results of impacts on pyrex and mild steel bars, given in Chapter V, show that the time of impact is primarily dependent on the mass of the impacting hammer and perhaps slightly dependent on the kinetic energy of impact. The Herzian theory of impact of spheres[6], which may be applied to impact of rods with rounded ends, shows that the time of impact should be influenced primarily by the radii of contact and the masses of the objects. It also shows that the time of impact should vary inversely as the one-tenth power of the kinetic energy of impact. Therefore, although the impact time is slightly dependent on the kinetic energy of impact the effect is almost negligible and the graphs in Figures 18 and 19, which show time of impact as a function of the mass of the impacting hammer only, may be assumed correct for the correlation of impact time and absorbed strain energy.

D. Correlation of Impact Time and Strain Energy Absorbed

(a). Experimental

The experimental work of this investigation of impacts on pyrex and mild steel rods furnished information for the calculation of strain energy absorption coefficients as a function of the impacting hammer weight. Times of impact were also measured as a function of impacting hammer weight and therefore a relationship between the strain energy absorption coefficients and the times of impact can easily be obtained.

The curves marked A in Figures 30 and 31 show the variation of strain energy absorption coefficients with the ratios of impact time to oscillation period for the cases of impact on the pyrex glass and mild steel rods. In these figures the peaks show that there exists a time of impact of the rods

for which the transfer of impact energy to strain energy is a maximum. The maximum amounts of strain energy obtained within the glass and steel rods are respectively 0.5 and 0.3 times the kinetic energy of impact and are obtained from loading pulses lasting, respectively 75 and 50 microseconds. Examination of the strain-time traces shows that these particular loading pulses consisted of single blows. Therefore, the main conclusion from the experimental work of this investigation is that a maximum transfer of kinetic energy of impact to strain energy is obtained when the impact time is a fractional part of the period of vibration of the impacted object and when the loading pulse consists of a single blow. It may further be concluded that the time of impact and the character of the loading pulse are important factors if fracture of an object or failure of a structure is to be predicted.

The relative values for the strain energy absorption coefficients for the pyrex glass and mild steel rods indicate that the transfer of kinetic energy of impact to strain energy for similar conditions of impact is lower for the case of mild steel. Two possible explanations may be given for this fact. Firstly, if significant amounts of plastic deformation occurred at the points of contact of the steel rod and hammers then appreciable amounts of energy may be lost in this form. However, since the effects of plastic deformation should be proportionally greater for the more severe impacts then no linear relationship between strain at any gage section and the square root of the impact energy would be obtained as in Figures 22 and 23. If plastic deformation was an important consideration then the lines in the above figures would tend to flatten off. The trend, however, of the experimental points through which the straight lines have been drawn

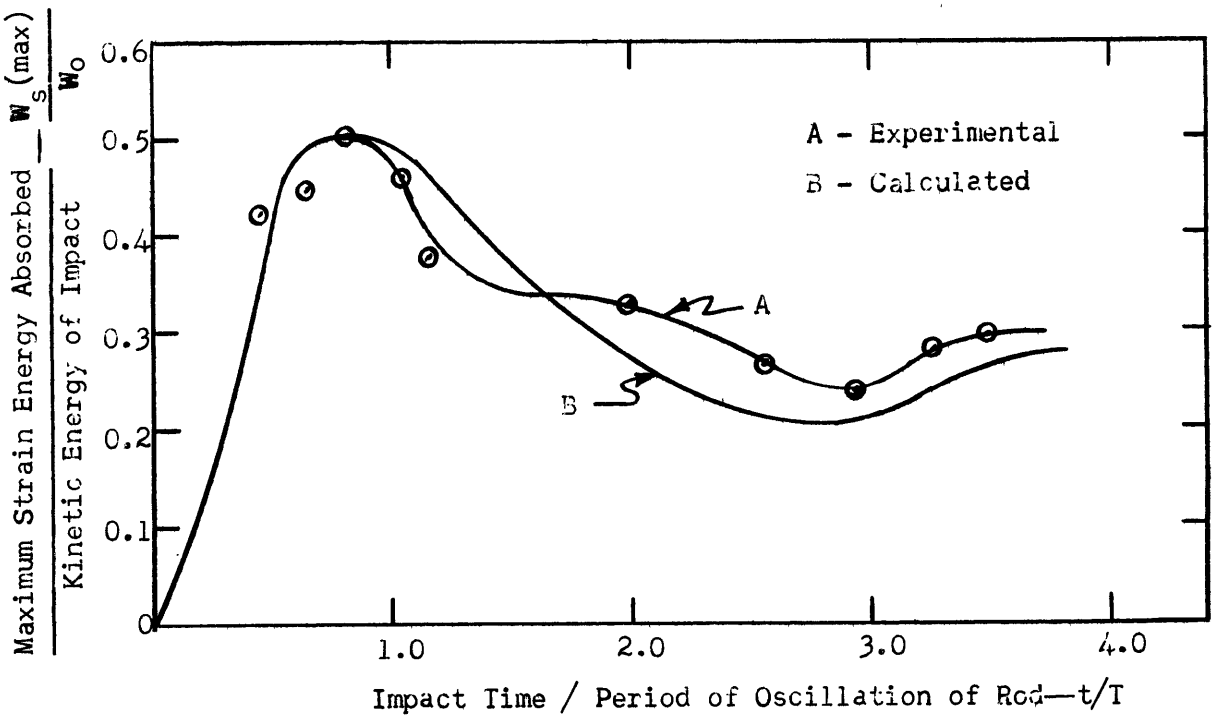

Figure 30. Strain Energy Absorption Coefficients Versus Impact Time-Period of Oscillation Ratios for Impacts on Pyrex Rod

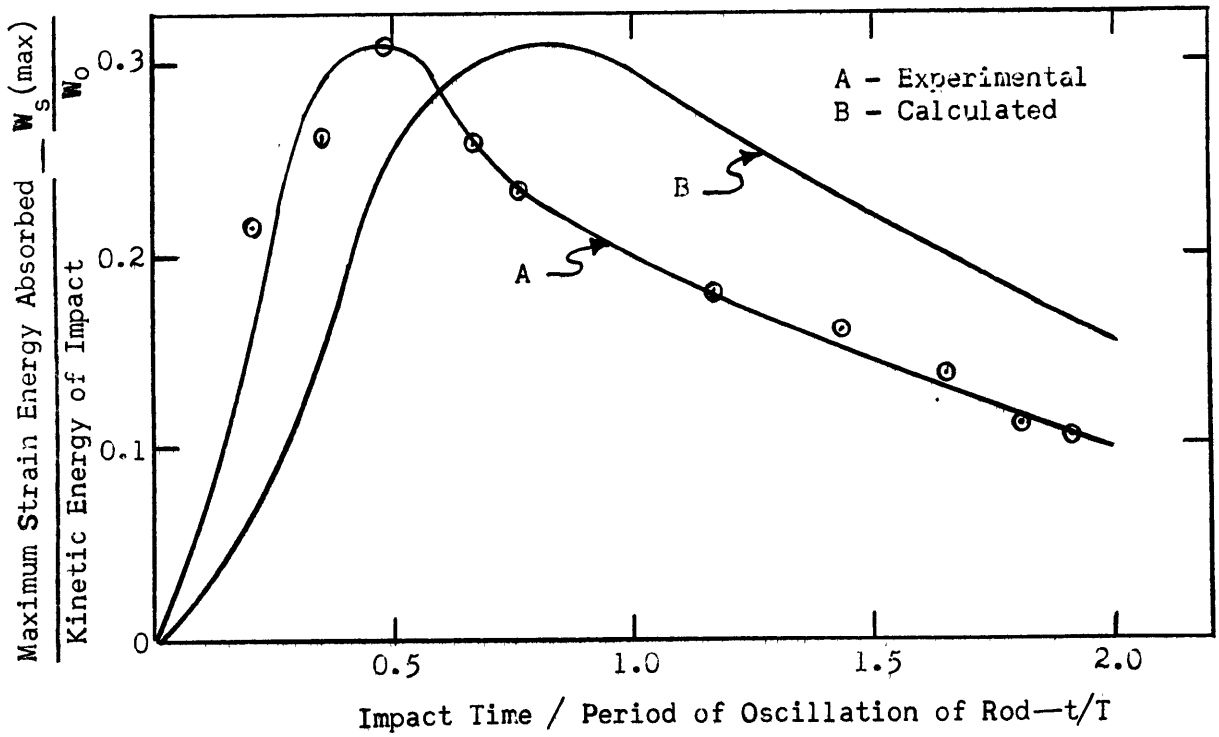

Figure 31. Strain Energy Absorption Coefficients Versus Impact Time-Period of Oscillation Ratios for Impacts on Mild Steel Rod

is upward rather than downward from the lines and consequently, it would appear that no appreciable plastic deformation occurred.

A second possible explanation for the higher energy transfer in the case of glass is that the Young's Modulus of glass is lower than steel. Under impact loading the strain at any section of the rod is a complex function of the kinetic energy of impact and the reciprocal of the Young's Modulus of the material. In the determination of the strain energy absorbed the reciprocal relation may be preserved and thus the transfer of energy to strain energy would be the more complete the less is the Young's Modulus of the material impacted. Qualitatively this hypothesis appears correct if one considers the extreme case where a rubber rod is subjected to impact. The impacting object would be decelerated slowly by forces of small magnitude and when the impacting object had decelerated to zero velocity its kinetic energy would have been almost completely absorbed as strain energy of the rubber.

The experimental portion of this work was carried out on rods composed of only two materials of differing Young's Modulus and therefore experimental results cannot be given to fully illustrate the effect of Young's Modulus on the transfer of kinetic energy of impact to strain energy; however, the results obtained on these two materials are in agreement with the hypothesis brought out in the above discussion.

(b). Theoretical

Frankland's theory of impact, as given previously, shows that for impacts on simple systems of one degree of freedom the responses of the systems are greatly dependent on how long the impacts last. A graph has been presented (Figure 4) which shows some of the effects of the sudden

application of a sinusoidally varying pulse force on a simple system consisting of a rigid mass and a spring. In this figure the dynamic load factor (the maximum value for the response for any single impact) is given as a function of the ratio of the time of impact and the period of fundamental oscillation of the system.

The spring reactive force at any time has previously been shown to be proportional to the response of the system at that time and therefore the maximum spring reactive force would be proportional to the dynamic load factor for the specific impact considered. The strain energy absorbed by the spring when exerting the maximum reactive force is proportional to the square of that reactive force and is, therefore, proportional to the square of the dynamic load factor. For sinusoidal impact pulses of constant amplitude but of variable durations, a graph may be constructed showing the relative amounts of strain energy absorbed by the spring versus the ratio of times of impact and the period of fundamental oscillation of the system. Such a graph is illustrated in Figure 32 and was obtained by squaring the ordinates of Figure 4 and plotting the resultant values against the original abscissa values. Since the strain energy values are relative the ordinate scale has been so arranged that the maximum ordinate of the curve has a value of unity. The curve in Figure 32 has a striking similarity to Curve A in Figures 30 and 31 and has therefore been redrawn as Curve B in these latter figures. Since the theoretical curves give only relative values of strain energy absorption the maximum ordinates have been made equal to those of the experimentally determined curves. Although the theoretical strain energy versus impact time curves do not predict specific values of the absorption coefficients they do show the manner in which they should vary with impact time if the impact pulses varied sinusoidally with time and if the experimental

systems could be considered as having a single degree of freedom.

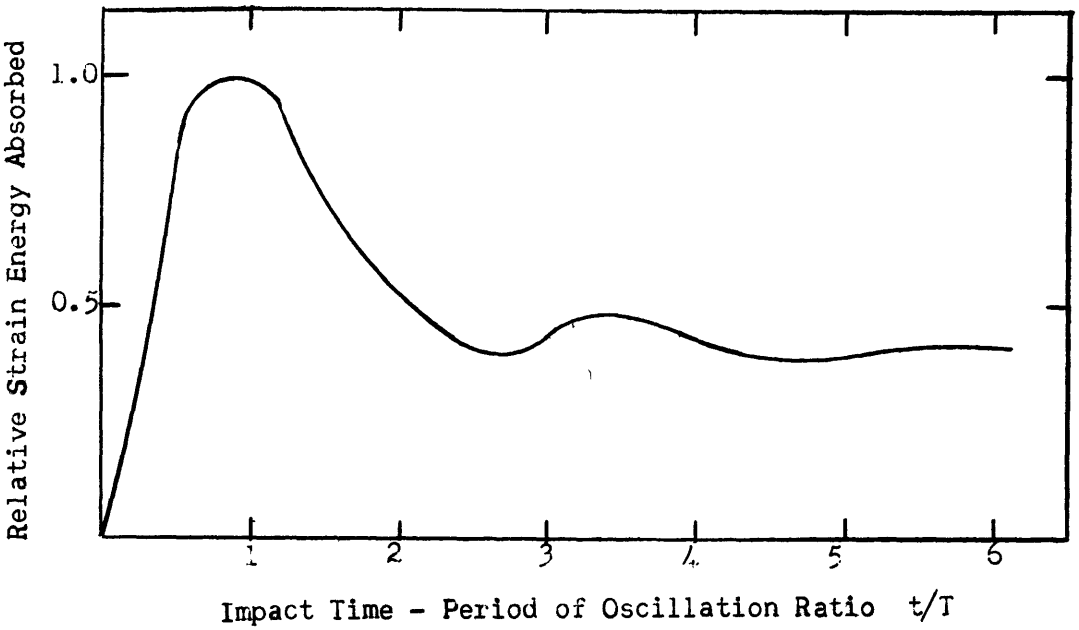

Figure 32. Relative Strain Energy Absorbed versus the Ratio of Contact Time to Period of Oscillation

For the case of impacts on the pyrex glass rods the variation of the experimental strain energy absorption coefficients with the impact time-oscillation period ratios is very nearly that predicted by the theory developed from Frankland's work. Examination of the strain-time traces for the pyrex rods however, shows that only in the case of impact hammers weighing less than 100 grams do the impact pulses at the struck end of the rod assume a sinusoidal shape. For impacts with hammers weighing greater than 100 grams a double peaked impact pulse was always obtained at the struck end of the rods. It may be observed, by examining Figures 12 and 13, that the stress at the fixed end of the rods, however, varies nearly sinusoidally with time when double peaked impacting pulses are obtained at the struck end of the rods. Moreover, the time at which the strain values were determined was at the moment when the stress at the fixed ends

of the rods was a maximum. Thus for the purposes of analysis the rod may be assumed to have been struck at the fixed end rather than at the end where hammer contact was made. Under these conditions and since the assumed impact pulse at the fixed end has a nearly sinusoidal shape, the basic requirements for Frankland's theory have been fulfilled.

For the case of impact on the mild steel rod the theoretical and experimental curves in Figure 31 have the same shape but the portions of the curves to the right of the peaks are displaced one from another by an almost constant amount. This difference would suggest that all the impact times measured were shorter than those demanded by the theory. A check of the experimental data failed to bring to light any recognizable constant error or other effect to explain the discrepancy. Consequently it would appear that the theory developed from Frankland's work is only partially applicable to the impacts on the mild steel rod.

It may be concluded that the theory of impact as derived by Frankland on the basis of a single degree of freedom is upheld by the experimental results of impact on the glass rods and is also partially upheld by the experiments on the steel rod. Frankland's theory, therefore, should find useful application in the analysis of impact problems that arise in a study of comminution.

VII. SUMMARY AND CONCLUSIONS

The transfer of kinetic energy by impact to strain energy is a process which plays an important role in the comminution of brittle solids. Considered as a process, separate from the fracture process, the mechanism of energy transfer must be more fully understood before a complete analysis of size reduction can be realized. Studies of impact, which give information on energy transfer and stress conditions arising from impact, have been made for the simple case of a rod fixed at one end and struck longitudinally at the other end with a moving object.

The information which was obtained in the experimental studies is summarized as follows:

1) The transfer of the kinetic energy of impact to strain energy of the rods is greatly dependent on the time during which the hammer and rod remain in contact. The experimental values of the impact times for which the energy transfer is a maximum for the pyrex and mild steel rods are, respectively, 0.8 and 0.5 times the period of fundamental oscillations of the rods. The maximum values of the ratios of strain energy absorbed to impact kinetic energy were 0.50 for the pyrex rod and 0.31 for the steel rod. Although the evidence is not conclusive, the lower strain energy absorption coefficient for the steel rod appears to be due to the fact that the Young's Modulus for steel is higher than that for pyrex glass.

2) The impact times, which have been shown to be the controlling feature in the transfer of impact kinetic energy to strain energy of the rods, are determined mainly by the weight of the impacting hammers and the physical characteristics of the rods. The experimental results showed that

for impacts on either the glass or the steel rods the time of impact decreased with decreasing hammer weight. Theoretical considerations indicate that the energy of impact should have a small effect on the time of impact; the accuracy with which these measurements can be made, however, prevent any specific conclusions as to this effect.

3) Light weight impacting hammers generated simple loading pulses, consisting of single blows, at the struck end of the pyrex rod. As the weight of the impacting hammer was increased the time of contact also increased so that the vibrational motions of the rods increasingly affected the shape of the loading pulse. With a maximum impacting weight of about 600 grams on the 25.4 cm pyrex rod the loading pulse consisted of two separate blows of almost equal intensity.

4) The maximum stress could be either at the fixed end or the struck end of the bar depending on the shape of the loading pulse. In general, when the loading pulse consisted of two well defined blows the maximum stress was developed at the fixed end of the rod and when the loading pulse consisted of a single blow the maximum stress was developed at the struck end of the rod.

5) The experimental results showed, qualitatively, that in the rebound of light hammers from the rod the amount of energy left in the rod as vibrational energy was much greater than in the case of rebound of relatively heavy hammers. Apparently the longer times of impact and the greater forces required for acceleration of the heavier masses in rebound caused a very significant damping action on the vibrations of the rods set up during impact.

From the experimental results as summarized above a number of general

conclusions may be made as to the application of the impact studies to comminution. The most obvious conclusion is that if kinetic energy is to be most efficiently utilized in an impact process for size reduction, the time of impact should be as short as possible, for all practical purposes, and the intensity of impact as large as possible. The former condition assures a substantial transfer of kinetic energy to strain energy and the latter condition assures the development of stress values sufficient to initiate and propagate fractures.

Since the time of impact can be controlled only indirectly through adjustment of the masses and other physical characteristics of the impacting objects, short impact times can only be obtained by using impacting masses that are small compared to the impacted mass. The use of such impacting masses necessitates the development of relatively high velocities of impact in order that sufficient amounts of kinetic energy are available for the size reduction process. Unfortunately, there are great mechanical difficulties in accelerating large numbers of particles to high velocities and the efficiency of developing high velocity impacts may more than offset the expected gain in efficiency of the size reduction process which makes use of these impacts.

From the experimental results it would appear that the use of small impacting masses at high velocities would have two other advantages in a size reduction process. The loading pulse would undoubtedly consist of a single blow of short duration and therefore it is more likely that the maximum stress would be developed at the point of contact rather than at the points which support the impacted mass. Thus the energy of impact would be transferred to strain energy within the impacted mass and the major portion localized near the point of impact for the short period of

time necessary for fracture. In this manner only a small amount of energy would be passed through the impacted object and absorbed by the supports.

If the interpretation of the experimental results is correct in that light impacting hammers in rebounding cause only slight damping of the vibrations set up during impact then the use of small impacting masses in comminution may have another advantage. Rapid, successive impacts may have a cumulative effect on the internal vibrations set up in the impacted mass. It would be very unlikely that the internal vibrations would be neutralized by impacts occurring exactly out of phase with the preceding vibrations and therefore, the most probable condition with successive impacts would be that the internal vibrations would increase in intensity. Thus, fracture and size reduction may be accomplished by a succession of rapid, light blows of which any one of them taken singly would have no lasting effect on the impacted object.

VIII. SUGGESTIONS FOR FUTURE WORK

The experimental evidence obtained from this study of impact indicates that further work along the following lines may contribute to the knowledge of comminution.

1) Carry out fracturing experiments in which a great range of velocities of impact are investigated but in which the kinetic energies of impact are held constant. The experimental equipment could be quite simple consisting of the following.

(a) A rifle firing bullets for very high impact velocities.

(b) A wheel which could be made to rotate at various speeds and which contained a magnetic release so that an attached projectile could be released tangentially at various velocities from the wheel.

(c) A drop weight device for relatively slow impact velocities.

(d) A velocity measuring device similar to that used in the investigations outlined in this thesis.

The experimental procedure would consist of fracturing tests on glass cylinders or spheres and determining the resulting size distributions and productions of new surface area. The impact fracturing results could be compared to a standard test obtained by measuring the strain energy absorbed and the size distribution and new surface produced in slow compression breakage of duplicate test pieces of glass.

2) The present work indicates the importance of time of impact in the transfer of kinetic energy to strain energy through impact. The release of the stored strain energy by fracture is necessarily a time dependent process and thus the question of crack velocities enters the picture. A comprehensive study of crack velocity in brittle solids is, therefore, an important phase of research in comminution. There are numerous reports of

cracks propagating at the speed of sound within the fractured material: yet, tests incidental to the work of this thesis show that fractures in glass plates can be made to propagate slow enough so that they may be followed and observed with a microscope. A series of experiments are therefore proposed to observe and measure crack velocities and fracture patterns in fractured solids. Numerous electronic and photographic techniques, involving electronic switches, strain gage devices, photo-flash units, etc., may be applied to a research program of this kind.

3) Impact experiments, similar to those outlined in this work but in which the Young's Modulus and hardness of the hammers and rods are treated as variables, would provide important additional information on the energy transfer process during impact. A preliminary mathematical investigation of the problem along the lines suggested by Timoshenko[4] and Frankland[5] would undoubtedly reduce the amount of experimental work required.

4) A strain energy measuring method, in which the relationship of strain energy absorbed versus time could be evaluated from a single impact, would be of great value in impact-fracturing tests. Such a method could be realized if the signals from gages, which sample strain at various sections of the impacted body, could be electronically squared and a total voltage representing the sum of the squared signals applied to a recording device such as an oscilloscope. Such a device, although made difficult by the low level signals put out by strain gages, should not be impossible to construct. With this instrument the strain energy absorbed, when fracture begins, could be evaluated and correlated to the conditions of impact.

BIBLIOGRAPHY

1. Griffith, A. A., "The Phenomena of Rupture and Flow in Solids", Trans. Roy. Soc. (London), series A, vol. 221, p.163, 1921.

2. Joffe, A. F., "The Physics of Crystals", McGraw-Hill, New York, 1928.

3. Piret, E. L., Johnson, J. F., Axelson, J., "Energy - New Surface Relationship in the Crushing of Solids", Chem. Eng. Prog., vol. 45, No. 12, p. 713, 1949.

4. Timoshenko, S., "Vibration Problems in Engineering", D. Van Nostrand Co. Inc., New York, 1937.

5. Frankland, J. M., "Effects of Impact on Simple Elastic Structures", Proc. Soc. Exp. Stress Anal., vol. VI, No. 2, p. 7, 1948.

6. Hertz, H., "Ueber die Berührung fester elasticher Körper", J. Math. (Crelle's J.), vol. 92, 1881.

7. Morey, G. W., "The Properties of Glass", Reinhold Pub. Corp., New York, 1938.

8. Williams, A. E., "The Strength of Glass", J. Am. Ceram. Soc., vol. 6, p. 980, 1923.

9. Fyffe, R. J., Arobone, A., "Strain Gage Transducers for Measurement and Control", Prod. Eng., p. 127, Nov. 1952.

10. "Handbook of Chemistry and Physics", Chemical Rubber Publishing Co., Cleveland, 31st. Ed., 1949

11. Timoshenko, S., "Zur Frage nach der Wirkung eines Stosses auf einen Balken", Zeitschr. f. Math. u. Phys., Vol. 62, p. 198, 1913.

APPENDIX I

EXPERIMENTAL EQUIPMENT

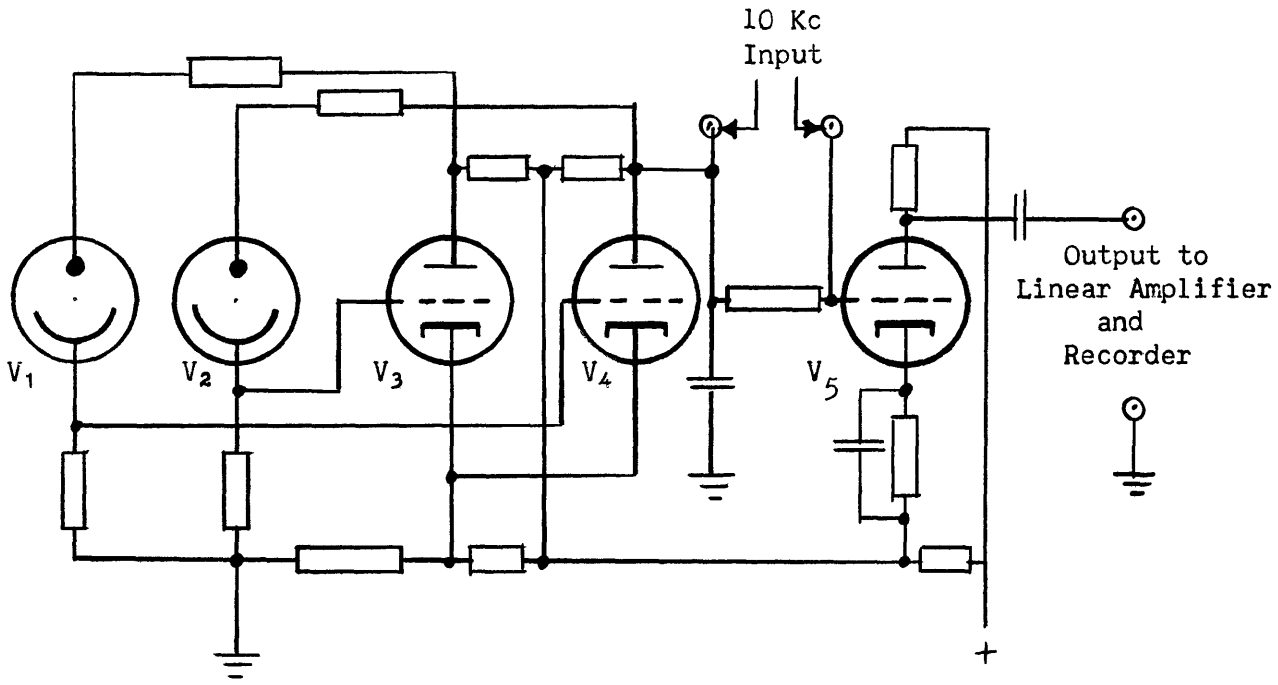

Figure 1. Schematic Circuit for Velocity Measuring Apparatus

A. Method of Operation of Velocity Meter

1) In stable operating conditions V_4 conducts and V_5 is biased below cut off.

2) Interruption of light on V_1 transfers conductance from V_4 to V_3 thus removing negative bias to V_5 and therefore V_5 conducts and amplifies the 10 Kc signal.

3) The pulses of the amplified 10 Kc signal are counted by the recorder.

4) Interruption of light on V_2 transfers conduction from V_3 back to V_4 and V_5 stops conducting.

5) The number of pulses counted as the projectile passes between V_1 and V_2 allows the calculation of the average velocity of the projectile as it passes between the phototubes.

B. Calculation of the Accuracy of the Measurements of Velocity from the Spring Loaded Gun

If R is the coefficient of friction between the projectile and the gun barrel then,

$$v^2 = v_o^2 - 2Rgs$$

where v = impact velocity of projectile

v_o = measured velocity of projectile

R = coefficient of friction

g = acceleration of gravity

s = distance between point of impact and the point where the velocity is measured

For the case of the spring loaded gun used in the investigation,

$R = 0.17$

$s = 6$ cm

$g = 980$ cm/sec^2

then $v^2 = v_o^2 - 2000$

The following table shows the percent error of the measured velocity with respect to the calculated velocity of impact.

TABLE 1

Calculated Versus Measured Impact Velocities for the Spring Loaded Gun

Measured Velocity v_o(cm/sec)	Calculated Velocity v	% Difference $(\frac{v_o - v}{v_o})$ 100
100	89.5	10.5
200	195.0	2.5
300	297.0	1.0
400	398.0	0.5
500	499.0	0.2

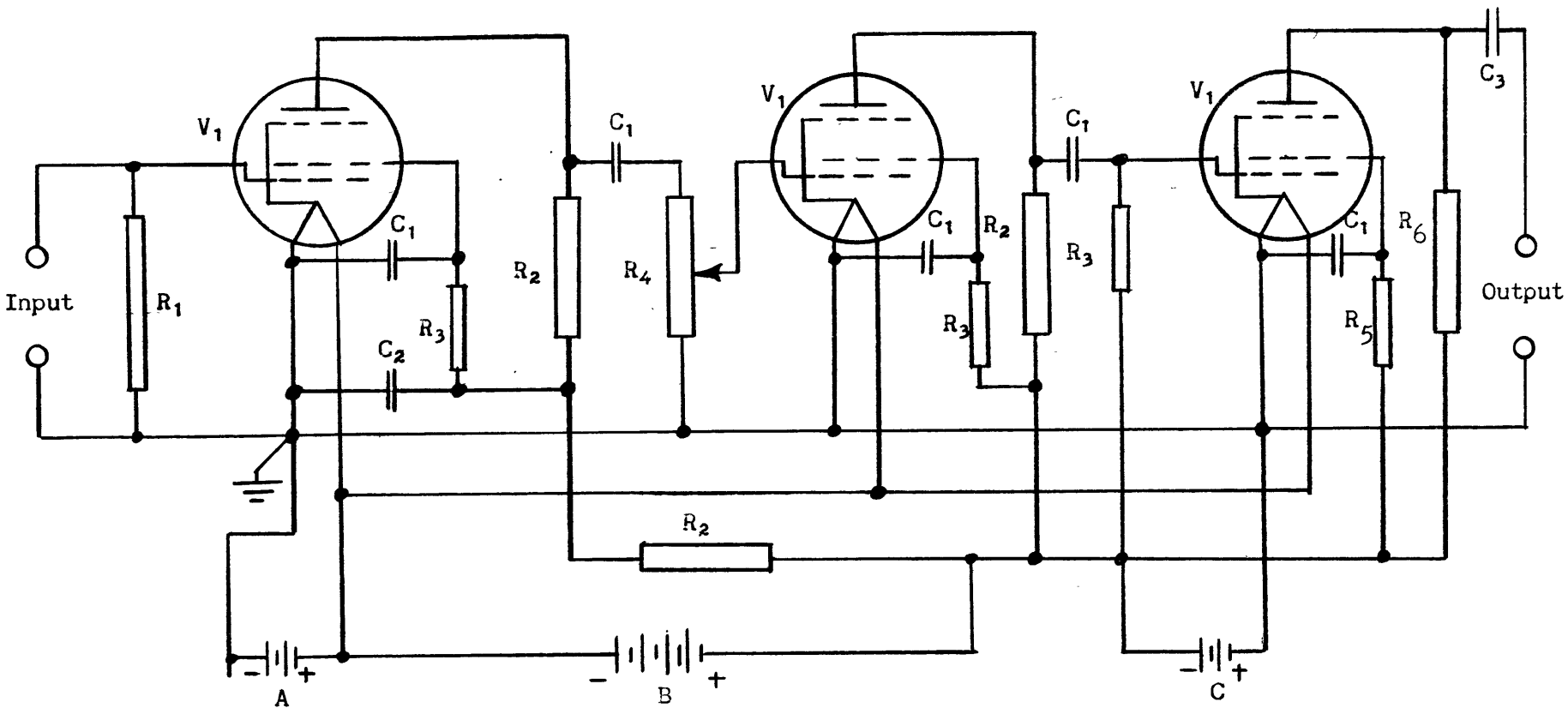

V_1 - type 34 pentodes	R_4 - .5 M	C_1 - .02 mfd	A - 2 volts
R_1 - 5 M	R_5 - .25 M	C_2 - .2 mfd	B - 135 volts
R_2 - .1 M	R_6 - 50 K	C_3 - 1 mfd	C - 1 1/2 volts
R_3 - 2 M			

Figure 2. Schematic Diagram of Strain Gage Amplifier

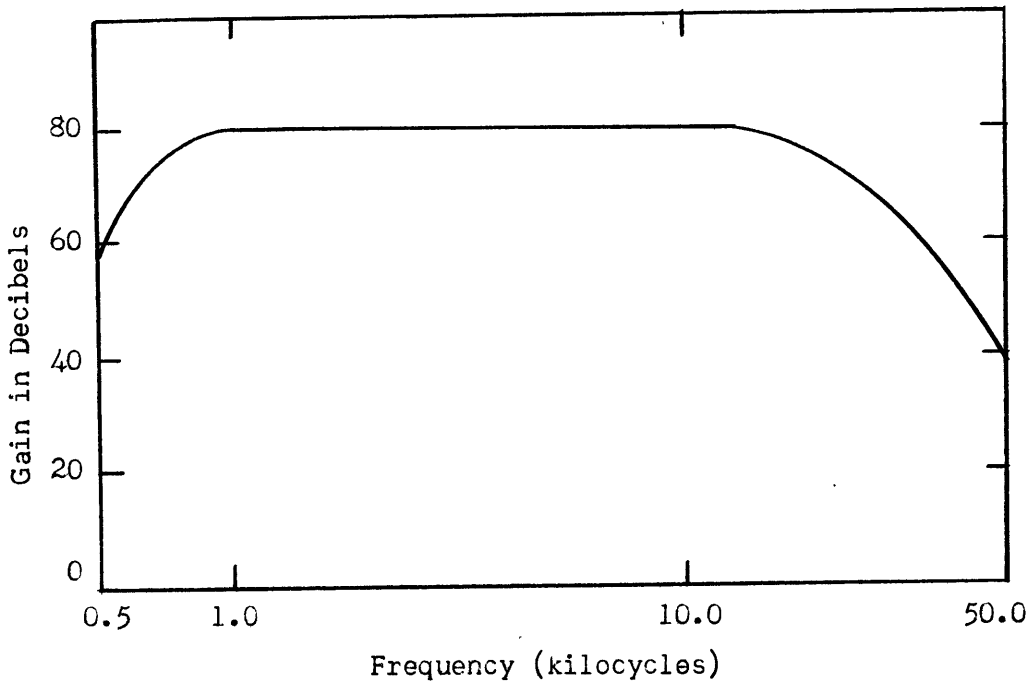

Figure 3. Frequency Response of Strain Gage Amplifier

TABLE 2

Manufacturers Data on Strain Gages
(Baldwin-Lima Corp., Philadelphia)

Type	Resistance	Gage Factor
AB - 3	$119 \pm 0.5\ \Omega$	$2.09 \pm 1\%$
AB - 7	$121 \pm 0.5\ \Omega$	$1.98 \pm 1\%$
AB - 11	$121 \pm 0.5\ \Omega$	$1.91 \pm 1\%$

APPENDIX II

EXPERIMENTAL DATA

Table 1

Impact Times as a Function of Hammer Weight
(Impacts on Pyrex Glass Rods)

Hammer Weight (gm)	Impact Energy w_o (gm.cm.)	Impact Time (microsecs.)	Hammer Weight (gm)	Impact Energy w_o (gm.cm.)	Impact Time (microsecs.)
59.3	1200	75	393	511	290
	2080	80		800	320,320
	2600	75		933	280
	3180	80		2000	320,310
	3430	75			300,310
93.0	336	90			320,300
	493	120		2980	275
	986	90		3000	305,300
	1832	100			280,305
199	388	190			305,290
	500	185,185			290,280
		185,195	493	497	320
		195,195		900	280
	1010	175		1270	290
	1642	175		1990	280
	1970	175		3065	280
	2000	175,165		4410	255
		165,165	593	510	350
		165,165		1000	355,340
	2500	175			350,350
	3020	180			340,330
296	686	270		1020	330
	1110	240		1570	330
	2030	220		2000	325,350
	3450	260			310,315
393	460	275			320,300
				3000	350

TABLE 2

Impact Times as a Function of Hammer Weight
(Impacts on Mild Steel Rod)

Hammer Weight (gm)	Impact Energy w_o (gm.cm.)	Impact Time (microsecs.)	Hammer Weight (gm)	Impact Energy w_o (gm.cm.)	Impact Time (microsecs.)
39.5	1260	35	199	1010	110
	1800	35		1016	130
	2260	33		1510	110
	2520	35		2000	120,125
	3000	33			105,105
	4600	33			100,105
78.1	1920	58			100,100
	2760	58		2420	110
	4700	57		2510	120
93	374	84	296	592	140
	598	90		806	130
	935	77		1000	125,160
	1000	70,75			120,130
		75,90			110,120
		80,80		1070	130
		90,90		1110	140
	1300	78,80		1600	130
	1600	73		1810	120
	2000	75,75		2000	110,120
		80,80			120,100
		80,80			110,110
	3000	70,70		2990	130
199	505	120	393	800	160,170
	700	110			140,145
	808	130			150,160
	910	120			140,140
	1000	125,105		2000	135,145
		105,105			165,150
		105,105			140,135
		105,140			130
		135,110		3000	135,140

TABLE 2 - CONTINUED

Hammer Weight (gm)	Impact Energy w_o (gm.cm.)	Impact Time (microsecs.)
493	508	150
	1000	175,160
		175,160
	1010	140
	1780	140
	2000	150,180
		140,150
	3020	140
593	778	210
	813	200
	1000	190,180
		190,175
		180,175
		175,200
	1210	170
	1715	190
	2000	175,175
		175,160
		160,170
		160,160
		180,180
	2820	170
	3000	175,170
		160,190
		210

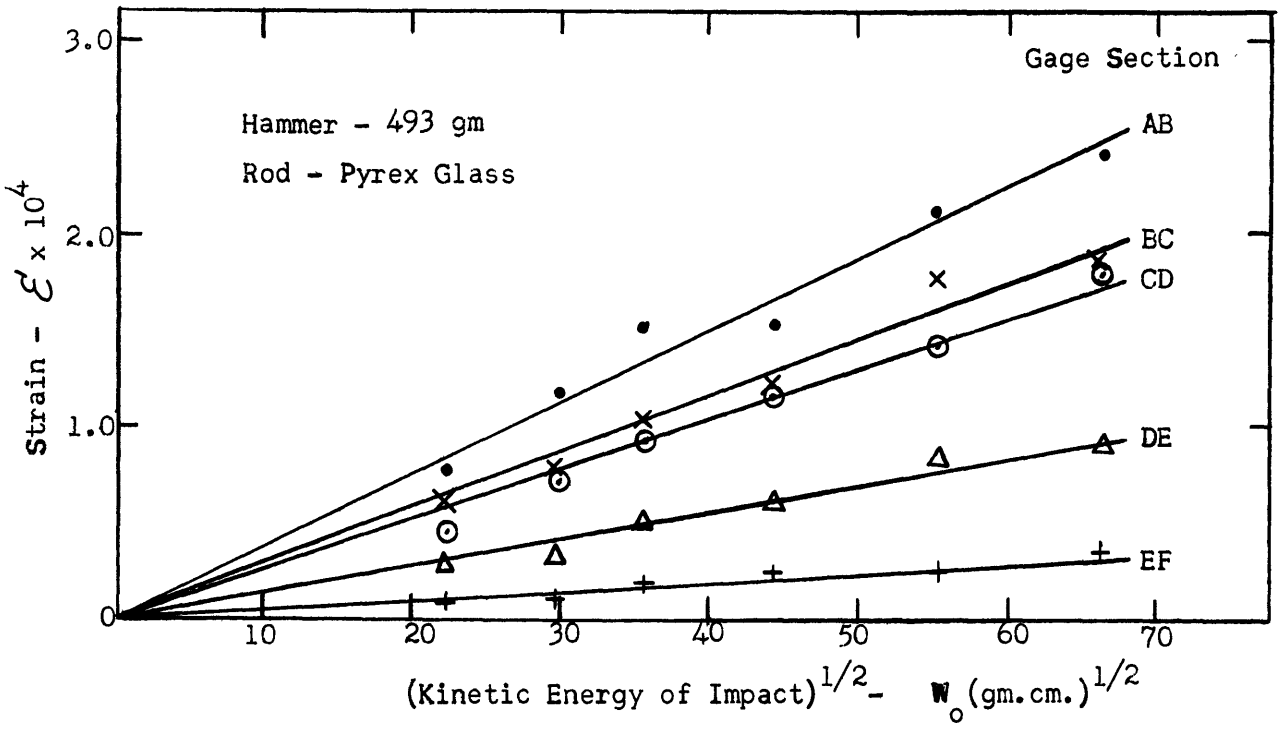

Figure 1. Strain Versus Square Root of Kinetic Energy of Impact

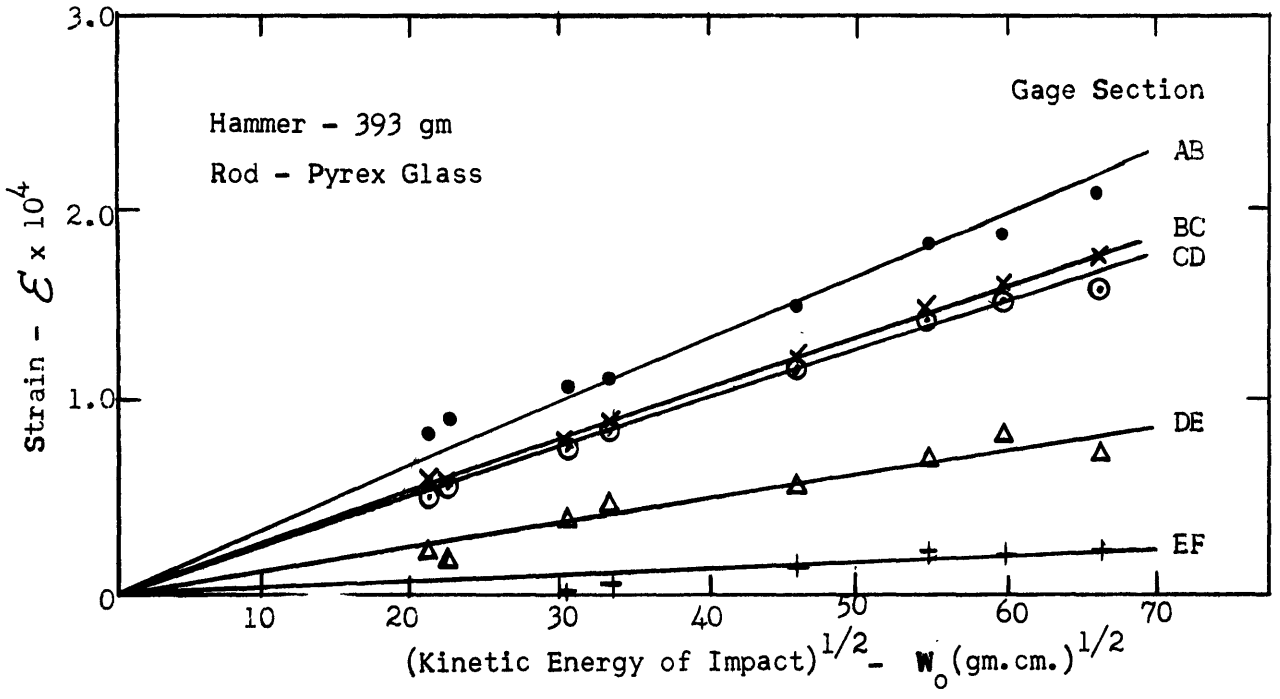

Figure 2. Strain Versus Square Root of Kinetic Energy of Impact

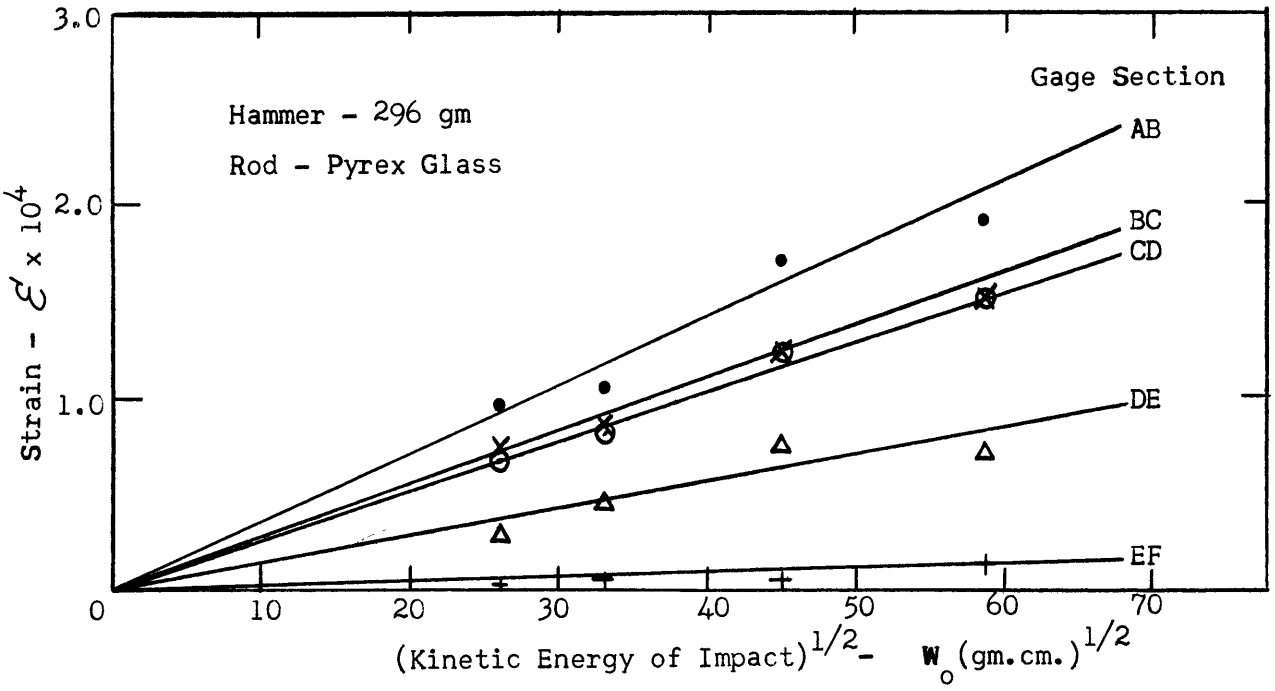

Figure 3. Strain Versus Square Root of Kinetic Energy of Impact

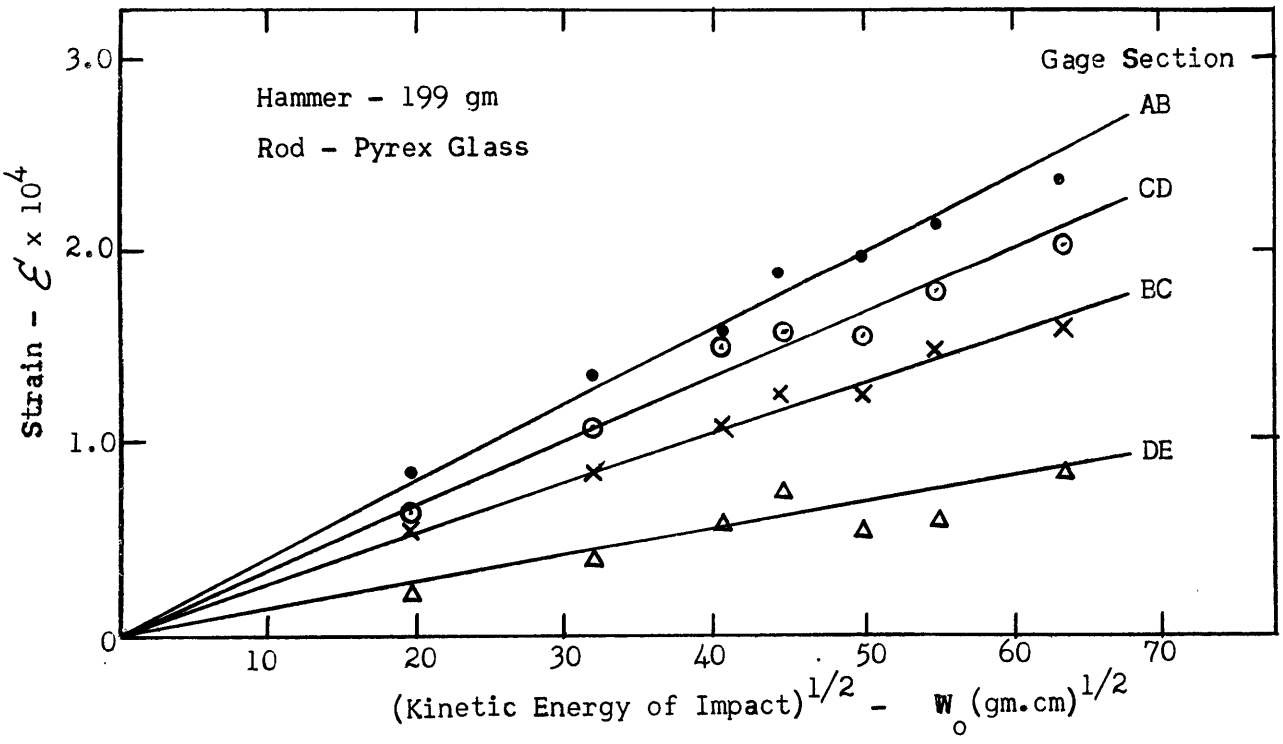

Figure 4. Strain Versus Square Root of Kinetic Energy of Impact

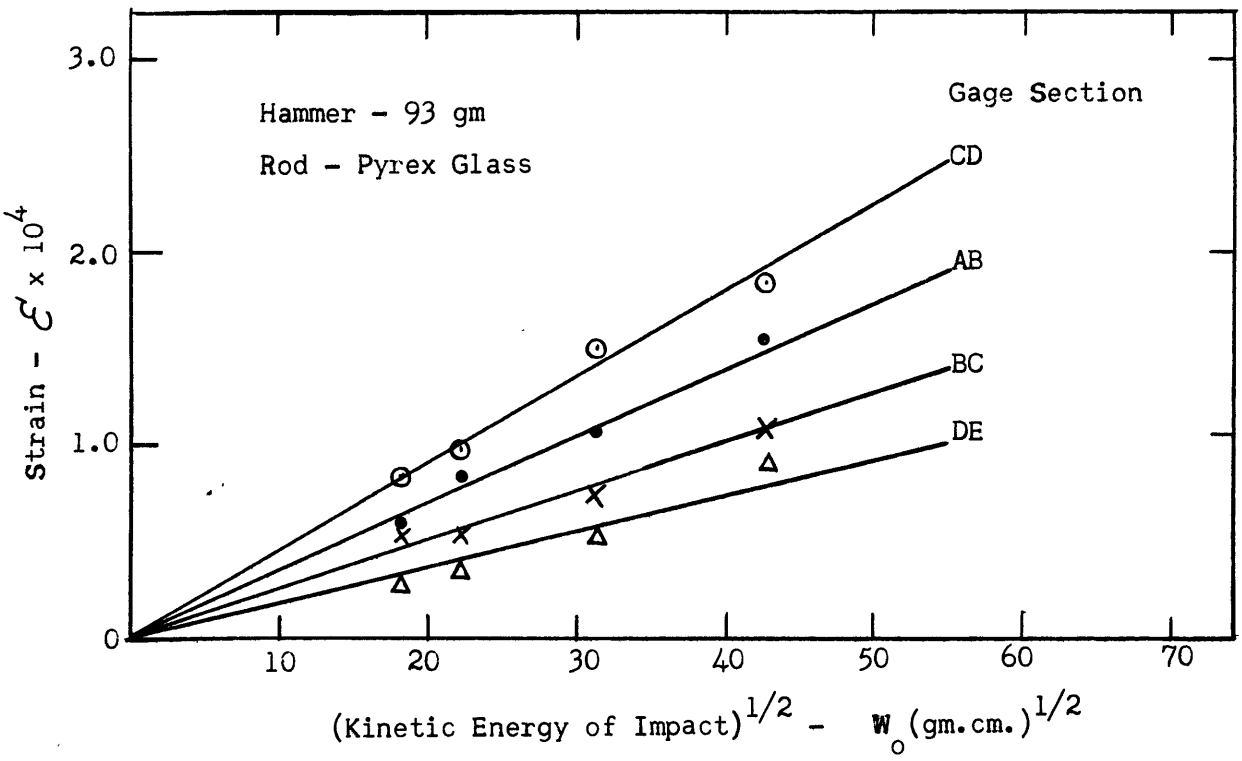

Figure 5. Strain Versus Square Root of Kinetic Energy of Impact

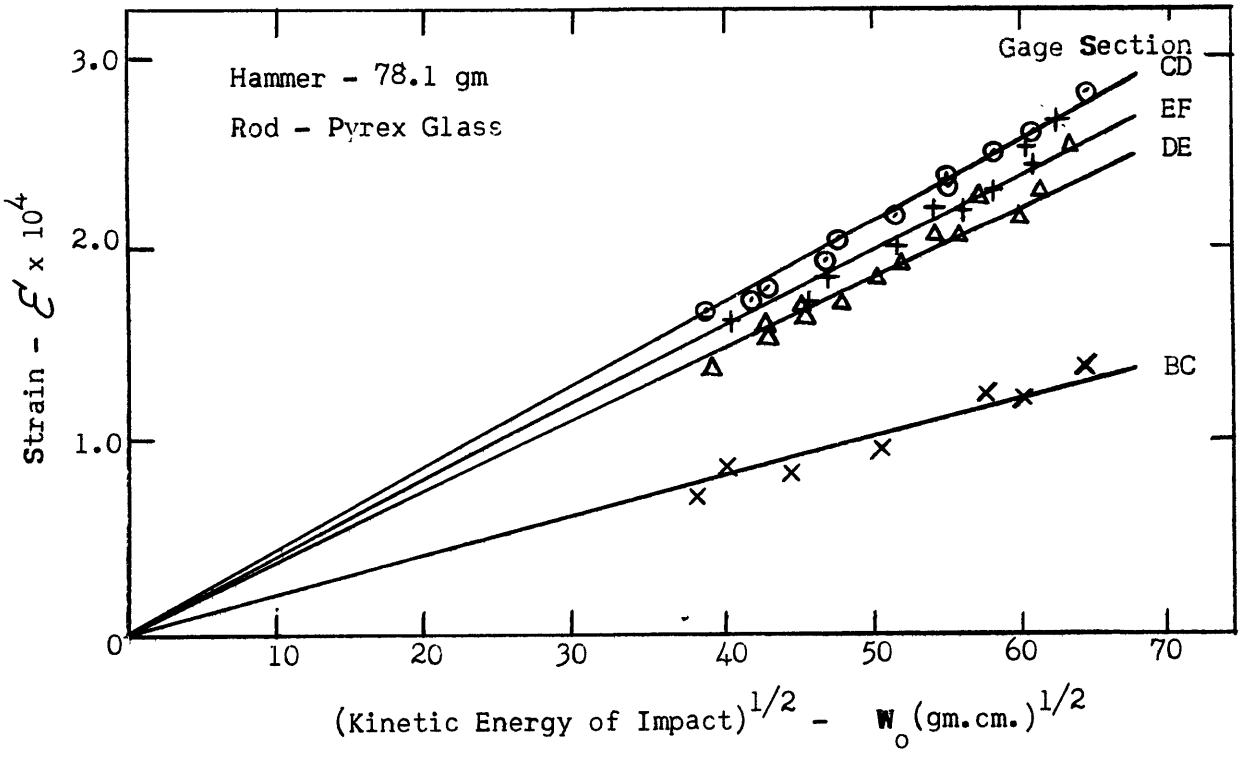

Figure 6. Strain Versus Square Root of Kinetic Energy of Impact

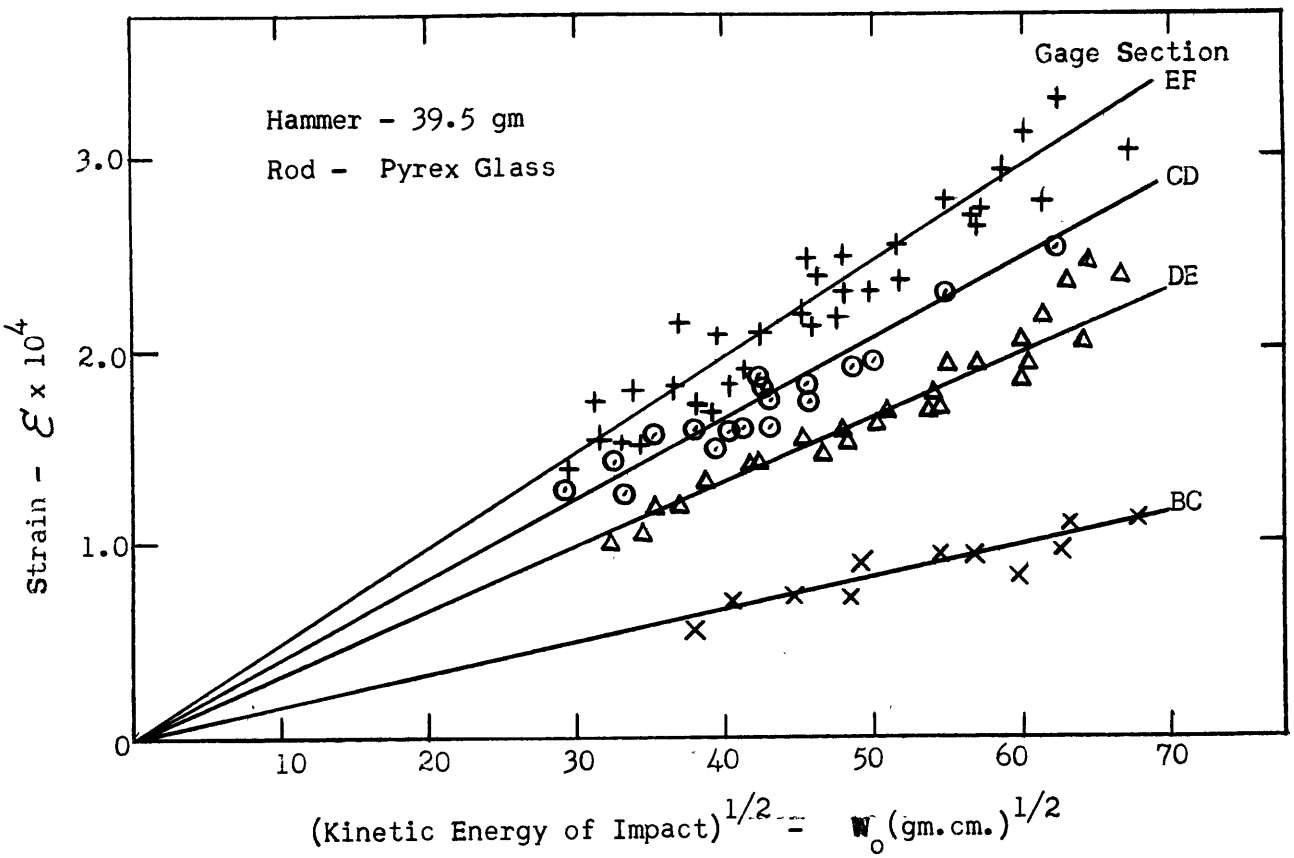

Figure 7. Strain Versus Square Root of Kinetic Energy of Impact

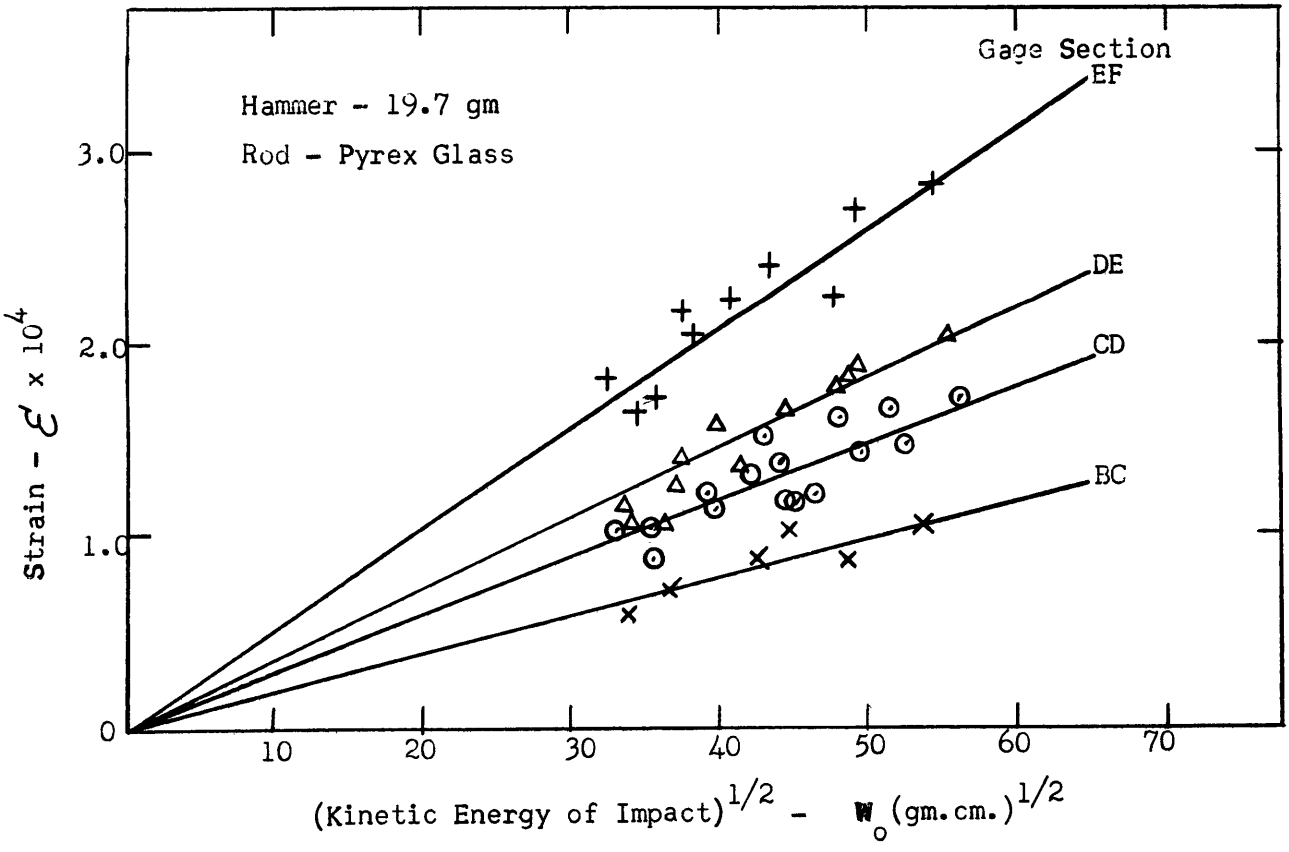

Figure 8. Strain Versus Square Root of Kinetic Energy of Impact

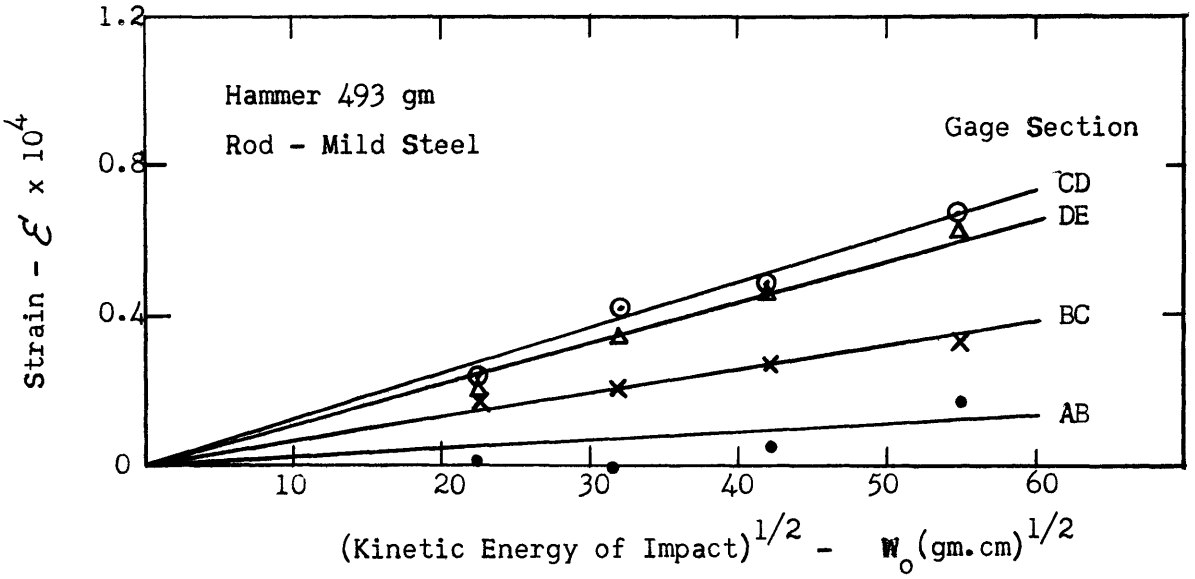

Figure 9. Strain Versus Square Root of Kinetic Energy of Impact

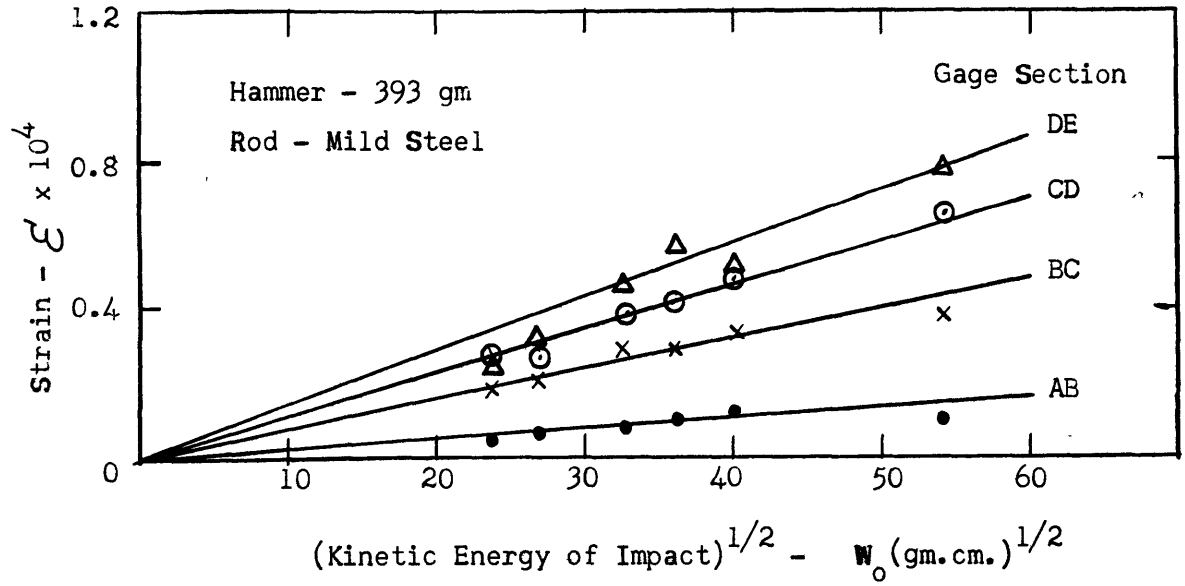

Figure 10. Strain Versus Square Root of Kinetic Energy of Impact

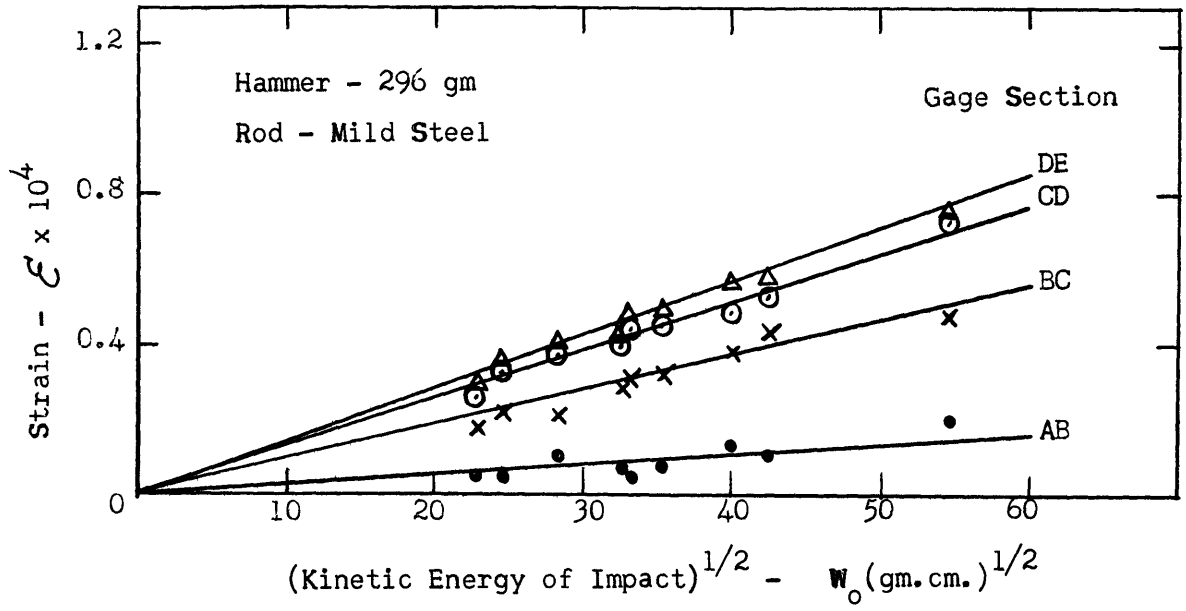

Figure 11. Strain Versus Square Root of Kinetic Energy of Impact

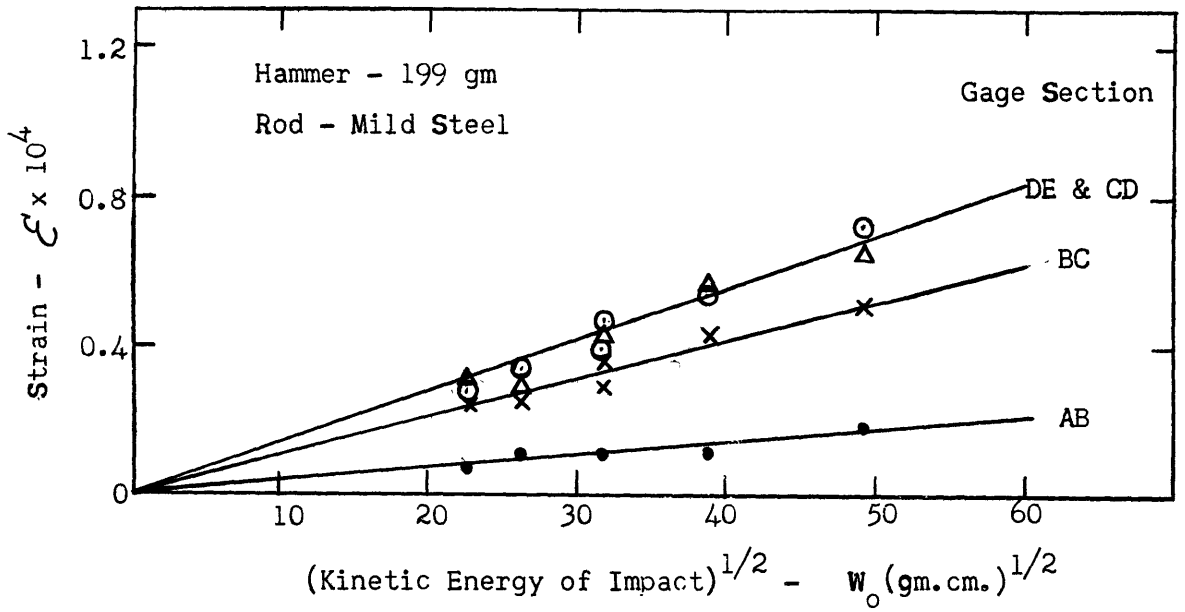

Figure 12. Strain Versus Square Root of Kinetic Energy of Impact

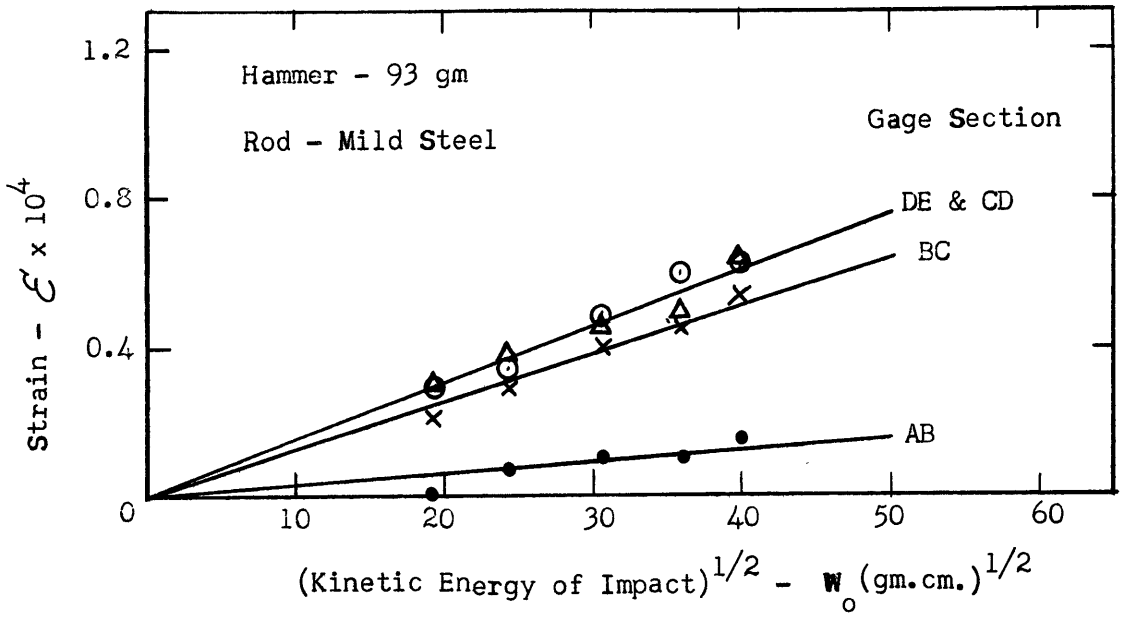

Figure 13. Strain Versus Square Root of Kinetic Energy of Impact

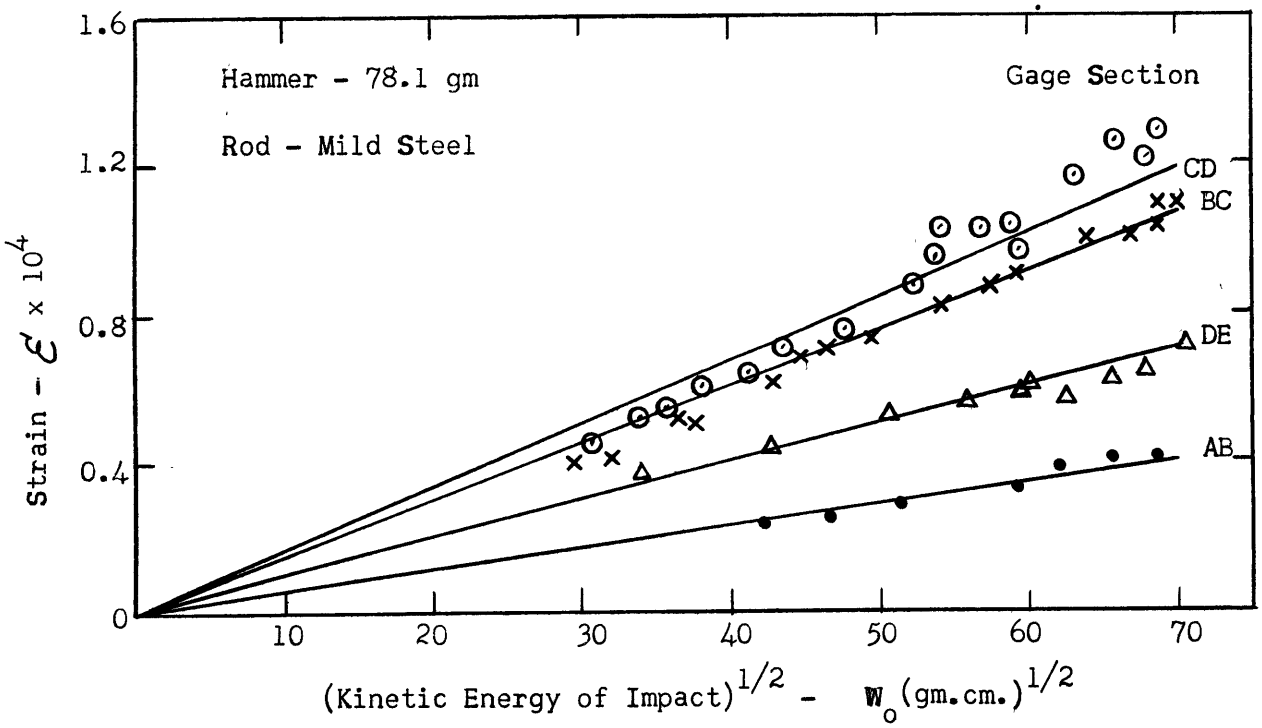

Figure 14. Strain Versus Square Root of Kinetic Energy of Impact

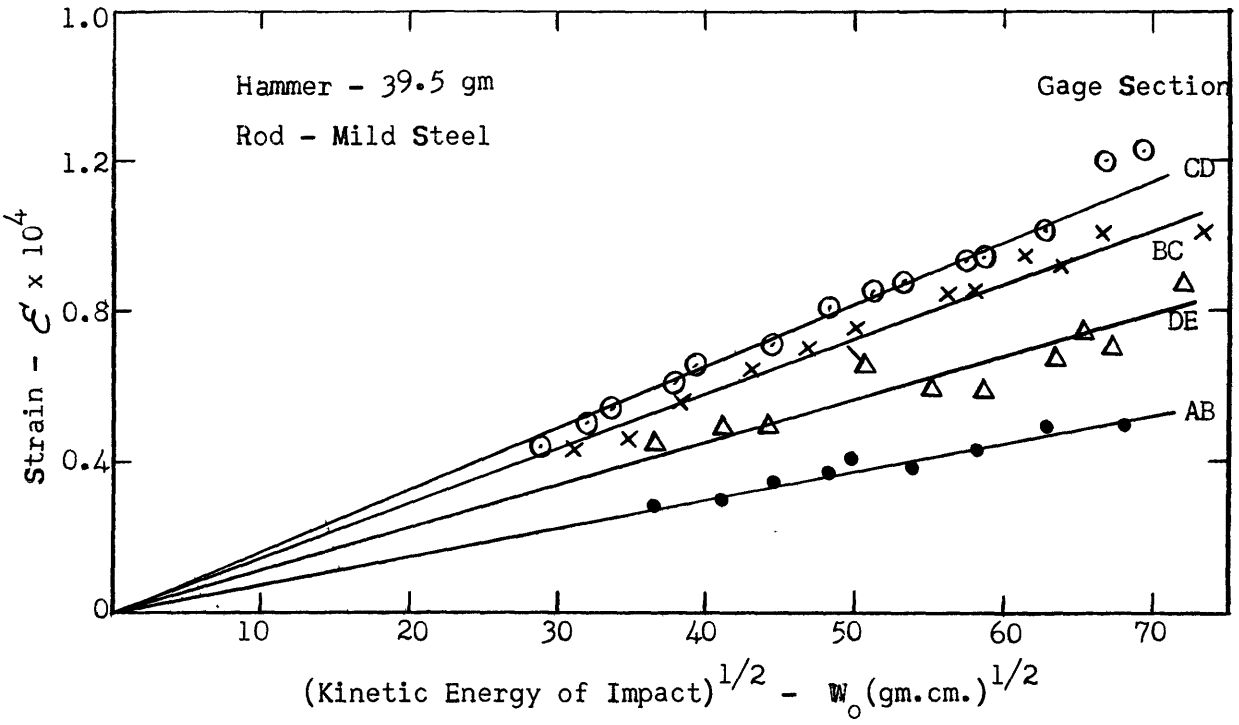

Figure 15. Strain Versus Square Root of Kinetic Energy of Impact

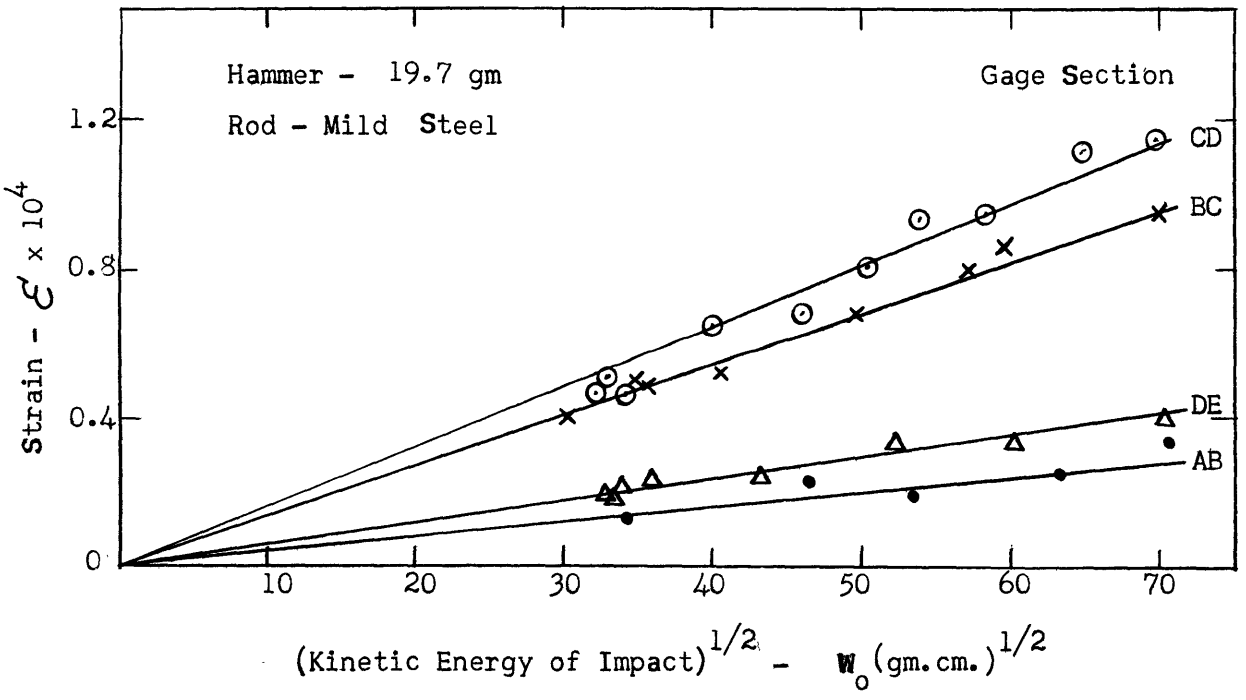

Figure 16. Strain Versus Square Root of Kinetic Energy of Impact

APPENDIX III

THEORETICAL CALCULATIONS

A. Method of Solution of the General Impact Equation

The following equation has been derived in Chapter II for longitudinal impact of a fixed end rod.

$$v_o t - \left(\int_o^t \frac{dt_1}{m}\right)\int_o^t P dt_1 = k_1 P^{2/3} + \sum_{i=1,3,5\ldots}^{\infty} (K/i)\int_o^t P \sin(i\pi a/2\,l)(t-t_1)dt_1$$

v_o = velocity of impact
m = mass of impacting object
t = specific value of time
t_1 = time
k_1 = constant
P = contact force
K = constant
a = velocity of sound in rod material
l = length of rod

A solution, as given by Timoshenko[11], which expresses the contact force, P, as a function of time, t_1, may be obtained for the above equation by stepwise numerical integration. The time of integration, t, is divided into n equal intervals such that the force, P, may be considered constant during any single interval, thus,

$$\tau = t/n \qquad \tau = \text{interval length}$$

Then the term

$$\int_o^t \frac{dt_1}{m}\int_o^{t_1} P dt_1 \cong \frac{\tau^2}{2m}\left[P_1 + P_2 + P_3 + \cdots + P_n\right]$$

and the term

$$\sum_{i=1,3,5\ldots}^{i=\infty} (K/i)\int_o^t P \sin(i\pi a/2\,l)(t-t_1)dt_1 \cong K\left\{P_1 \sum_{i=1,3,5\ldots}^{i=\infty}\left[\frac{\cos(i\pi a/2\,l)(t-\tau)}{i^2} - \frac{\cos(i\pi a/2\,l)t}{i^2}\right] + P_2 \sum_{i=1,3,5\ldots}^{i=\infty}\left[\frac{\cos(i\pi a/2\,l)(t-2\tau)}{i^2} - \frac{\cos(i\pi a/2\,l)(t-\tau)}{i^2}\right] + \cdots + P_n \sum_{i=1,3,5\ldots}^{i=\infty}\left[\frac{1-\cos(i\pi a/2\,l)\tau}{i^2}\right]\right\}$$

The approximations for the above two terms are introduced into the original equation and starting with the first interval the equation is solved for P_1. The value obtained for P_1 permits rewriting of the equation so that a value of P_2, during the second interval, may be obtained. The procedure is repeated until a value for P_n is arrived at and thus a relationship of contact force, P, and time, t_1, is obtained.

B. Strain Energy Distribution in Pyrex Rods as a Function of Kinetic Energy of Impact and Hammer Weight

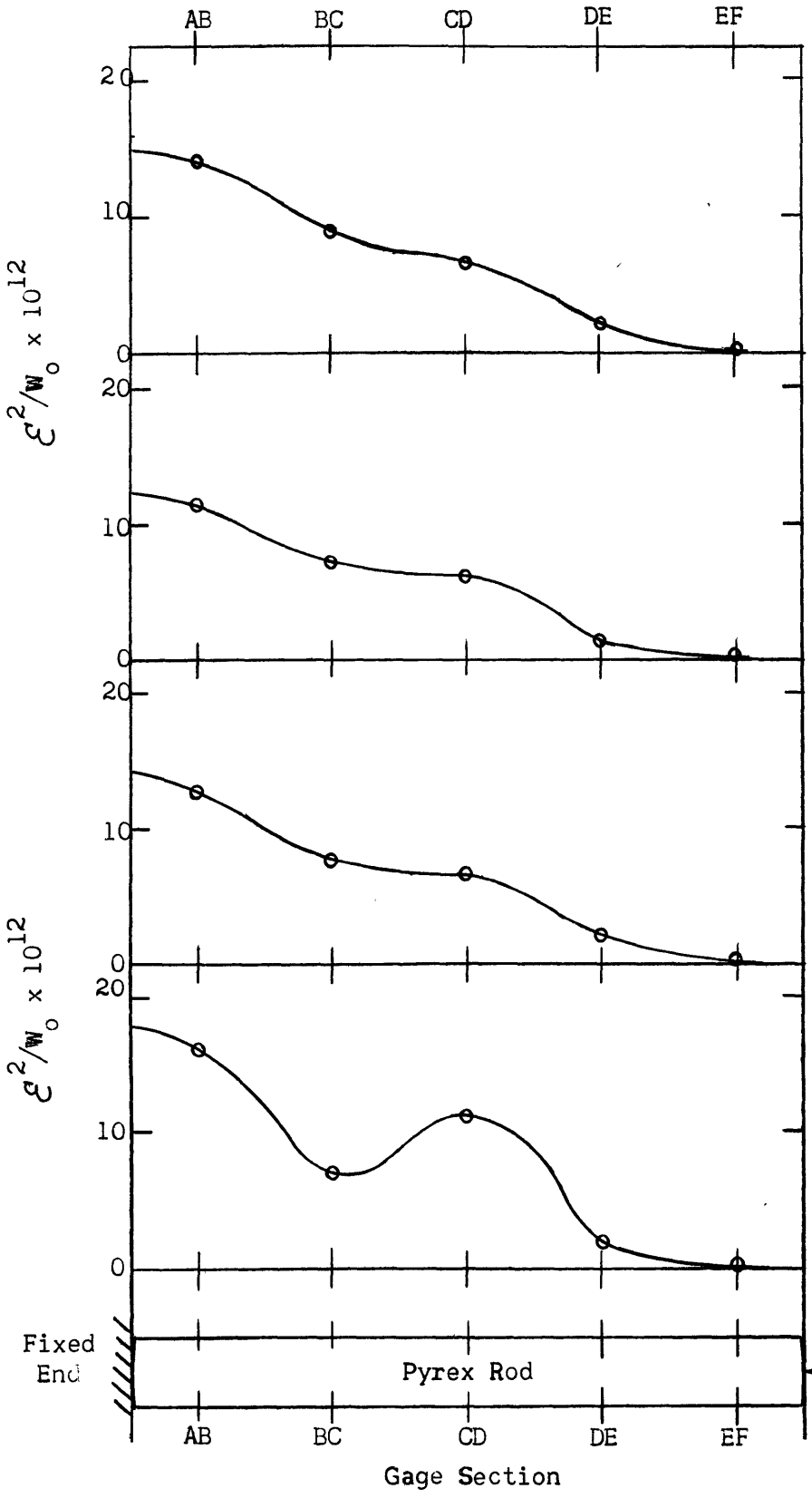

Figure 1
Hammer - 493 gm

Figure 2
Hammer - 393 gm

Figure 3
Hammer - 296 gm

Figure 4
Hammer - 199 gm

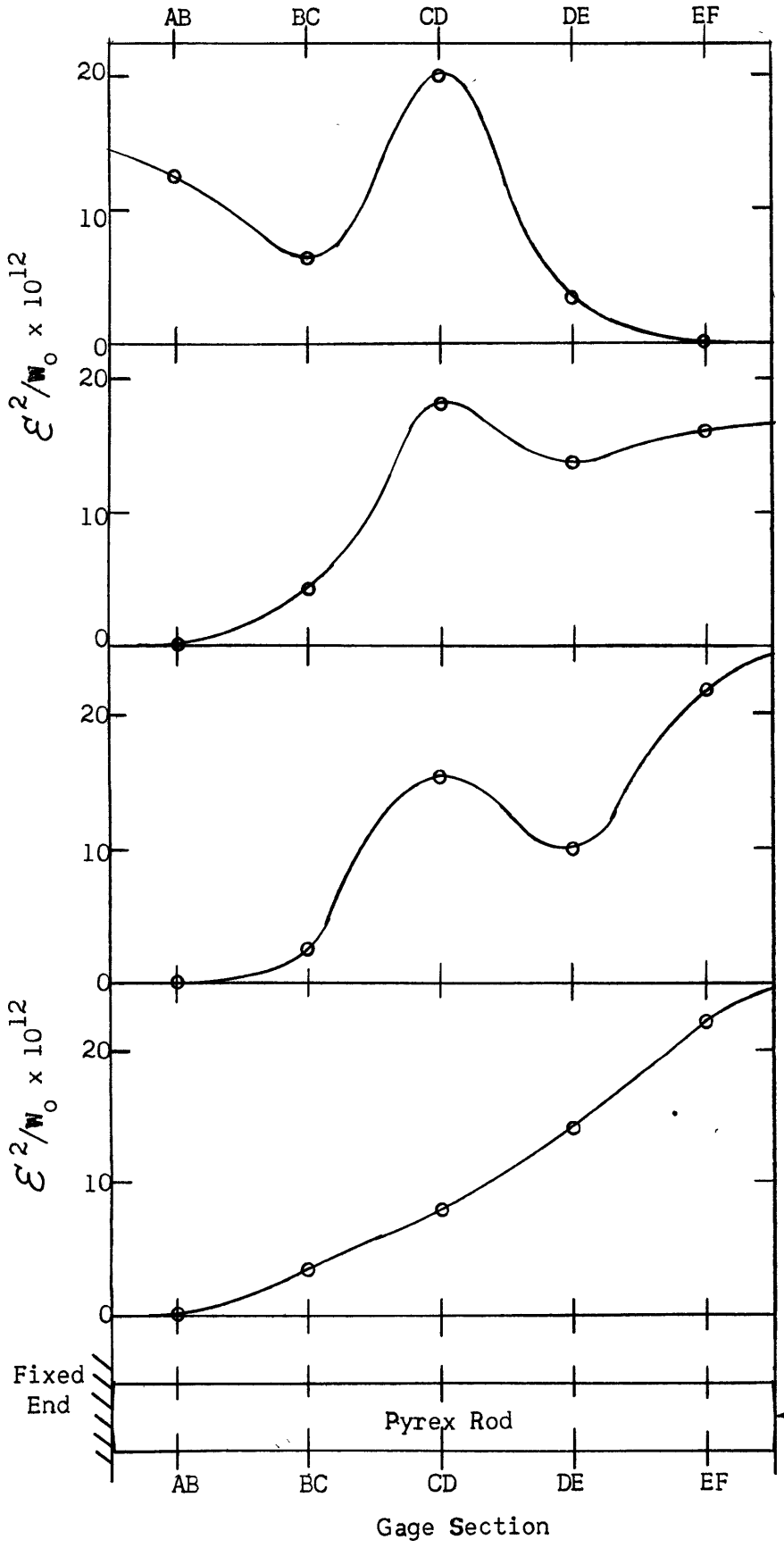

Figure 5
Hammer - 939 gm

Figure 6
Hammer - 78.1 gm

Figure 7
Hammer - 39.5 gm

Figure 8
Hammer - 19.7 gm

C. Strain Energy Distribution in Mild Steel Rods as a Function of Kinetic Energy of Impact and Hammer Weight

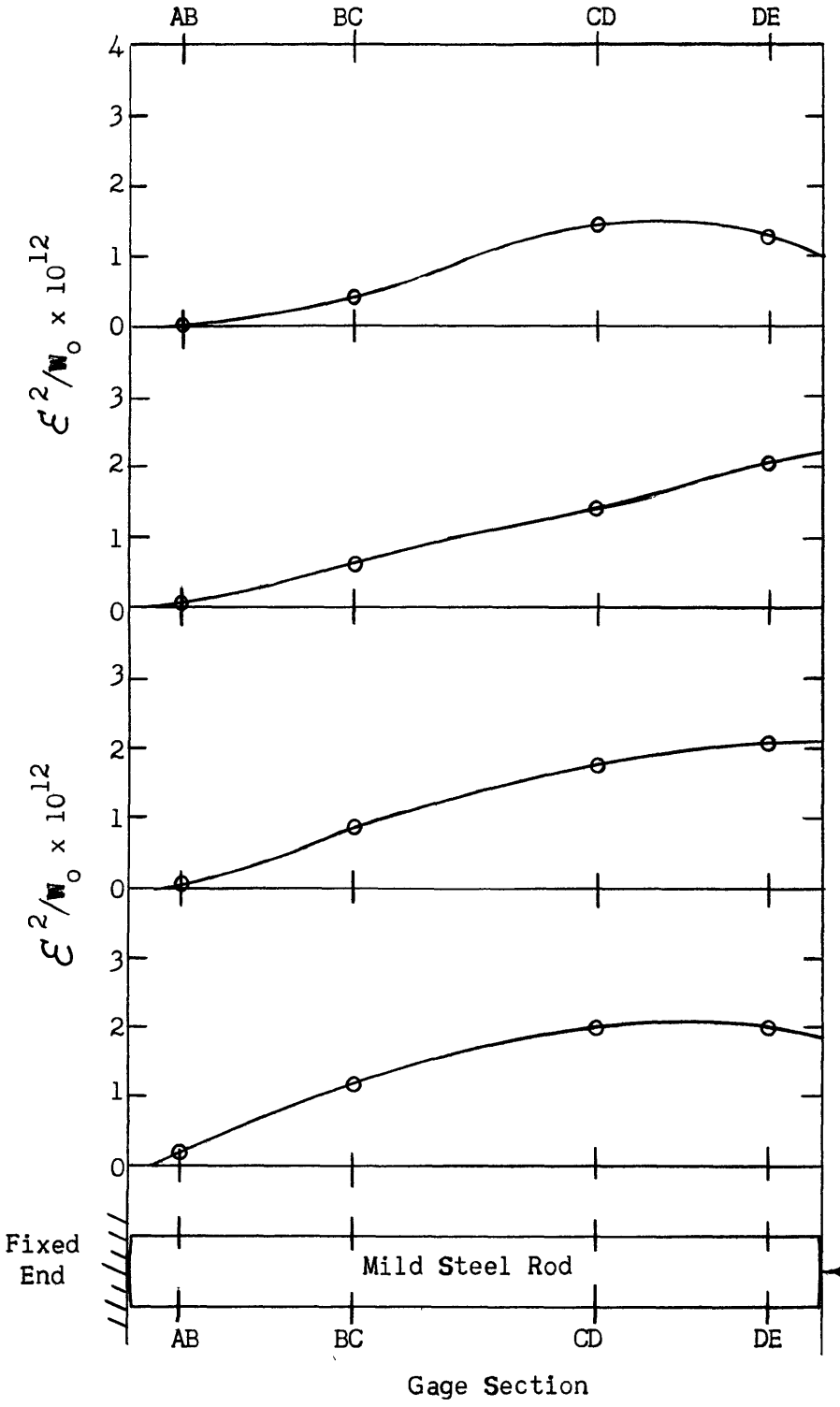

Figure 9
Hammer - 493 gm

Figure 10
Hammer - 393 gm

Figure 11
Hammer 296 gm

Figure 12
Hammer - 199 gm

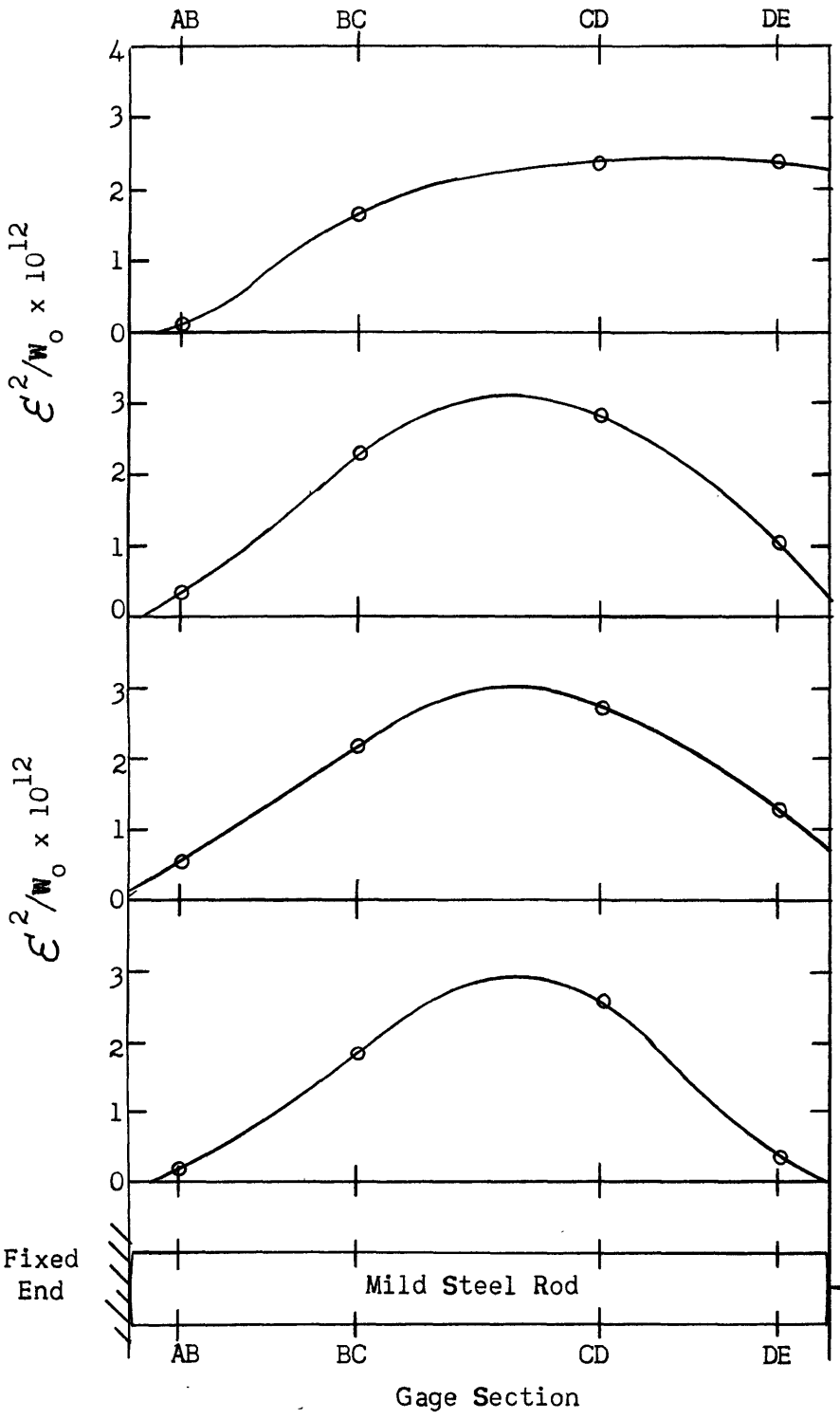

Figure 13
Hammer - 93 gm

Figure 14
Hammer - 78.1 gm

Figure 15
Hammer - 39.5 gm

Figure 16
Hammer - 19.9 gm

BIOGRAPHICAL SKETCH

The author was born in Elfros, Saskatchewan, Canada on September 8, 1925. After completing the required courses at Lord Byng High School at Vancouver, B. C., in 1943, he entered the University of British Columbia and received a B.A.Sc. degree in Mining Engineering in June, 1948. He was awarded a scholarship by the Britannia Mining and Smelting Corporation for further study and received an M.A.Sc. degree in Metallurgical Engineering in September, 1949.

His industrial experience prior to graduation included working as a surveyor for the Quebec Gold Mining Corporation, Montreal, Quebec, and a Junior Engineer for the Caribou Gold Quartz Mining Company, Wells, B. C. Further industrial experience was obtained after graduation as Mine Engineer for the Base Metals Mining Corporation, Field, B. C., and as Engineer in Charge for the El Alamein Gold Mines, Tulameen, B. C.

In February, 1951 he was admitted to the Graduate School of the Massachusetts Institute of Technology. During his stay at the Institute he was employed as a research assistant and instructor in the Department of Metallurgy.